# VOLUMETRIC MR-HIFU ABLATION OF UTERINE FIBROIDS

Marlijne Elisabeth Ikink

**Volumetric MR-HIFU ablation of uterine fibroids**
Marlijne Elisabeth Ikink

PhD thesis, Utrecht University, The Netherlands

ISBN/EAN: 978-94-6108-833-8
Cover art: IKEA B.V. Nederland (adapted)
Lay out: A.L.L. Adams
Printed by: Gildeprint, Enschede



Financial support for the publication of this thesis was kindly provided by Philips Healthcare.

# Volumetric MR-HIFU ablation of uterine fibroids

# Volumetrische MR-HIFU-ablatie van vleesbomen in de baarmoeder

(met een samenvatting in het Nederlands)

**Proefschrift**

ter verkrijging van de graad van doctor aan de Universiteit Utrecht
op gezag van de rector magnificus, prof.dr. G.J. van der Zwaan,
ingevolge het besluit van het college voor promoties
in het openbaar te verdedigen op maandag 8 december 2014 des middags te 2.30 uur

door

Marlijne Elisabeth Ikink

geboren op 6 juni 1984 te Nieuwegein

| | |
|---|---|
| Promotoren: | Prof.dr. M.A.A.J. van den Bosch<br>Prof.dr. W.P.Th.M. Mali |
| Copromotor: | Dr.ir. L.W. Bartels |

*Voor mijn ouders*

# Contents

# 1 General introduction

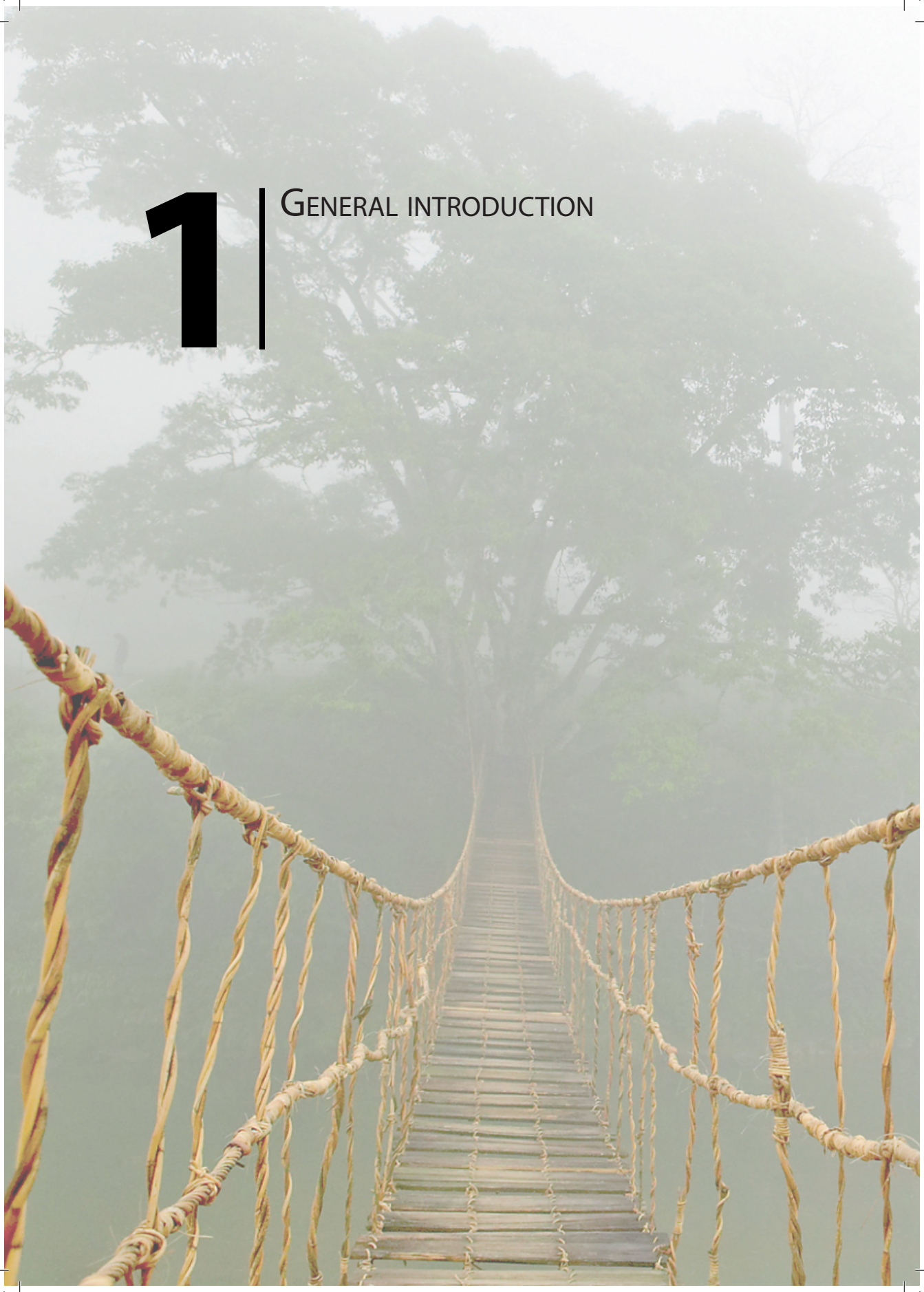

## Uterine fibroids

Uterine fibroids (or leiomyomas) are benign hormone-sensitive tumours that originate from the smooth muscle layer (i.e. myometrium) of the uterus. They are characterised by the proliferation of myometrial smooth muscle cells and the excessive deposition of collagenous extracellular matrix[1-4]. The aetiology of uterine fibroids is unknown and their biology poorly understood. Promoters of fibroid formation and tumour growth are found in the female sex hormones oestrogen and progesterone by increased mitotic activity[5-7], elevated levels of growth factors and angiogenetic factors[8], and the impaired process of apoptosis[9,10]. Uterine fibroids are considered the most common benign solid pelvic tumours in women, and typically appear and grow during middle and late reproductive age[11-13]. Available data reporting the incidence of uterine fibroids in women over the age of 45 years is more than 60%, with a higher prevalence in African-American women with a younger age[14,15]. The most reported symptoms include menorrhagia and hypermenorrhoea leading to anaemia, dysmenorrhoea, pelvic pain (unrelated to menstruation), pressure related symptoms such as frequent micturition and gastrointestinal disturbances, and reproductive dysfunction[16-18]. These symptoms can have a severe impact on the women's quality of life and are associated with substantially higher healthcare and work loss costs[19-22]. Uterine fibroids are often classified according to their location in the uterus. The international federation of gynaecology and obstetrics (FIGO) recommended the following subclassification system[23]: submucous (FIGO types 0, 1, 2), intramural (FIGO types 3, 4), subserosal (FIGO types 5, 6, 7), and an additional 'parasitic' category (FIGO type 8) reserved for e.g. cervical or transmural uterine fibroids as shown in *Figure 1*. Multiple treatment options are available to treat symptomatic uterine fibroids[24,25]: (1) a conservative drug-based approach (e.g. progestins, GnRH-agonists or ulipristal acetate[26]), (2) surgical treatment (e.g. endometrial ablation, laparoscopic, hysteroscopic or trans-abdominal myomectomy, (sub-)total hysterectomy), and (3) interventional radiology procedures such as fluoroscopy-guided uterine artery embolisation (UAE), and more recently, high-intensity focused ultrasound (HIFU) ablation performed under the guidance of magnetic resonance imaging (MRI) or ultrasound imaging. The treatment approach has to be optimally tailored for each patient, depending on the symptoms' severity, the patient's preferences, the importance of uterine preservation, location, and size of the uterine fibroids. However, many of the available conventional treatment methods, although effective, are known to have unattractive side-effects and are of limited use for women who wish to preserve their uterus and fertility[27-31]. For instance, most of the pharmacotherapy may produce significant reductions in both uterine fibroid size and symptoms, although the improvements are often temporary. Hysterectomy will eliminate the symptoms permanently, but is associated with surgical risks and postoperative complications, lengthy recovery times, health-related productivity loss, and potentially negative impact on the quality of life related to the removal of the uterus[32]. Myomectomy is often recommended as the treatment of choice in patients desiring future fertility[33], but is again associated with disadvantages such as surgical morbidity and may be quite difficult to perform for women with large, multiple uterine fibroids[12,27,34]. Compared with hysterectomy and myomectomy UAE is known for its lower major complication rate, yet associated with a higher risk of minor complications with more unscheduled visits and higher rehospitalisation rates[35,36].

## Magnetic resonance-guided high-intensity focused ultrasound

For many decades, the replacement of the surgeon's scalpel with image-guided tools has been explored[37-40]. Focused ultrasound in combination with MR-guidance has become a leading method for realising non-invasive image-guided tissue ablation. In clinical practice, MR-HIFU ablation has already been applied to treat a variety of solid tumours, such as fibroadenomas of the breast[41,42], uterine fibroids[43-46], uterine adenomyosis[47,48], palliative pain treatment of bone metastases[49,50], and prostate cancer[51]. The most widely used clinical application of MR-HIFU ablation is the treatment of patients with symptomatic uterine fibroids. Magnetic resonance-guided high-intensity focused ultrasound (MR-HIFU) is a modality for uterus-sparing thermoablation through the intact skin. Advantages over conventional therapies - like surgery and UAE - are that MR-HIFU is completely non-invasive, does not require the use of ionising radiation, and does not involve an overnight hospital stay. This rapidly developing treatment modality combines the excellent soft-tissue contrasts achievable using MRI[52] with transcutaneous focal heat delivery (while avoiding adjacent normal tissue damage)[40,53], real-time temperature mapping[54], and immediate post-treatment confirmation (typically with contrast-enhanced MRI) of the extent of tissue destruction. Several mechanisms are involved in thermal tissue ablation using HIFU[55]. The primary mechanism is the thermal effect from the conversion of mechanical ultrasound energy into heat, causing coagulative necrosis through the denaturation of cellular proteins. The second mechanism, which is generally clinically avoided as a result of its unpredictable thermal control[56-58], is acoustic cavitation. The low peak negative pressure applied under ultrasound stimulation can generate a cluster of gas-filled bubbles oscillating around an equilibrium size. Rapid growth and violent collapses of these bubbles may fractionate the target tissue to a liquid homogenate with unrecognizable cellular structures[59]. Recently, new treatment protocols are being developed to exploit cavitation-induced HIFU to generate enhanced heating with larger treatment effects[60-62]. Third, high-intensity focused ultrasound has been shown to produce a spectrum of vascular changes[63-67]. Its acoustic radiation force (i.e. tissue displacement and acoustic streaming) may cause vascular compression and (temporary) cessation of blood flow

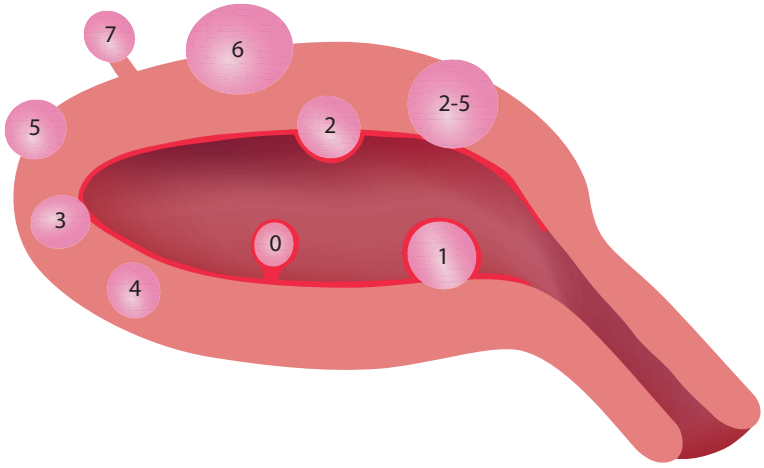


**Figure 1.** FIGO classification (adapted from Munro *et al.*[23])

achieved through vascular spasm, cell shrinkage, endothelial damage, and accumulation of subendothelial tissue oedema. Increasing thermal endothelial destruction of small tumour vessels may eventually lead to the activation of platelets leading to occlusive thrombus formation within the lumen. These mechanisms may provoke ischaemia which will eventually lead to coagulative necrosis[45,63,68].

To date, several systems for MR-HIFU ablation have been clinically introduced. In 2004, the first commercially available MR-HIFU system was released (ExAblate® 2000, Insightec Ltd, Haifa, Israel) using the point-by-point ablation technique[69]. The ultrasound beam, produced by a concave piezoelectric multielement-phased array ultrasound transducer, is iteratively converged into a very small cigar-shaped focal point (6 mm radius, 25 mm long) until the entire tissue volume is ablated[43]. However, this time-consuming procedure is limited due to suboptimal utilisation of the energy deposition which may lead to somewhat inhomogeneous thermal lesions. In order to overcome this limitation and to reduce treatment time, a volumetric heating approach using a spiral trajectory of the focal point was suggested with the intention to optimise temperature uniformity within a larger target volume[70,71]. This volumetric approach has been further developed by electronically steering the focal point along multiple outwards-moving concentric circles (i.e. sub-trajectories) of increasing diameter (range 4-16 mm)[72]. Volumetric MR-HIFU ablation is thought to be more energy efficient than the point-by-point technique, since intrinsic heat diffusion - occurring during the sonication of the inner circles - is used to preheat the region later covered by the outer circle sub-trajectories without losing heat from the targeted area. On account of the spatiotemporal temperature distribution realised while sonicating the sub-trajectories, large well-defined thermal lesions can be achieved[73]. The clinical MR-HIFU platform (Sonalleve®, Philips Healthcare, Vantaa, Finland) as used in our department is depicted in *Figure 2*.

**Figure 2.** Clinical MR-HIFU platform (Sonalleve®, Philips Healthcare, Vantaa, Finland). Adapted from Ikink *et al.*[100]

## Challenges in MR-HIFU ablation of uterine fibroids

Despite the obvious benefits related to its fully non-invasive character, it should be recognised that MR-HIFU ablation also has limitations. An important factor that determines the success of MR-HIFU treatment is patient selection[74-78]. MR-HIFU ablation cannot be applied on all patients with symptomatic uterine fibroids. Each patient should be screened for eligibility based on their medical history, physical assessment, and diagnostic pelvic MRI examination. Diagnostic pelvic MR imaging before and after the administration of a gadolinium-based contrast agent is essential in obtaining the anatomical information on the exact size, number, location, and contrast enhancement of the uterine fibroids, which will be used for treatment planning[79]. Moreover, MRI is used to exclude confounding diagnoses such as pelvic inflammatory disease (PID), and other pelvic neoplasms (e.g. malignancies). Other primary anatomical restrictions for MR-HIFU ablation are device-inaccessible uterine fibroids (deeper than 12-14 cm from the abdominal skin and/or fibroids shielded by bowel loops, ovaries, bone, or metal implants), obesity (excessive thickness of the subcutaneous fat layer of the anterior abdominal wall), and the presence of abdominal scars in the intended beam path. However, advanced mitigation methods used during patient preparation and patient positioning[78,80-84] have developed treatment of uterine fibroids in previously disadvantageous locations, and will continue to amend exclusion criteria.

Previous studies have demonstrated that the non-enhancing part within the treated uterine fibroid (i.e. non-perfused volume (NPV)) on contrast-enhanced T1-weighted (CE-T1w) MRI is a predictor of clinical success with regard to fibroid volume reduction and symptom relief after treatment[85-90]. If the immediate NPV ratio (non-perfused volume divided by fibroid volume) is limited, the patient will most likely not significantly benefit from an MR-HIFU ablation. This suggests that in order to obtain a clinically significant outcome, the highest possible NPV ratios should be achieved in an acceptable time frame while ensuring safety is still guaranteed[91]. To determine clinically significant improvement, a disease-specific uterine fibroid symptom and health-related quality of life (UFS-QoL) questionnaire has been developed[92-94], consisting of an 8-item transformed symptom severity score (tSSS) and 29 health-related quality of life (HRQoL) items.

Several research groups have observed that the immediate NPV ratio was smaller and corresponding fibroid volume reduction and symptom improvement after MR-HIFU ablation reduced in uterine fibroids with a high (brighter) signal intensity on pre-treatment T2-weighted (T2w) MRI[86,89,95,96]. The exact cause of this finding is not entirely clear, but various histopathological features of uterine fibroids, such as cellularity, vascularity, perfusion, necrosis, oedema, and calcification that could be reflected in the signal intensity on T2w MRI[97-99] may influence the therapeutic effect. Therefore, elucidating the tissue's organisational features in relation to the imaging characteristics of uterine fibroids is important to further optimise treatment with MR-HIFU ablation.

## Thesis outline

The aim of the work presented in this thesis is twofold. First, to investigate the mid-term clinical efficacy of volumetric MR-HIFU ablation for treatment of uterine fibroids and, in addition, to compare the efficacy of MR-HIFU with those obtained in patients treated with UAE. Second, to investigate the use of novel MRI techniques that may help to improve the treatment effect of patients with symptomatic uterine fibroids. The thesis is organised as follows:

**Part I. Clinical treatment evaluation**

After this introduction, *Chapter 2* describes the clinical efficacy of volumetric MR-HIFU ablation for the treatment of patients with symptomatic uterine fibroids. Six month clinical outcomes are presented, as assessed with the validated disease-specific UFS-QoL questionnaire and volume changes of the treated uterine fibroids. Using the follow-up data, the clinical efficacy of MR-HIFU can be further compared with a commonly used radiological treatment modality, i.e. UAE. In *Chapter 3*, the treatment efficacy of volumetric MR-HIFU ablation is compared with the results achieved in patients treated with UAE. Follow-up and MR imaging were compared in two groups of patients who fulfilled the eligibility criteria for MR-HIFU ablation. Efficacy was defined as (1) changes in the patient-reported tSSS and total HRQoL scores, and (2) the risk of reintervention.

The clinical success of an MR-HIFU ablation is closely related to the immediate NPV ratio. However, as with other treatment modalities, the balance between clinical efficacy and patients' safety is important. The treatment of larger ablation volumes requires more thermal energy which may lead to a temperature increase along the ultrasound beam axis in the near field area (close to the skin). Although MR-HIFU ablation of uterine fibroids is related to a low complication rate, thermal skin damage and abdominal discomfort has been reported. *Chapter 4* aims to assess the safety and technical feasibility of volumetric MR-HIFU ablation using a direct skin cooling (DISC) device during treatments of uterine fibroids. This technique may further mitigate undesired heating by shifting the baseline skin temperature, potentially increasing effectiveness of treatment effect and reducing treatment time.

**Part II. Prediction and measurement of treatment effect**

As with other non-invasive techniques, there is a need for methods to evaluate the (intraprocedural) treatment effect, preferably without the need to use a contrast agent. An imaging method that has been suggested to determine the extent of tissue ablation during MR-HIFU ablation is diffusion-weighted magnetic resonance imaging (DWI). In *Chapter 5* we describe the value of DWI and apparent diffusion coefficient (ADC) mapping using different *b*-value combinations for the evaluation of treatment results after volumetric MR-HIFU ablation of uterine fibroids. The purpose of this study was to investigate how the choice of *b*-values influences ADC values and contrasts in ADC maps before and immediately after MR-HIFU ablation of uterine fibroids. We hypothesised that by using five different *b*-values ($b$= 0, 200, 400, 600, and 800 s/mm$^2$), the effects of tissue ablation on perfusion and diffusion could selectively be emphasized.

The investigation of perfusion and diffusion contributions can be enhanced by performing intravoxel incoherent motion (IVIM) analyses. The IVIM model takes both the molecular movement of water (diffusion) and the microcirculation of blood in the

capillaries (perfusion) into account by extracting the perfusion fraction (*f*), the static perfusion-free diffusion coefficient (*D*), and the flow-related pseudodiffusion coefficient (*D**). In *Chapter 6*, this method was used to investigate whether pre-treatment IVIM diffusion and perfusion characteristics could predict the therapeutic heating effect of volumetric MR-HIFU ablation.

Finally, in *Chapter 7*, an overview of our findings is given, and future prospects of MR-HIFU ablation for the treatment of symptomatic uterine fibroids are discussed.

# References

1. Islam MS, Protic O, Stortoni P, Grechi G, Lamanna P, Petraglia F, Castellucci M, Ciarmela P. Complex networks of multiple factors in the pathogenesis of uterine leiomyoma. *Fertil Steril.* 2013;100:178-193
2. Flake GP, Andersen J, Dixon D. Etiology and pathogenesis of uterine leiomyomas: a review. *Environ Health Perspect.* 2003;111:1037-1054
3. Ciarmela P, Islam MS, Reis FM, Gray PC, Bloise E, Petraglia F, Vale W, Castellucci M. Growth factors and myometrium: biological effects in uterine fibroid and possible clinical implications. *Hum Reprod Update.* 2011;17:772-790
4. Moore AB, Yu L, Swartz CD, Zheng X, Wang L, Castro L, Kissling GE, Walmer DK, Robboy SJ, Dixon D. Human uterine leiomyoma-derived fibroblasts stimulate uterine leiomyoma cell proliferation and collagen type I production, and activate RTKs and TGF beta receptor signaling in coculture. *Cell Commun Signal.* 2010;8:10
5. Rein MS, Barbieri RL, Friedman AJ. Progesterone: a critical role in the pathogenesis of uterine myomas. *Am J Obstet Gynecol.*1995;172:14-18
6. Andersen J, Barbieri RL. Abnormal gene expression in uterine leiomyomas. *J Soc Gynecol Investig.* 1995;2:663-672
7. Andersen J, Grine E, Eng CL, Zhao K, Barbieri RL, Chumas JC, Brink PR. Expression of connexin-43 in human myometrium and leiomyoma. *Am J Obstet Gynecol.* 1993;169:1266-1276
8. Andersen J. Growth factors and cytokines in uterine leiomyomas. *Semin Reprod Endocrinol.* 1996;14:269-282
9. Okolo S. Incidence, aetiology and epidemiology of uterine fibroids. *Best Pract Res Clin Obstet Gynaecol.* 2008;22:571-588
10. Walker CL, Stewart EA. Uterine fibroids: the elephant in the room. *Science.* 2005;308:1589-1592
11. Buttram VC Jr, Reiter RC. Uterine leiomyomata: etiology, symptomatology, and management. *Fertil Steril.* 1981;36:433-445
12. Wallach EE, Vlahos NF. Uterine myomas: an overview of development, clinical features, and management. *Obstet Gynecol.* 2004;104:393-406
13. Cramer SF, Patel A. The frequency of uterine leiomyomas. *Am J Clin Pathol.* 1990;94:435-438
14. Jacoby VL, Fujimoto VY, Giudice LC, Kuppermann M, Washington AE. Racial and ethnic disparities in benign gynecologic conditions and associated surgeries. *Am J Obstet Gynecol.* 2010;202:514-521
15. Baird DD, Dunson DB, Hill MC, Cousins D, Schectman JM. High cumulative incidence of uterine leiomyoma in black and white women: ultrasound evidence. *Am J Obstet Gynecol.* 2003;188:100-107
16. Gupta S, Jose J, Manyonda I. Clinical presentation of fibroids. *Best Pract Res Clin Obstet Gynaecol.* 2008;22:615-626
17. Zimmermann A, Bernuit D, Gerlinger C, Schaefers M, Geppert K. Prevalence, symptoms and management of uterine fibroids: an international internet-based survey of 21,746 women. *BMC Womens Health.* 2012;12:6
18. Parker WH. Etiology, symptomatology, and diagnosis of uterine myomas. *Fertil Steril.* 2007;87:725-736
19. Spies JB, Bradley LD, Guido R, Maxwell GL, Levine BA, Coyne K. Outcomes from leiomyoma therapies: comparison with normal controls. *Obstet Gynecol.* 2010;116:641-652
20. Hartmann KE, Birnbaum H, Ben-Hamadi R, Wu EQ, Farrell MH, Spalding J, Stang P. Annual costs associated with diagnosis of uterine leiomyomata. *Obstet Gynecol.* 2006;108:930-937
21. Flynn M, Jamison M, Datta S, Myers E. Health care resource use for uterine fibroid tumors in the United States. *Am J Obstet Gynecol.* 2006;195:955-964
22. Lee DW, Ozminkowski RJ, Carls GS, Wang S, Gibson TB, Stewart EA. The direct and indirect cost burden of clinically significant and symptomatic uterine fibroids. *J Occup Environ Med.* 2007;49:493-506
23. Munro MG, Critchley HO, Fraser IS. The FIGO classification of causes of abnormal uterine bleeding in the reproductive years. *Fertil Steril.* 2011;95:2204-2208, 2208 e2201-2203
24. Hoellen F, Griesinger G, Bohlmann MK. Therapeutic drugs in the treatment of symptomatic uterine fibroids. *Expert Opin Pharmacother.* 2013;14:2079-2085
25. Levy BS. Modern management of uterine fibroids. *Acta Obstet Gynecol Scand.* 2008;87:812-823
26. Talaulikar VS, Manyonda IT. Ulipristal acetate: a novel option for the medical management of symptomatic uterine fibroids. *Adv Ther.* 2012;29:655-663
27. American College of Obstetricians and Gynecologists. ACOG practice bulletin: Alternatives to hysterectomy in the management of leiomyomas. *Obstet Gynecol.* 2008;112:387-400
28. Perez-Lopez FR, Ornat L, Ceausu I, Depypere H, Erel CT, Lambrinoudaki I, Schenck-Gustafsson K, Simoncini T, Tremollieres F, Rees M. EMAS position statement: Management of uterine fibroids. *Maturitas.* 2014;79:106-116

29. Sankaran S, Manyonda IT. Medical management of fibroids. *Best Pract Res Clin Obstet Gynaecol.* 2008;22:655-676
30. Khan AT, Shehmar M, Gupta JK. Uterine fibroids: current perspectives. *Int J Womens Health.* 2014;6:95-114
31. Leather AT, Studd JW, Watson NR, Holland EF. The prevention of bone loss in young women treated with GnRH analogues with "add-back" estrogen therapy. *Obstet Gynecol.* 1993;81:104-107
32. Beinfeld MT, Bosch JL, Isaacson KB, Gazelle GS. Cost-effectiveness of uterine artery embolization and hysterectomy for uterine fibroids. *Radiology.* 2004;230:207-213
33. Goldberg J, Pereira L. Pregnancy outcomes following treatment for fibroids: uterine fibroid embolization versus laparoscopic myomectomy. *Curr Opin Obstet Gynecol.* 2006;18:402-406
34. Parker WH. Laparoscopic myomectomy and abdominal myomectomy. *Clin Obstet Gynecol.* 2006;49:789-797
35. Gupta JK, Sinha A, Lumsden MA, Hickey M. Uterine artery embolization for symptomatic uterine fibroids. *Cochrane Database Syst Rev.* 2012;5:CD005073
36. Hehenkamp WJ, Volkers NA, Donderwinkel PF, de Blok S, Birnie E, Ankum WM, Reekers JA. Uterine artery embolization versus hysterectomy in the treatment of symptomatic uterine fibroids (EMMY trial): peri- and postprocedural results from a randomized controlled trial. *Am J Obstet Gynecol.* 2005;193:1618-1629
37. Lynn JG, Zwemer RL, Chick AJ, Miller AE. A New Method for the Generation and Use of Focused Ultrasound in Experimental Biology. *J Gen Physiol.* 1942;26:179-193
38. Fry WJ, Barnard JW, Fry EJ, Krumins RF, Brennan JF. Ultrasonic lesions in the mammalian central nervous system. *Science.* 1955;122:517-518
39. Lynn JG, Putnam TJ. Histology of Cerebral Lesions Produced by Focused Ultrasound. *Am J Pathol.* 1944;20:637-649
40. ter Haar GR. High intensity focused ultrasound for the treatment of tumors. *Echocardiography.* 2001;18:317-322
41. Hynynen K, Pomeroy O, Smith DN, Huber PE, McDannold NJ, Kettenbach J, Baum J, Singer S, Jolesz FA. MR imaging-guided focused ultrasound surgery of fibroadenomas in the breast: a feasibility study. *Radiology.* 2001;219:176-185
42. Furusawa H, Namba K, Thomsen S, Akiyama F, Bendet A, Tanaka C, Yasuda Y, Nakahara H. Magnetic resonance-guided focused ultrasound surgery of breast cancer: reliability and effectiveness. *J Am Coll Surg.* 2006;203:54-63
43. Tempany CM, Stewart EA, McDannold N, Quade BJ, Jolesz FA, Hynynen K. MR imaging-guided focused ultrasound surgery of uterine leiomyomas: a feasibility study. *Radiology.* 2003;226:897-905
44. Stewart EA, Gedroyc WM, Tempany CM, Quade BJ, Inbar Y, Ehrenstein T, Shushan A, Hindley JT, Goldin RD, David M, Sklair M, Rabinovici J. Focused ultrasound treatment of uterine fibroid tumors: safety and feasibility of a noninvasive thermoablative technique. *Am J Obstet Gynecol.* 2003;189:48-54
45. Hindley J, Gedroyc WM, Regan L, Stewart E, Tempany C, Hynyen K, Mcdannold N, Inbar Y, Itzchak Y, Rabinovici J, Kim HS, Geschwind JF, Hesley G, Gostout B, Ehrenstein T, Hengst S, Sklair-Levy M, Shushan A, Jolesz F. MRI guidance of focused ultrasound therapy of uterine fibroids: early results. *AJR Am J Roentgenol.* 2004;183:1713-1719
46. Clement GT. Perspectives in clinical uses of high-intensity focused ultrasound. *Ultrasonics.* 2004;42:1087-1093
47. Rabinovici J, Stewart EA. New interventional techniques for adenomyosis. *Best Pract Res Clin Obstet Gynaecol.* 2006;20:617-636
48. Fukunishi H, Funaki K, Sawada K, Yamaguchi K, Maeda T, Kaji Y. Early results of magnetic resonance-guided focused ultrasound surgery of adenomyosis: analysis of 20 cases. *J Minim Invasive Gynecol.* 2008;15:571-579
49. Hurwitz MD, Ghanouni P, Kanaev SV, Iozeffi D, Gianfelice D, Fennessy FM, Kuten A, Meyer JE, LeBlang SD, Roberts A, Choi J, Larner JM, Napoli A, Turkevich VG, Inbar Y, Tempany CM, Pfeffer RM. Magnetic resonance-guided focused ultrasound for patients with painful bone metastases: phase III trial results. *J Natl Cancer Inst.* 2014;106
50. Liberman B, Gianfelice D, Inbar Y, Beck A, Rabin T, Shabshin N, Chander G, Hengst S, Pfeffer R, Chechick A, Hanannel A, Dogadkin O, Catane R. Pain palliation in patients with bone metastases using MR-guided focused ultrasound surgery: a multicenter study. *Ann Surg Oncol.* 2009;16:140-146
51. Crouzet S, Rouviere O, Martin X, Gelet A. High-intensity focused ultrasound as focal therapy of prostate cancer. *Curr Opin Urol.* 2014;24:225-230
52. LiPuma JP, Bryan PJ, Butler HE, Resnick MI. Magnetic resonance imaging of the genitourinary tract. *Urol Clin North Am.* 1986;13:531-550
53. Hynynen K, Darkazanli A, Unger E, Schenck JF. MRI-guided noninvasive ultrasound surgery. *Med Phys.* 1993;20:107-115

54. Quesson B, de Zwart JA, Moonen CT. Magnetic resonance temperature imaging for guidance of thermotherapy. *J Magn Reson Imaging.* 2000;12:525-533
55. O'Brien WD Jr. Ultrasound-biophysics mechanisms. *Prog Biophys Mol Biol.* 2007;93:212-255
56. Clarke RL, ter Haar GR. Temperature rise recorded during lesion formation by high-intensity focused ultrasound. *Ultrasound Med Biol.* 1997;23:299-306
57. Holt RG, Roy RA. Measurements of bubble-enhanced heating from focused, MHz-frequency ultrasound in a tissue-mimicking material. *Ultrasound Med Biol.* 2001;27:1399-1412
58. Arvanitis CD, McDannold N. Integrated ultrasound and magnetic resonance imaging for simultaneous temperature and cavitation monitoring during focused ultrasound therapies. *Med Phys.* 2013;40:112901
59. Apfel RE. Acoustic cavitation: a possible consequence of biomedical uses of ultrasound. *Br J Cancer Suppl.* 1982;5:140-146
60. Khokhlova TD, Canney MS, Lee D, Marro KI, Crum LA, Khokhlova VA, Bailey MR. Magnetic resonance imaging of boiling induced by high intensity focused ultrasound. J *Acoust Soc Am.* 2009;125:2420-2431
61. Melodelima D, Chapelon JY, Theillere Y, Cathignol D. Combination of thermal and cavitation effects to generate deep lesions with an endocavitary applicator using a plane transducer: ex vivo studies. *Ultrasound Med Biol.* 2004;30:103-111
62. Farny CH, Glynn Holt R, Roy RA. The correlation between bubble-enhanced HIFU heating and cavitation power. *IEEE Trans Biomed Eng.* 2010;57:175-184
63. Shaw CJ, ter Haar GR, Rivens IH, Giussani DA, Lees CC. Pathophysiological mechanisms of high-intensity focused ultrasound-mediated vascular occlusion and relevance to non-invasive fetal surgery. *J R Soc Interface.* 2014;11:20140029
64. Hynynen K, Colucci V, Chung A, Jolesz F. Noninvasive arterial occlusion using MRI-guided focused ultrasound. *Ultrasound Med Biol.* 1996;22:1071-1077
65. Hynynen K, Chung AH, Colucci V, Jolesz FA. Potential adverse effects of high-intensity focused ultrasound exposure on blood vessels in vivo. *Ultrasound Med Biol.* 1996;22:193-201
66. Ishikawa T, Okai T, Sasaki K, Umemura S, Fujiwara R, Kushima M, Ichihara M, Ichizuka K. Functional and histological changes in rat femoral arteries by HIFU exposure. *Ultrasound Med Biol.* 2003;29:1471-1477
67. Ichihara M, Sasaki K, Umemura S, Kushima M, Okai T. Blood flow occlusion via ultrasound image-guided high-intensity focused ultrasound and its effect on tissue perfusion. *Ultrasound Med Biol.* 2007;33:452-459
68. Wu F, Chen WZ, Bai J, Zou JZ, Wang ZL, Zhu H, Wang ZB. Tumor vessel destruction resulting from high-intensity focused ultrasound in patients with solid malignancies. *Ultrasound Med Biol.* 2002;28:535-542
69. Fennessy FM, Tempany CM. MRI-guided focused ultrasound surgery of uterine leiomyomas. *Acad Radiol.* 2005;12:1158-1166
70. Salomir R, Palussiere J, Vimeux FC, de Zwart JA, Quesson B, Gauchet M, Lelong P, Pergrale J, Grenier N, Moonen CT. Local hyperthermia with MR-guided focused ultrasound: spiral trajectory of the focal point optimized for temperature uniformity in the target region. *J Magn Reson Imaging.* 2000;12:571-583
71. Mougenot C, Salomir R, Palussiere J, Grenier N, Moonen CT. Automatic spatial and temporal temperature control for MR-guided focused ultrasound using fast 3D MR thermometry and multispiral trajectory of the focal point. *Magn Reson Med.* 2004;52:1005-1015
72. Kohler MO, Mougenot C, Quesson B, Enholm J, Le Bail B, Laurent C, Moonen CT, Ehnholm GJ. Volumetric HIFU ablation under 3D guidance of rapid MRI thermometry. *Med Phys.* 2009;36:3521-3535
73. Kim YS, Keserci B, Partanen A, Rhim H, Lim HK, Park MJ, Köhler MO. Volumetric MR-HIFU ablation of uterine fibroids: role of treatment cell size in the improvement of energy efficiency. *Eur J Radiol.* 2012;81:3652-3659
74. Behera MA, Leong M, Johnson L, Brown H. Eligibility and accessibility of magnetic resonance-guided focused ultrasound (MRgFUS) for the treatment of uterine leiomyomas. *Fertil Steril.* 2010;94:1864-1868
75. Arleo EK, Khilnani NM, Ng A, Min RJ. Features influencing patient selection for fibroid treatment with magnetic resonance-guided focused ultrasound. *J Vasc Interv Radiol.* 2007;18:681-685
76. Zaher S, Gedroyc WM, Regan L. Patient suitability for magnetic resonance guided focused ultrasound surgery of uterine fibroids. *Eur J Obstet Gynecol Reprod Biol. 2009*;143:98-102
77. Al Hilli MM, Stewart EA. Magnetic resonance-guided focused ultrasound surgery. *Semin Reprod Med.* 2010;28:242-249
78. Hesley GK, Gorny KR, Woodrum DA. MR-guided focused ultrasound for the treatment of uterine fibroids. *Cardiovasc Intervent Radiol.* 2013;36:5-13

79. Yoon SW, Lee C, Cha SH, Yu JS, Na YJ, Kim KA, Jung SG, Kim SJ. Patient selection guidelines in MR-guided focused ultrasound surgery of uterine fibroids: a pictorial guide to relevant findings in screening pelvic MRI. *Eur Radiol.* 2008;18:2997-3006
80. Trumm CG, Stahl R, Clevert DA, Herzog P, Mindjuk I, Kornprobst S, Schwarz C, Hoffmann RT, Reiser MF, Matzko M. Magnetic resonance imaging-guided focused ultrasound treatment of symptomatic uterine fibroids: impact of technology advancement on ablation volumes in 115 patients. *Invest Radiol.* 2013;48:359-365
81. Kim YS, Bae DS, Park MJ, Viitala A, Keserci B, Rhim H, Lim HK. Techniques to expand patient selection for MRI-guided high-intensity focused ultrasound ablation of uterine fibroids. *AJR Am J Roentgenol.* 2014;202:443-451
82. Wang W, Wang Y, Wang T, Wang J, Wang L, Tang J. Safety and efficacy of US-guided high-intensity focused ultrasound for treatment of submucosal fibroids. *Eur Radiol.* 2012;22:2553-2558
83. Park H, Yoon SW, Kim KA, Jung Kim D, Jung SG. Magnetic resonance imaging-guided focused ultrasound treatment of pedunculated subserosal uterine fibroids: a preliminary report. *J Vasc Interv Radiol.* 2012;23:1589-1593
84. Smart OC, Hindley JT, Regan L, Gedroyc WG. Gonadotrophin-releasing hormone and magnetic-resonance-guided ultrasound surgery for uterine leiomyomata. *Obstet Gynecol.* 2006;108:49-54
85. Stewart EA, Gostout B, Rabinovici J, Kim HS, Regan L, Tempany CM. Sustained relief of leiomyoma symptoms by using focused ultrasound surgery. *Obstet Gynecol.* 2007;110:279-287
86. Lenard ZM, McDannold NJ, Fennessy FM, Stewart EA, Jolesz FA, Hynynen K, Tempany CM. Uterine leiomyomas: MR imaging-guided focused ultrasound surgery-imaging predictors of success. *Radiology.* 2008;249:187-194
87. LeBlang SD, Hoctor K, Steinberg FL. Leiomyoma shrinkage after MRI-guided focused ultrasound treatment: report of 80 patients. *AJR Am J Roentgenol.* 2010;194:274-280
88. Okada A, Morita Y, Fukunishi H, Takeichi K, Murakami T. Non-invasive magnetic resonance-guided focused ultrasound treatment of uterine fibroids in a large Japanese population: impact of the learning curve on patient outcome. *Ultrasound Obstet Gynecol.* 2009;34:579-583
89. Machtinger R, Inbar Y, Cohen-Eylon S, Admon D, Alagem-Mizrachi A, Rabinovici J. MR-guided focus ultrasound (MRgFUS) for symptomatic uterine fibroids: predictors of treatment success. *Hum Reprod.* 2012;27:3425-3431
90. Morita Y, Ito N, Hikida H, Takeuchi S, Nakamura K, Ohashi H. Non-invasive magnetic resonance imaging-guided focused ultrasound treatment for uterine fibroids - early experience. *Eur J Obstet Gynecol Reprod Biol.* 2008;139:199-203
91. Park MJ, Kim YS, Rhim H, Lim HK. Safety and therapeutic efficacy of complete or near-complete ablation of symptomatic uterine fibroid tumors by MR imaging-guided high-intensity focused US therapy. *J Vasc Interv Radiol.* 2014;25:231-239
92. Spies JB, Coyne K, Guaou Guaou N, Boyle D, Skyrnarz-Murphy K, Gonzalves SM. The UFS-QOL, a new disease-specific symptom and health-related quality of life questionnaire for leiomyomata. *Obstet Gynecol.* 2002;99:290-300
93. Harding G, Coyne KS, Thompson CL, Spies JB. The responsiveness of the uterine fibroid symptom and health-related quality of life questionnaire (UFS-QOL). *Health Qual Life Outcomes.* 2008;6:99
94. Coyne KS, Margolis MK, Bradley LD, Guido R, Maxwell GL, Spies JB. Further validation of the uterine fibroid symptom and quality-of-life questionnaire. *Value Health.* 2012;15:135-142
95. Funaki K, Fukunishi H, Funaki T, Sawada K, Kaji Y, Maruo T. Magnetic resonance-guided focused ultrasound surgery for uterine fibroids: relationship between the therapeutic effects and signal intensity of preexisting T2-weighted magnetic resonance images. *Am J Obstet Gynecol.* 2007;196:184 e181-186
96. Funaki K, Fukunishi H, Funaki T, Kawakami C. Mid-term outcome of magnetic resonance-guided focused ultrasound surgery for uterine myomas: from six to twelve months after volume reduction. *J Minim Invasive Gynecol.* 2007;14:616-621
97. Yamashita Y, Torashima M, Takahashi M, Tanaka N, Katabuchi H, Miyazaki K, Ito M, Okamura H. Hyperintense uterine leiomyoma at T2-weighted MR imaging: differentiation with dynamic enhanced MR imaging and clinical implications. *Radiology.* 1993;189:721-725
98. Swe TT, Onitsuka H, Kawamoto K, Ueyama T, Tsuruchi N, Masuda K. Uterine leiomyoma: correlation between signal intensity on magnetic resonance imaging and pathologic characteristics. *Radiat Med.* 1992;10:235-242
99. Oguchi O, Mori A, Kobayashi Y, Horiuchi A, Nikaido T, Fujii S. Prediction of histopathologic features and proliferative activity of uterine leiomyoma by magnetic resonance imaging prior to GnRH analogue therapy: correlation between T2-weighted images and effect of GnRH analogue. *J Obstet Gynaecol.* 1995;21:107-117
100. Ikink ME, Voogt MJ, Verkooijen HM, Lohle PN, Schweitzer KJ, Franx A, Mali WP, Bartels LW, van den Bosch MA. Mid-term clinical efficacy of a volumetric magnetic resonance-guided high-intensity focused ultrasound technique for treatment of symptomatic uterine fibroids. *Eur Radiol.* 2013;23:3054-3061

# PART I

# CLINICAL TREATMENT EVALUATION

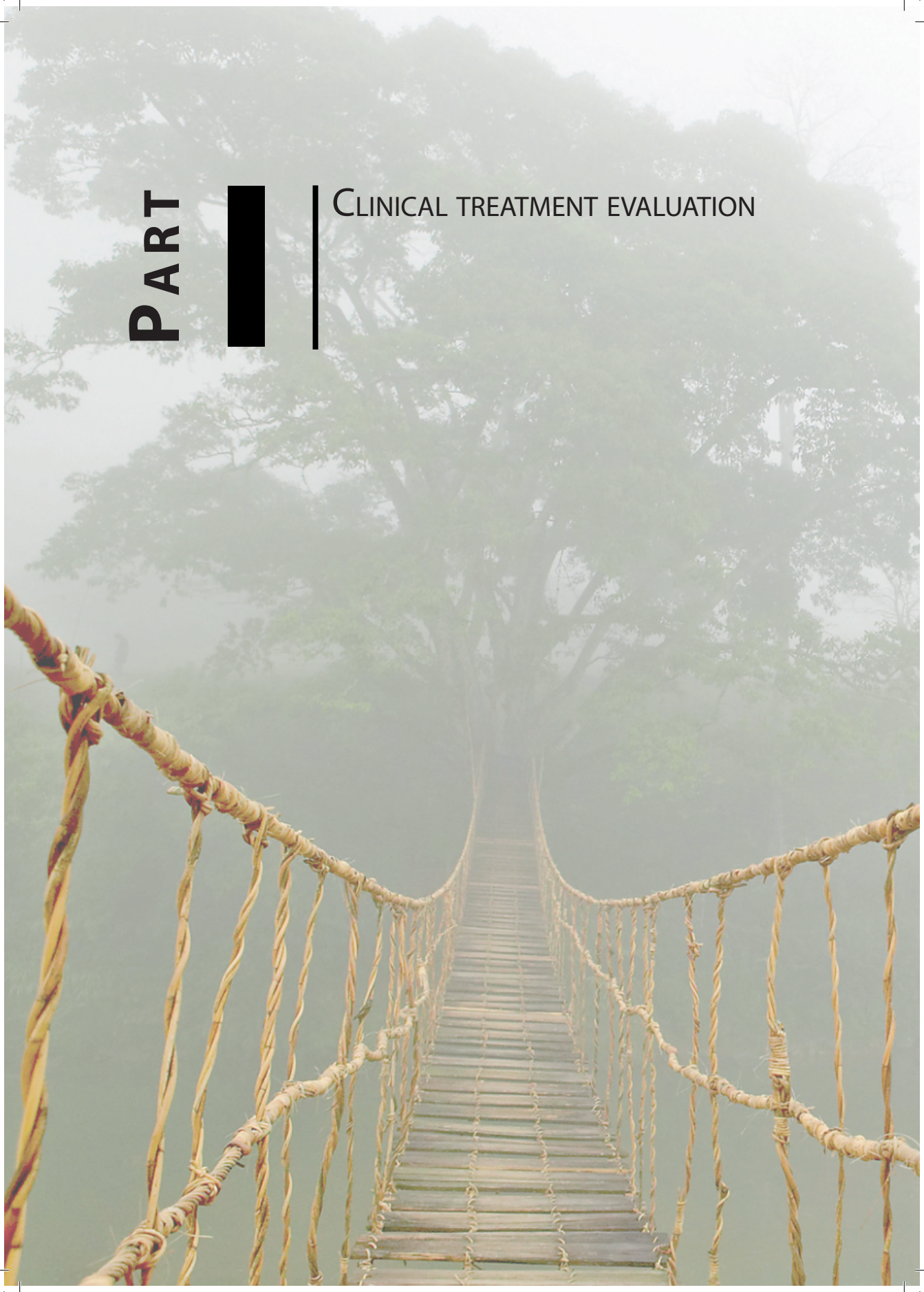

# 2 Mid-term clinical efficacy of a volumetric MR-guided high-intensity focused ultrasound technique for treatment of symptomatic uterine fibroids

Marlijne E. Ikink
Marianne J. Voogt
Helena M. Verkooijen
Paul N.M. Lohle
Karlijn J. Schweitzer
Arie Franx
Willem P.Th.M. Mali
Lambertus W. Bartels
Maurice A.A.J. van den Bosch

*Eur Radiol. 2013;23:3054-3061*

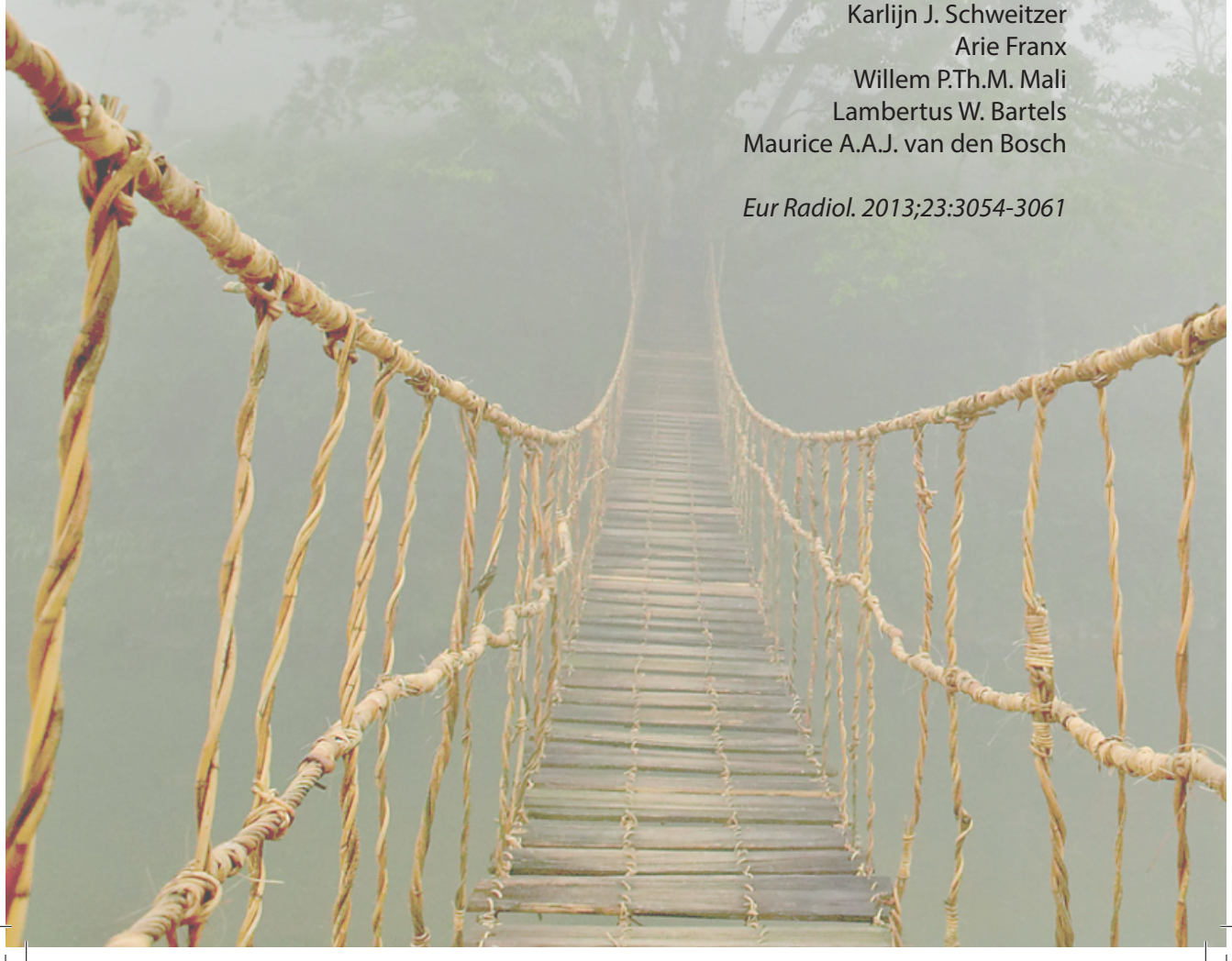

# Abstract

**Objective**

To assess the mid-term efficacy of magnetic resonance-guided high-intensity focused ultrasound (MR-HIFU) using a volumetric ablation technique for treating uterine fibroids.

**Methods**

Forty-six premenopausal women with 58 symptomatic uterine fibroids were prospectively included for MR-HIFU. After treatment, contrast-enhanced T1-weighted magnetic resonance imaging (MRI) allowed measurement of the non-perfused volume (NPV) ratio, defined as the non-enhancing part of the fibroid divided by the fibroid volume. Clinical symptoms and fibroid size on T2-weighted MRI were quantified at 3 and 6 months' follow-up. The primary endpoint was a clinically relevant improvement in the transformed symptom severity score (tSSS) of the Uterine Fibroid Symptom and health-related quality of life questionnaire, defined as a 10-point reduction.

**Results**

Volumetric ablation resulted in a mean NPV ratio of 0.40±0.22, with a mean NPV of 141±135 $cm^3$. The mean fibroid volume was 353±269 $cm^3$ at baseline, which decreased to 271±225 $cm^3$ at 6 months ($p<0.001$), corresponding to a mean volume reduction of 29±20%. Clinical follow-up showed that 54% (25/46) of the patients reported a more than 10-point reduction in the tSSS. Mean tSSS improved from 50.9±18.4 at baseline to 34.7±20.2 after 6 months ($p<0.001$).

**Conclusion**

Volumetric MR-HIFU is effective for patients with symptomatic uterine fibroids. At 6 months, significant symptom improvement was observed in 54% of patients.


## Introduction

Uterine fibroids are benign tumours arising from the uterine myometrium and the accompanying connective tissue of the uterus. Epidemiological data are limited, and prevalence data range from 5% to 20%[1-4]. Although most women are asymptomatic, 25% have symptoms such as menorrhagia and pelvic pain[5,6]. Many therapeutic options are available for treatment of symptomatic uterine fibroids, including medication, endometrial ablation, and myomectomy[7,8]. Traditionally, hysterectomy has been the gold standard therapy, which makes uterine fibroids the leading indication for female pelvic surgery[9,10]. In recent years, less invasive alternatives have been successfully introduced, including uterine artery embolisation (UAE)[11-15]. However, UAE may cause post-embolisation syndrome and is accompanied by hospital admission and recovery periods of up to several weeks[16,17].

Magnetic resonance-guided high-intensity focused ultrasound (MR-HIFU) is a novel non-invasive ablation technique that uses heat generated by convergent ultrasound waves. Multiple focal energy depositions (sonications) are realised by emitting focused ultrasound into the fibroid, causing thermal coagulation and necrosis of treated tissue in the focal zone[18]. The ablations are preferentially performed under magnetic resonance imaging (MRI) for anatomic visualisation, beam guidance, and real-time dynamic thermal monitoring by the proton resonance frequency shift (PRFS) method[19]. This allows the radiologist to change ultrasound power levels depending on the perfusion of the fibroid and to plan sonications such that injury to adjacent vital structures is avoided[20]. Most women undergoing MR-HIFU for symptomatic uterine fibroids reported sustained symptom improvement for up to 24 months after treatment[21-23].

Many recent studies have focused on the conventional 'point-by-point' ablation strategy[24]. In 2009, the European Union approved an MR-HIFU system with volumetric ablation capabilities for the treatment of uterine fibroids. This system uses a volumetric ablation strategy, which utilises treatment cells of various sizes that are realised by rapidly steering the focal spot along concentric circles of increasing diameter. Compared with the conventional 'point-by-point' method, it is expected to be more energy efficient[25], to ablate larger volumes per sonication, and to reduce treatment time. The initial safety and feasibility of this volumetric MR-HIFU technique for the treatment of uterine fibroids has been previously reported[26]. The purpose of this study is to assess the clinical efficacy of volumetric MR-HIFU ablation for the treatment of patients with symptomatic uterine fibroids at 6 months' follow-up.

## Materials and methods

**Patient selection**

Patients were referred to our institute for clinical MR-HIFU treatment of symptomatic uterine fibroids between March 2010 and May 2012. Premenopausal or perimenopausal women, 18 years or older, with symptomatic fibroids referred by a general practitioner or gynaecologist were screened for eligibility. Exclusion criteria included women who wished future fertility, other pelvic diseases (e.g. adenomyosis uteri or pelvic inflammatory disease), extensive abdominal scar tissue, and contraindications for MRI.

Before the procedure, patients underwent a diagnostic pelvic MRI examination on a clinical 1.5-T MRI (Achieva, Philips Healthcare, Best, The Netherlands) in prone position to determine if the fibroids could be treated technically and safely with the MR-HIFU system. T2-weighted (T2w) turbo spin echo MR images were acquired in two orthogonal planes (i.e. axial and sagittal), and T1-weighted (T1w) sequences before and after administration of a gadolinium-based contrast agent (Gadovist® 1.0 mmol/ml, gadobutrol, 0.1 mmol/kg, Bayer Schering Pharma). Patients proceeded to MR-HIFU treatment if there was: (1) a dominant fibroid with a largest diameter ≥ 3 cm and ≤ 12 cm, (2) a maximum of ten fibroids (only the largest dominant fibroid was treated), (3) not more than 8 cm distance from the skin, (4) no evidence of degeneration or calcification in the uterine fibroid[27], (5) no pedunculated fibroids with a stalk base less than 30% of the fibroid volume, (6) no hyper-intense (bright) signal of the fibroid on T2w MRI[28], and (6) an acoustic beam path through the anterior abdominal wall into the fibroid unobstructed by the pubic bone and the bowel. Our local institutional review board approved this study, all patients were counselled on the nature of the procedure, and all provided written informed consent to this treatment.

**MR-HIFU system**

Treatments were performed using a clinical MR-HIFU platform (Sonalleve, Philips Healthcare, Vantaa, Finland) integrated into a 1.5-T MRI (Achieva, Philips Healthcare, Best, The Netherlands), depicted in *Figure 1*. The platform included a 256-channel phased-array HIFU transducer (120 mm in radius; operating at 1.2 or 1.45 megahertz [MHz]) embedded


**Figure 1.** Clinical Sonalleve MR- HIFU platform

in an MR table top, a radiofrequency (RF) generator cabinet, and a dedicated treatment console with a user interface for therapy planning and execution. Volumetric ablations were performed using ellipsoidal treatment cells with an axial (and longitudinal) diameter of 4 (10), 8 (20), 12 (30), and 16 mm (40 mm), equivalent to volumes of 0.08, 0.67, 2.26, and 5.36 ml. Volumetric ablation was achieved by automatically steering the focal point along several concentric circles of increasing diameter, viz. sub-trajectories. The temperature differences during the sonications were calculated from the observed changes in MR signal phase using the PRFS MR thermometry method[29,30].

**MR imaging**

Three-dimensional (3D) T2w turbo spin echo (TSE) and T1w spoiled gradient echo ($T_1$-FFE) MR images were acquired for treatment planning and lesion targeting. The T2w TSE parameters were as follows: repetition time (TR), 1425 ms; echo time (TE), 130 ms; flip angle, 90°; matrix size, 208×179; 133 slices; field of view (FOV), 250 mm×250 mm; slice thickness, 1.50 mm; number of signal averages (NSA), 2. T1w FFE parameters were: TR, 3.6 ms; TE, 1.9 ms; flip angle, 7°; matrix size, 176×157; 120 slices; FOV, 220 mm×240 mm; slice thickness, 1.25 mm; NSA, 8. Immediately after HIFU treatment, a contrast-enhanced (CE) T1w MRI was acquired to visualise the treatment result. The 3D fat suppressed T1w high-resolution isotropic volume examination (THRIVE) sequences were: TR, 5.4 ms; TE, 2.6 ms; flip angle, 10°; matrix size, 168×132; 80 slices; FOV, 250 mm ×250 mm; slice thickness, 1.50 mm; NSA, 4.

**MR-HIFU procedure**

The participants were treated as outpatients with a standardised procedure. After the introduction of an intravenous line and a Foley catheter, the patient was positioned prone on the MR table top, with the dominant fibroid directly above the HIFU transducer. A thin gel pad (20 mm) wetted with some degassed water provided optimal acoustic coupling between the transducer window and the depilated skin of the patient. At the start of the treatment, patients received a benzodiazepine (oxazepam 10 mg orally) and an intravenous analgesic (Voltaren® 25 mg/ml, diclofenacnatrium, maximum dose 75 mg, Navartis Pharma). In the case of breakthrough pain, intravenous administration of a short-acting opioid analgesic was given (Fentanyl-Janssen® 0.05 mg/ml, fentanyl citrate, maximum dose 0.1 mg, Janssen-Cilag B.V.), still allowing communication with the operator. Patients were asked to use the hand-held patient emergency stop button (PESB) if they experienced intolerable pain, discomfort, or anxiety. The vital functions were continuously monitored, and patients were visually observed using a multi-camera observation system. During treatment planning, the ultrasound beam was projected onto the MR images. Sensitive structures (i.e. bowel, bladder with catheter, pubic bone, spinal column, and sacral nerve) were identified and kept out of the HIFU beam path. The power level used for the therapeutic sonications (range 60-200 Watt [W]) was based on the observed temperature increase realised using a small low-power test sonication (40 W), which was also used to confirm the system's geometrical accuracy. When the temperature reached a certain predefined threshold (55-60°C) during the ablation of a sub-trajectory, the treatment point moved to the next sub-trajectory. Further technical details and feasibility of the system have been published elsewhere[25,26]. During ablations, colour temperature maps were acquired to allow the practitioner to monitor the heating in a sagittal and a coronal slice through the focus, and in coronal slices positioned in the

near field close to the skin and in the far field near the spinal column. The choice of size, location, and number of treatment cells was made according to the experience of the practitioner, depending on the volume of the targeted fibroid. Generally, treatment was started by placing 16 mm treatment cells (or the largest possible) in the centre of the fibroid, while smaller cells were used to treat the outer parts of the tumour. The volume that was successfully treated was defined as the non-perfused volume (NPV), i.e. the non-enhancing part of the fibroid on the CE-T1w MRI. Patients were observed for about 1 hour and then discharged home guided by a relative.

**Data collection**

The primary endpoint of the study was a clinically significant improvement in the transformed symptom severity score (tSSS) as assessed using the disease-specific uterine fibroid symptom and health-related quality of life (UFS-QoL) questionnaire[31], obtained at baseline and 1, 3, and 6 months after treatment. Based on previous research it has been suggested that a 10-point reduction in the tSSS can be considered clinically relevant[21,32,33]. Adverse events (AEs) were recorded and classified according to the Society of Interventional Radiology classification[34]. Details recorded with respect to the duration of the MR-HIFU treatment procedure were (1) room time, which included preparation time and treatment duration, defined as the time in between the moment the patient entered the HIFU room and the moment she went out and (2) treatment time, defined as the time from the start of the first to the end of the last sonication. Total treatment time was limited to 180 minutes (min) or adapted according to patient tolerance. Volume changes of the treated fibroids were assessed during follow-up, using volumes determined before treatment and after 3 and 6 months on T2w MRI. All volumes were measured by summing the volumes circumscribed by contour segmentations of all individual slices (sum-of-slice method).



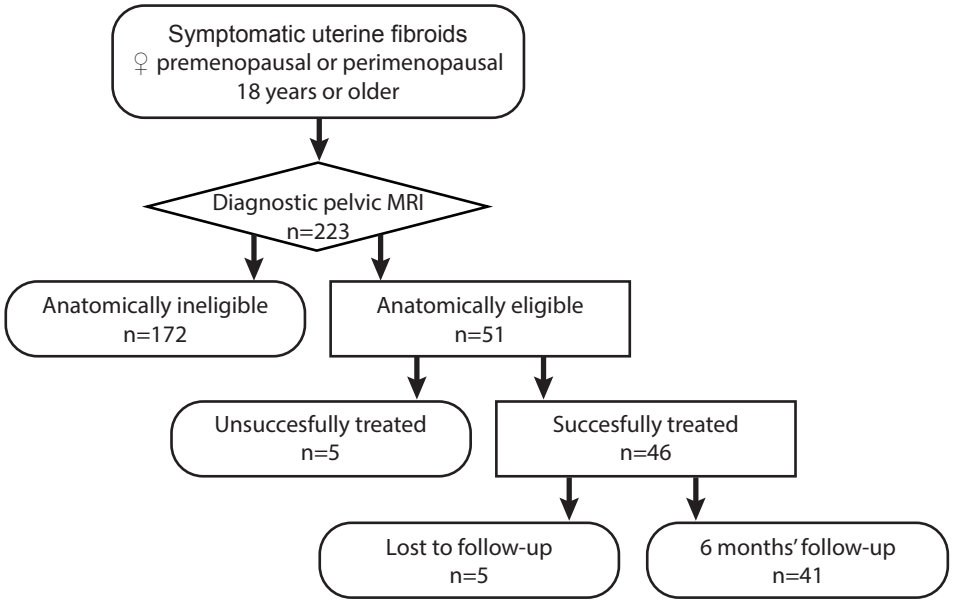


**Figure 2.** Study inclusion

**Table 1.** Characteristics of patients eligible for MR-HIFU (n=46)

| Characteristics | Value |
|---|---|
| Age (years)[a] | 45.3±4.1 |
| BMI (kg/m$^2$)[a] | 23.4±2.9 |
| Ethnicity[b] | |
| Caucasian | 39 (85%) |
| South American | 4 (9%) |
| African | 2 (4%) |
| Asian | 1 (2%) |
| Current medication for uterine fibroids[b] | |
| None | 25 (54%) |
| Oral contraception | 13 (28%) |
| Mirena IUD | 5 (11%) |
| Depo-provera | 1 (2%) |
| Homeopathy | 3 (7%) |
| Earlier treatments for uterine fibroids[b] | |
| None | 32 (70%) |
| Oral contraception | 8 (17%) |
| Mirena IUD | 4 (9%) |
| Progesterone | 2 (4%) |
| GnRH agonist | 1 (2%) |
| NSAIDs | 1 (2%) |
| HIFU | 4 (9%) |
| UAE | 1 (2%) |
| Myomectomy | 2 (4%) |
| Homeopathy | 3 (6%) |
| Symptoms[b] | |
| Bloating | 40 (87%) |
| Frequent urination | 35 (76%) |
| Abdominal pain | 32 (70%) |
| Menorrhagia | 32 (70%) |
| Constipation | 20 (43%) |
| Number of fibroids (per patient)[b] | |
| Solitary fibroid | 10 (22%) |
| Multiple fibroids | 36 (78%) |
| 2-5 fibroids | 28 (78%) |
| 6-10 fibroids | 8 (22%) |
| Location of the fibroids[b] | |
| Intramural | 37 (64%) |
| Subserosal | 14 (24%) |
| Submucosal | 6 (10%) |
| Pedunculated | 1 (2%) |

[a]Mean ± standard deviation; [b]number (percentage); BMI, body mass index; IUD, intrauterine device; GnRH, gonadotropin-releasing hormone; NSAIDs, non-steroidal anti-inflammatory drugs; HIFU, high-intensity focused ultrasound; UAE, uterine artery embolisation

**Statistical analysis**

A retrospective analysis of prospectively collected data was performed. Categorical data are presented as frequency and proportions; for continuous data the mean and standard deviation are reported. In order to evaluate the changes in fibroid volume and UFS-QoL within subjects over time, a one-way repeated measures analysis of variance with pairwise comparisons was used. Tests of the 27 a priori hypotheses were conducted using Bonferroni adjusted alpha levels of 0.0019 per test (0.05/27). Statistical analyses were performed using IBM SPSS Statistics, version 20.0 (Armonk, New York, USA).

## Results

Two hundred twenty-three (n=223) women were referred for MR-HIFU treatment and screened with MRI (*Figure 2*). Fifty-one patients (23%) were considered anatomically eligible and underwent MR-HIFU ablation. The remaining 172 women (77%) were excluded, for example as a result of obstructed beam path (n=50), unsuitable fibroid size (n=20), number (n=34), type (n=31), location (n=10), lack of contrast enhancement (n=9), or other causes (n=18). Forty-six patients were successfully treated with MR-HIFU (*Table 1*). Bloating and frequent urination were the most commonly reported symptoms. Twelve women had two uterine fibroids ablated during the same session, so in total 58 fibroids were treated, most of which were located intramurally (64%). Four patients underwent the treatment twice because of insufficient symptom improvement after a complete first 6 months' follow-up; in total 46 patients underwent 50 interventions. Immediately after treatment, the mean NPV was 141±135 $cm^3$, which corresponded to 40±22% of the fibroid volume treated. The mean room time amounted to 234±54 min; the treatment time was 148±53 min.

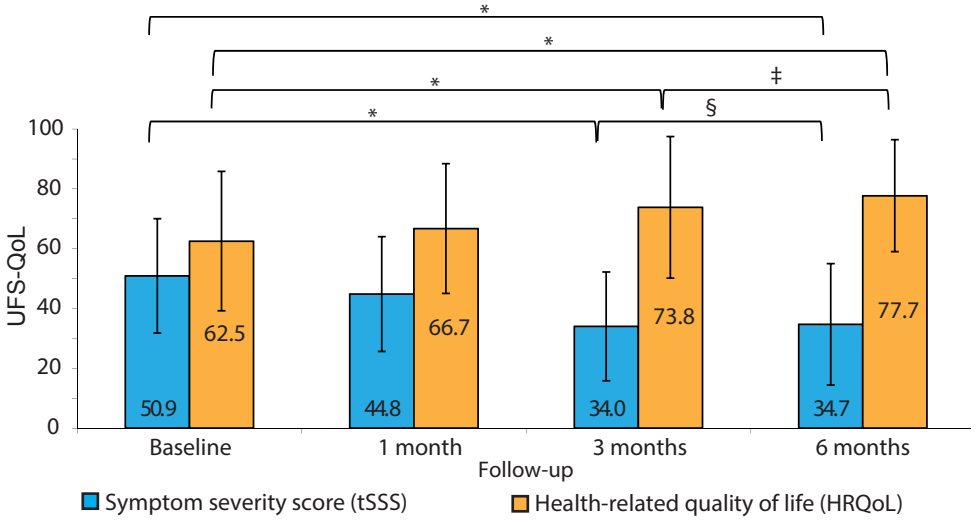


**Figure 3.** Uterine fibroid symptom and quality of life (UFS-QoL) scores before treatment (baseline), and at 3 and 6 months' follow-up. Error bars represent the standard deviation.
* p<0.001; ‡ p=0.084; § p=0.734

**Table 2.** Changes in uterine fibroid symptom and quality of life (UFS-QoL) scores

| | BL | 1MFU | 3MFU | Δ | p | 6MFU | Δ | p |
|---|---|---|---|---|---|---|---|---|
| tSSS | 50.9±18.4 | 44.8±18.7 | 34.0±18.1 | -16.9 | <0.001 | 34.7±20.2 | -16.2 | <0.001 |
| Total HRQoL* | 62.5±22.9 | 66.7±21.4 | 73.8±23.2 | +11.3 | <0.001 | 77.7±18.1 | +15.2 | <0.001 |
| Concern | 64.0±27.2 | 64.9±26.9 | 73.2±24.8 | +9.2 | =0.011 | 78.6±20.1 | +14.6 | <0.001 |
| Activities | 65.2±25.3 | 70.4±24.8 | 76.8±24.5 | +11.6 | <0.001 | 79.3±21.1 | +14.1 | <0.001 |
| Energy/mood | 59.8±30.9 | 65.3±25.7 | 72.1±27.1 | +12.3 | <0.001 | 74.8±24.3 | +15.0 | <0.001 |
| Control | 68.3±26.3 | 70.7±25.0 | 75.9±22.5 | +7.6 | =0.014 | 78.7±22.5 | +10.3 | =0.002 |
| Self-consciousness | 50.9±26.6 | 55.6±25.6 | 68.7±27.2 | +17.8 | <0.001 | 69.8±26.1 | +18.9 | <0.001 |
| Sexual Function* | 68.2±30.9 | 73.5±27.6 | 76.5±26.2 | +8.3 | =0.053 | 78.6±29.5 | +10.4 | =0.013 |

Values expressed in mean ± standard deviation; tSSS, transformed symptom severity score; HRQoL, health-related quality of life; BL, baseline; MFU, months' follow-up; Δ, change from baseline; * n=38, due to missing data



Five patients with six uterine fibroids did not complete the 6 months' follow-up. These patients were not satisfied with the treatment result and sought additional treatment after MR-HIFU ablation. Two patients underwent surgery (hysterectomy), and two patients received uterine artery embolisation. One patient withdrew from further follow-up; unfortunately, we were not able to acquire additional information. Of 41 patients, the mean volume of the uterine fibroids at baseline was 353±269 $cm^3$. At 3 and 6 months' follow-up, the mean fibroid volume had decreased significantly to 289±232 ($p<0.001$) and 271±225 $cm^3$ ($p<0.001$), respectively. This corresponds to a fibroid volume reduction of 22±15% and 29±20%, respectively. Clinical follow-up showed that 54% (25/46) of the patients achieved more than a 10-point reduction in the tSSS assessed using the UFS-QoL questionnaire. The mean tSSS improved from 50.9±18.4 at baseline to 34.7±20.2 after 6 months ($p<0.001$). In addition to symptom severity, a significant change in all HRQoL subscales[31] was demonstrated at 6 months' follow up. The UFS-QoL scores before treatment (baseline) and at 1, 3, and 6 months after MR-HIFU ablation are presented in *Table 2*. Changes in endpoints occurred especially within 3 months after treatment and remained stable up to 6 months' follow-up. Distributions of changes in UFS-QoL scores are depicted in *Figure 3*. No serious complications or AEs were described during treatment and follow-up. The most common symptoms during the procedure were lower abdominal heat, nausea, back pain, and referred leg pain. Two patients reported first-degree skin burns that were adequately treated with conservative management.

## Discussion

This is the first study assessing the 6 month clinical outcome of volumetric MR-HIFU ablation of uterine fibroids. The volumetric HIFU ablation approach resulted in a mean NPV ratio of 0.40, with a NPV of 141 $cm^3$, within 148 minutes of treatment time. Factors that restricted entire fibroid ablation included time limitations, obstruction of the ultrasound beam (by bone, bowels, or abdominal scars) of peripheral fibroid areas, non-responsive hypervascular fibroids, or too deep location of the fibroid. Nevertheless, the results of this prospective study demonstrate that non-invasive volumetric MR-HIFU treatment leads to fibroid-related clinical symptom improvement in most (54%) of the treated patients. At 6 months, a mean fibroid volume reduction of 29% was seen, resulting in a significant improvement of clinical symptoms of 16.2 points from a mean tSSS of 50.9±18.4 at baseline to 34.7±20.2 after 6 months' follow-up. The total HRQoL score improved by 15.2 points at 6 months post-treatment, altering from 62.5±22.9 to 77.7±18.1 points. This clinical efficacy was determined by a validated questionnaire that assesses symptom severity and disease-specific quality of life in patients with uterine fibroids, the primary outcome measure used after MR-HIFU treatment. A larger cohort of patients will be required to perform sub-analyses and assess the outcome of MR-HIFU treatment in relation to the category of symptoms, i.e. the difference in outcome between patients with menorrhagia and those with bulk-related symptoms. Currently, all symptoms were measured together in a single symptom severity score. Additional questions arise whether other factors influence the treatment outcomes after MR-HIFU ablation. These factors include genetic, hormonal, medical uses, and tissue growth factor variations. Further studies addressing these questions will provide important information for optimising treatment efficacy.

The current results are based on all MR-HIFU treatments done in our hospital, including the first treatments where just relatively small volumes of the fibroids were ablated. We experienced that with increasing expertise, higher ablation volumes were achieved in time. This means that our results are partly a reflection of a learning curve for this new technique[35]. An already accepted minimally invasive therapy of symptomatic uterine fibroids is uterine artery embolisation[36]. In our study, the mean volume reduction of the treated fibroids is less than those reported in UAE studies. Following a technically successful bilateral embolisation, 6 months volume reductions are described ranging between 30% and 45%[16,37,38]. Data from UAE suggests that complete devascularisation is important for long-term success[13]. In addition, Leblang *et al*.[22] described larger thermal ablation volumes resulting in greater fibroid volume reduction and symptom improvement. With some adjustments to the treatment protocol, larger ablation volumes may be achieved with MR-HIFU. As scar tissue absorbs the acoustic energy and air in the bowels causes reflection of the ultrasound beam, abdominal scars and intermediate bowel loops may influence the propagation of ultrasound waves and were therefore identified as exclusion criteria for MR-HIFU treatment[39]. Increased absorption of ultrasound energy may lead to either skin or scar burns. By direct visualisation of the scar with paramagnetic contrast fluid[40], complete avoidance of the scar could be accomplished through various techniques, including bladder filling to raise the uterus above the scar and angulation of the beam. In addition, the scar tissue can be protected by placing acoustic reflector materials between the ultrasound transducer and the skin[41]. Zhang *et al*.[42] published a technique that displaced the bowels out of the pelvis by using a water balloon compressed against the anterior abdominal wall. Recent studies[43,44] described the use of urinary bladder filling (with saline) and rectal filling (with ultrasound gel) in order to avoid scars and bowel loops

in the acoustic beam path. Such techniques and experiences may further enhance the efficacy of MR-HIFU in the future.

The volumetric sonication approach was expected to result in faster HIFU treatment and larger homogeneous ablation volumes of up to 5.4 ml per treatment cell. The mean duration of our treatments was 148 min. The treatment time of several clinical trials that appointed an actual time ranged from 27-390 min, with an average of 3 hours[42,45-50]. Lénárd *et al*.[45] is the only group that realised shorter treatment times (123 min, range 75-180 min), but at the same time achieved significantly lower NPV ratios. This leads to the preliminary conclusion that volumetric ablation effectively shortens the 'in-bore' treatment time. This conclusion is supported by the findings in a study by Kim *et al*.[51], in which volumetric MR-HIFU ablation was used with a one-layer strategy for treatment of large uterine fibroids. Worth mentioning is that most hospitals performed the HIFU treatment under intravenous sedation (e.g. with use of midazolam), which reduced the need for communication with the patient considerably. This could further shorten the duration of the treatment, as less time is needed to reassure the patient.



Previously we reported on the safety of the Sonalleve MR-HIFU system[26]. Only minor adverse events were mentioned during the procedure, such as abdominal tenderness, malaise, or first-degree skin burns. In general, these complaints almost immediately disappeared after treatment. In order to achieve faster recovery, patients were advised to rest a few days. Patients could resume their daily activities after an average of 3-4 days. However, mostly because of the rather strict safety measures, only 40% of the fibroid volume was treated, with a corresponding mean of 29% volume reduction at the 6 months' follow-up period. Assuming treatment failure in those lost to follow-up - 5 patients (10%) received elective treatment for failed symptom control - most of our patients had persistent symptom relief. A possible clarification may be that other factors also affect the clinical treatment result after MR-HIFU. Recent studies demonstrated an altered expression of vasoactive growth factors or growth factor receptors in leiomyomatous myometrium[2,52]. This led to the hypothesis that a thermal stimulus causes endothelial damage of the vessel, resulting in dysregulation of these growth factors and thus inhibiting angiogenesis. Finally, there are several limitations of the present study. First, this is a small single-centre prospective non-randomised study that followed safety instructions by the manufacturer. There is no control group to assess the impact of a treatment, and biases may be present in the patient selection. Second, overall, we obtained a relatively low mean NPV ratio (0.40). The consensus by physicians performing this procedure is that a larger NPV ratio correlates to improved therapeutic outcomes.

In conclusion, volumetric MR-HIFU has great potential in patients with symptomatic uterine fibroids. This study shows that at 6 months, significant symptom improvement was obtained in 54% of the patients. A randomised controlled trial comparing MR-HIFU with another treatment technique, such as UAE, is required to set this new ablation technique in an appropriate context relative to other more established therapies.

## Acknowledgements

We would like to thank the technicians of the Department of Radiology for their help during the treatment procedure, in particular Niels Blanken, Greet Bouwman, Jørgen H. Mensinga, and Laura J.L. Gortzak-Mol. Further, we would like to thank Karin A. van Rijnbach, photography University Medical Center Utrecht, for providing *Figure 1*.

# References


1. Borgfeldt C, Andolf E. Transvaginal ultrasonographic findings in the uterus and the endometrium: low prevalence of leiomyoma in a random sample of women age 25-40 years. *Acta Obstet Gynecol Scand.* 2000;79:202-207
2. Buttram VC Jr, Reiter RC. Uterine leiomyomata: etiology, symptomatology, and management. *Fertil Steril.* 1981;36:433-445
3. Payson M, Leppert P, Segars J. Epidemiology of myomas. *Obstet Gynecol Clin North Am.* 2006;33:1-11
4. Walker CL, Stewart EA. Uterine fibroids: the elephant in the room. *Science.* 2005;308:1589–1592
5. Parker WH. Etiology, symptomatology, and diagnosis of uterine myomas. *Fertil Steril.* 2007;87:725-736
6. Stewart EA. Uterine fibroids. *Lancet.* 2001;357:293-298
7. Parker WH. Uterine myomas: management. *Fertil Steril.* 2007;88:255-271
8. Somigliana E, Vercellini P, Daguati R, Pasin R, De Giorgi O, Crosignani PG. Fibroids and female reproduction: a critical analysis of the evidence. *Hum Reprod Update.* 2007;13:465-476
9. Carlson KJ, Nichols DH, Schiff I. Indications for hysterectomy. *N Engl J Med.* 1993;328:856-860
10. Merrill RM. Hysterectomy surveillance in the United States, 1997 through 2005. *Med Sci Monit.* 2008;14:CR24-CR31
11. Broder MS, Goodwin S, Chen G, Tang LJ, Costantino MM, Nguyen MH, Yegul TN, Erberich H. Comparison of long-term outcomes of myomectomy and uterine artery embolization. *Obstet Gynecol.* 2002;100:864-868
12. Edwards RD, Moss JG, Lumsden MA, Wu O, Murray LS, Twaddle S, Murray GD; Committee of the Randomized Trial of Embolization versus Surgical Treatment for Fibroids. Uterine-artery embolization versus surgery for symptomatic uterine fibroids. *N Engl J Med.* 2007;356:360-370
13. Lohle PN, Voogt MJ, de Vries J, Smeets AJ, Vervest HA, Lampmann LE, Boekkooi PF. Long-term outcome of uterine artery embolization for symptomatic uterine leiomyomas. *J Vasc Interv Radiol.* 2008;19:319-326
14. Lumsden MA. Embolization versus myomectomy versus hysterectomy: which is best, when? *Hum Reprod.* 2002;17:253-259
15. Pinto I, Chimeno P, Romo A, Paúl L, Haya J, de la Cal MA, Bajo J. Uterine fibroids: uterine artery embolization versus abdominal hysterectomy for treatment - a prospective, randomized, and controlled clinical trial. *Radiology.* 2003;226:425-431
16. Pron G, Bennett J, Common A, Wall J, Asch M, Sniderman K; Ontario Uterine Fibroid Embolization Collaboration Group. The Ontario Uterine Fibroid Embolization Trial. Part 2. Uterine fibroid reduction and symptom relief after uterine artery embolization for fibroids. *Fertil Steril.* 2003;79:120-127
17. Spies JB, Spector A, Roth AR, Baker CM, Mauro L, Murphy-Skrynarz K. Complications after uterine artery embolization for leiomyomas. *Obstet Gynecol.* 2002;100:873-880
18. Tempany CM, Stewart EA, McDannold NJ, Quade BJ, Jolesz FA, Hynynen K. MR imaging-guided focused ultrasound surgery of uterine leiomyomas: a feasibility study. *Radiology.* 2003;226:897-905
19. Ishihara Y, Calderon A, Watanabe H, Okamoto K, Suzuki Y, Kuroda K, Suzuki Y. A precise and fast temperature mapping using water proton chemical shift. *Magn Reson Med.* 1995;34:814-823
20. McDannold NJ, Tempany CM, Fennessy FM, So MJ, Rybicki FJ, Stewart EA, Jolesz FA, Hynynen K. Uterine leiomyomas: MR imaging-based thermometry and thermal dosimetry during focused ultrasound thermal ablation. *Radiology.* 2006;240:263-272
21. Fennessy FM, Tempany CM, McDannold NJ, So MJ, Hesley G, Gostout B, Kim HS, Holland GA, Sarti DA, Hynynen K, Jolesz FA, Stewart EA. Uterine leiomyomas: MR imaging-guided focused ultrasound surgery–results of different treatment protocols. *Radiology.* 2007;243:885-893
22. LeBlang SD, Hoctor K, Steinberg FL. Leiomyoma shrinkage after MRI-guided focused ultrasound treatment: report of 80 patients. *AJR Am J Roentgenol.* 2010; 194:274-280
23. Stewart EA, Gostout B, Rabinovici J, Kim HS, Regan L, Tempany CM. Sustained relief of leiomyoma symptoms by using focused ultrasound surgery. *Obstet Gynecol.* 2007;110:279-287
24. Hesley GK, Gorny KR, Henrichsen TL, Woodrum DA, Brown DL. A clinical review of focused ultrasound ablation with magnetic resonance guidance: an option for treating uterine fibroids. *Ultrasound Q.* 2008;24:131-139
25. Kohler MO, Mougenot C, Quesson B, Enholm J, Le Bail B, Laurent C, Moonen CT, Ehnholm GJ. Volumetric HIFU ablation under 3D guidance of rapid MRI thermometry. *Med Phys.* 2009;36:3521-3535
26. Voogt MJ, Trillaud H, Kim YS, Mali WP, Barkhausen J, Bartels LW, Deckers R, Frulio N, Rhim H, Lim HK, Eckey T, Nieminen HJ, Mougenot C, Keserci B, Soini J, Vaara T, Köhler MO, Sokka S, van den Bosch MA. Volumetric feedback ablation of uterine fibroids using magnetic resonance-guided high intensity focused ultrasound therapy. *Eur Radiol.* 2012;22:411-417

27. Fennessy FM, Tempany CM. MRI-guided focused ultrasound surgery of uterine leiomyomas. *Acad Radiol.* 2005;12:1158-1166
28. Funaki K, Fukunishi H, Funaki T, Sawada K, Kaji Y, Maruo T. Magnetic resonance-guided focused ultrasound surgery for uterine fibroids: relationship between the therapeutic effects and signal intensity of preexisting T2-weighted magnetic resonance images. *Am J Obstet Gynecol.* 2007;196:184-186
29. Mougenot C, Quesson B, de Senneville BD, de Oliveira PL, Sprinkhuizen S, Palussière J, Grenier N, Moonen CT. Three-dimensional spatial and temporal temperature control with MR thermometry-guided focused ultrasound (MRgHIFU). *Magn Reson Med.* 2009;61:603-614
30. Rieke V, Butts PK. MR thermometry. *J Magn Reson Imaging.* 2008;27:376-390
31. Spies JB, Coyne K, Guaou Guaou N, Boyle D, Skyrnarz-Murphy K, Gonzalves SM. The UFS-QOL, a new disease-specific symptom and health-related quality of life questionnaire for leiomyomata. *Obstet Gynecol.* 2002;99:290-300
32. Hindley J, Gedroyc WM, Regan L, Stewart E, Tempany C, Hynyen K, McDannold NJ, Inbar Y, Itzchak Y, Rabinovici J, Kim HS, Geschwind JF, Hesley G, Gostout B, Ehrenstein T, Hengst S, Sklair-Levy M, Shushan A, Jolesz F. MRI guidance of focused ultrasound therapy of uterine fibroids: early results. *AJR Am J Roentgenol.* 2004;183:1713-1719
33. Stewart EA, Rabinovici J, Tempany CM, Inbar Y, Regan L, Gostout B, Hesley G, Kim HS, Hengst S, Gedroyc WM. Clinical outcomes of focused ultrasound surgery for the treatment of uterine fibroids. *Fertil Steril.* 2006;85:22-29
34. Hovsepian DM, Siskin GP, Bonn J, Cardella JF, Clark TW, Lampmann LE, Miller DL, Omary RA, Pelage JP, Rajan D, Schwartzberg MS, Towbin RB, Walker WJ, Sacks D; CIRSE and SIR Standards of Practice Committees. Quality improvement guidelines for uterine artery embolization for symptomatic leiomyomata. *J Vasc Interv Radiol.* 2009;20:S193-S199
35. Okada A, Morita Y, Fukunishi H, Takeichi K, Murakami T. Non-invasive magnetic resonance-guided focused ultrasound treatment of uterine fibroids in a large Japanese population: impact of the learning curve on patient outcome. *Ultrasound Obstet Gynecol.* 2009;34:579-583
36. van der Kooij SM, Hehenkamp WJ, Volkers NA, Birnie E, Ankum WM, Reekers JA. Uterine artery embolization vs hysterectomy in the treatment of symptomatic uterine fibroids: 5-year outcome from the randomized EMMY trial. *Am J Obstet Gynecol.* 2010;203:105-113
37. Brunereau L, Herbreteau D, Gallas S, Cottier JP, Lebrun JL, Tranquart F, Fauchier F, Body G, Rouleau P. Uterine artery embolization in the primary treatment of uterine leiomyomas: technical features and prospective follow-up with clinical and sonographic examinations in 58 patients. *AJR Am J Roentgenol.* 2000;175:1267-1272
38. Gupta JK, Sinha AS, Lumsden MA, Hickey M. Uterine artery embolization for symptomatic uterine fibroids. *Cochrane Database Syst Rev.* 2006;25:CD005073
39. Arleo EK, Khilnani NM, Ng A, Min RJ. Features influencing patient selection for fibroid treatment with magnetic resonance-guided focused ultrasound. *J Vasc Interv Radiol.* 2007;18:681-685
40. Zaher S, Gedroyc W, Lyons D, Regan L. A novel method to aid in the visualisation and treatment of uterine fibroids with MRgFUS in patients with abdominal scars. *Eur J Radiol.* 2010;76:269-273
41. Gorny KR, Chen S, Hangiandreou NJ, Hesley GK, Woodrum DA, Brown DL, Felmlee JP. Initial evaluation of acoustic reflectors for the preservation of sensitive abdominal skin areas during MRgFUS treatment. *Phys Med Biol.* 2009;54:N125-N133
42. Zhang L, Chen WZ, Liu YJ, Hu X, Zhou K, Chen L, Peng S, Zhu H, Zou HL, Bai J, Wang ZB. Feasibility of magnetic resonance imaging-guided high intensity focused ultrasound therapy for ablating uterine fibroids in patients with bowel lies anterior to uterus. *Eur J Radiol.* 2010;73:396-403
43. Park MJ, Kim YS, Keserci B, Rhim H, Lim HK. Volumetric MR-guided high-intensity focused ultrasound ablation of uterine fibroids: treatment speed and factors influencing speed. *Eur Radiol.* 2013;23:943-950
44. Trumm CG, Stahl R, Clevert DA, Herzog P, Mindjuk I, Kornprobst S, Schwarz C, Hoffmann RT, Reiser MF, Matzko M. Magnetic resonance imaging-guided focused ultrasound treatment of symptomatic uterine fibroids: impact of technology advancement on ablation volumes in 115 patients. *Invest Radiol.* 2013;48:359-365
45. Lenard ZM, McDannold NJ, Fennessy FM, Stewart EA, Jolesz FA, Hynynen K, Tempany CM. Uterine leiomyomas: MR imaging-guided focused ultrasound surgery–imaging predictors of success. *Radiology.* 2008;249:187-194
46. Mikami K, Murakami T, Okada A, Osuga K, Tomoda K, Nakamura H. Magnetic resonance imaging-guided focused ultrasound ablation of uterine fibroids: early clinical experience. *Radiat Med.* 2008;26:198-205
47. Rabinovici J, Inbar Y, Revel A, Zalel Y, Gomori JM, Itzchak Y, Schiff E, Yagel S. Clinical improvement and shrinkage of uterine fibroids after thermal ablation by magnetic resonance-guided focused ultrasound surgery. *Ultrasound Obstet Gynecol.* 2007;30:771-777
48. Smart OC, Hindley JT, Regan L, Gedroyc WG. Gonadotrophin-releasing hormone and magnetic-resonance-guided ultrasound surgery for uterine leiomyomata. *Obstet Gynecol*. 2006;108:49-54

49. Funaki K, Fukunishi H, Sawada K. Clinical outcomes of magnetic resonance-guided focused ultrasound surgery for uterine myomas: 24-month follow-up. *Ultrasound Obstet Gynecol.* 2009;34:584-589
50. Smart OC, Hindley JT, Regan L, Gedroyc WM. Magnetic resonance guided focused ultrasound surgery of uterine fibroids–the tissue effects of GnRH agonist pre-treatment. *Eur J Radiol.* 2006;59:163-167
51. Kim YS, Kim JH, Rhim H, Lim HK, Keserci B, Bae DS, Kim BG, Lee JW, Kim TJ, Choi CH. Volumetric MR-guided high-intensity focused ultrasound ablation with a one-layer strategy to treat large uterine fibroids: initial clinical outcomes. *Radiology.* 2012;263:600-609
52. Stewart EA, Nowak RA. Leiomyoma-related bleeding: a classic hypothesis updated for the molecular era. *Hum Reprod Update.* 1996;2:295-306

# 3 Volumetric MR-guided high-intensity focused ultrasound versus uterine artery embolisation for treatment of symptomatic uterine fibroids: comparison of symptom improvement and reintervention rates

Marlijne E. Ikink
Robbert J. Nijenhuis
Helena M. Verkooijen
Marianne J. Voogt
Paul J.H.M. Reuwer
Albert J. Smeets
Paul N.M. Lohle
Maurice A.A.J. van den Bosch

*Eur Radiol. 2014;24:2649-2657*

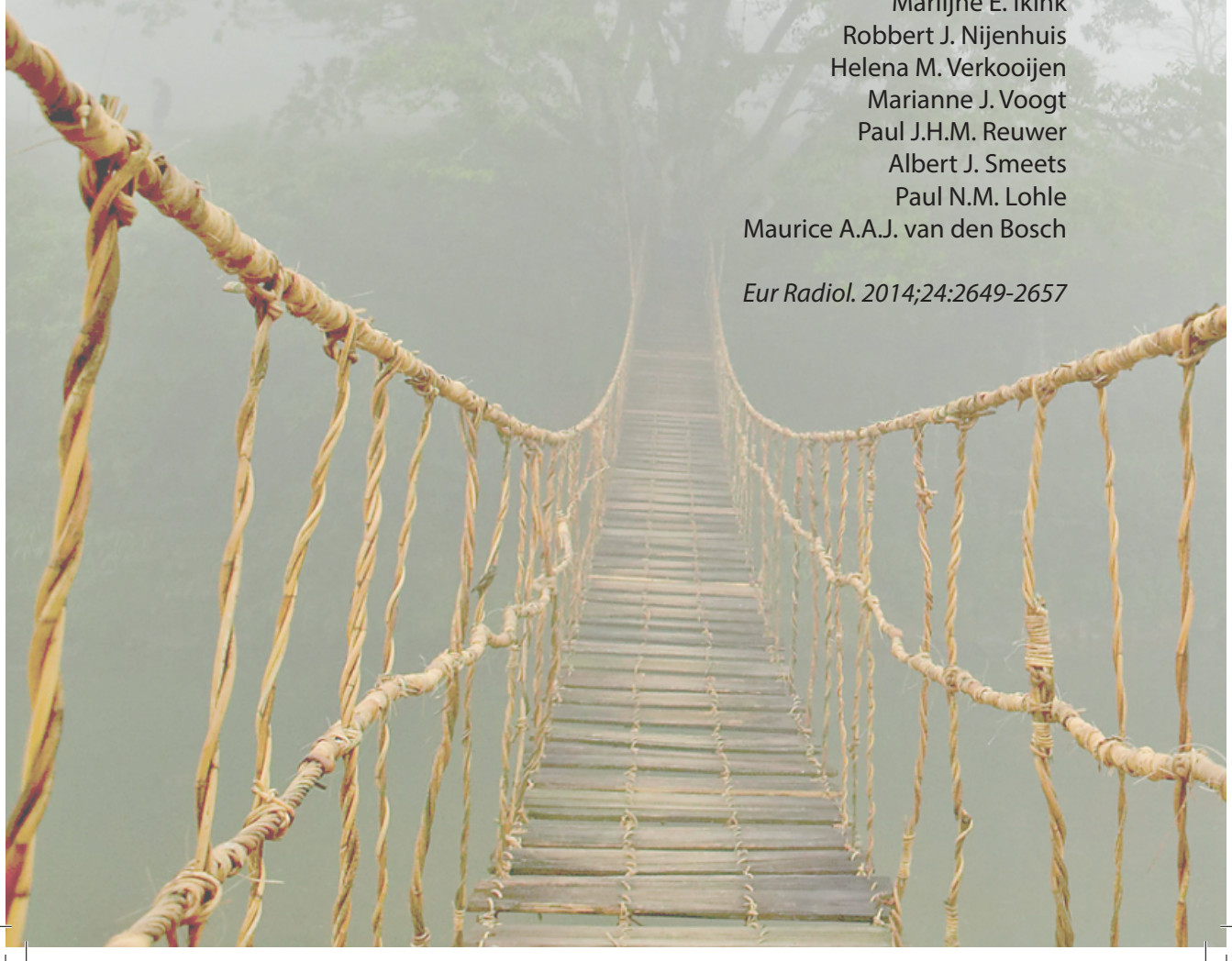

# Abstract

**Objective**

To compare the effectiveness of magnetic resonance-guided high-intensity focused ultrasound (MR-HIFU) with that of uterine artery embolisation (UAE) for treatment of uterine fibroids.

**Methods**

Between January 2010 and January 2013, 51 women with symptomatic fibroids underwent MR-HIFU. Follow-up and MR imaging were compared to 68 women treated with UAE, who fulfilled eligibility criteria for MR-HIFU: e.g. fibroid size (≤ 12 cm) and number (≤ 5). We compared median symptom severity (tSSS), total health-related quality of life (HRQoL) scores, and reintervention rates. The adjusted effect on symptom relief and HRQoL improvement was calculated using multivariable linear regression. Cox regression was applied to calculate the adjusted risk of reintervention between both treatments.

**Results**

Median tSSS improved significantly from baseline to 3 months' follow-up ($p<0.001$) for both MR-HIFU (53.1 (IQR [40.6-68.8]) to 34.4 (IQR [21.9-46.9])) and UAE (65.3 (IQR [56.3-74.2]) to 21.9 (IQR [9.4-34.4])). In addition, significantly better HRQoL scores were observed after 3 months ($p<0.001$). However, in multivariate analysis, UAE had a stronger effect on symptom relief and HRQoL improvement than MR-HIFU ($p<0.001$). Patients treated with MR-HIFU had a 7.1 (95% CI [2.00-25.3]; $p=0.002$) times higher risk of reintervention within 12 months (18/51 versus 3/68).

**Conclusion**

Both MR-HIFU and UAE result in significant symptom relief related to uterine fibroids. However, MR-HIFU is associated with a higher risk of reintervention.

## Introduction

In recent years, there has been a growing interest in uterus-conserving treatments for women with symptomatic uterine fibroids. These benign gynaecological tumours evolve from the smooth muscle cells of the uterus (i.e. myometrium). Although the exact aetiology or the molecular basis of uterine fibroids is still unknown, their cause seems to be multifactorial. Race, heredity, nulliparity, sex steroids, and insulin resistance (e.g. obesity, diabetes mellitus and hypertension) have been associated with an increased risk of fibroids[1,2]. Depending on their size and location within the uterus, uterine fibroids may cause excessive menstrual bleeding, and uterine discomfort or gynaecologic pain related to mechanical compression of the pelvic organs[3,4]. Several treatment options are available: (1) invasive surgery, e.g. abdominal hysterectomy and myomectomy; (2) minimally invasive alternatives, e.g. laparoscopic or hysteroscopic myomectomy, uterine artery embolisation (UAE), and (3) non-invasive treatment, i.e. high-intensity focused ultrasound (HIFU)[5]. Uterine fibroids come into being and grow in the reproductive age. Since many women currently postpone their motherhood, the number of patients with symptomatic uterine fibroids who want to preserve fertility is steadily growing[6,7]. Other factors frequently cited in the decision-making towards minimally or non-invasive treatments includes the wish to avoid invasive procedures, or maintain their uterus for psychological reasons[8]. This has fuelled interests in developing treatments such as in UAE and HIFU.

Uterine artery embolisation was first described in 1995[9], and rapidly gained acceptance as a safe and effective treatment method for uterine fibroids[10-12]. Hysterectomy and UAE are both equally effective in reducing symptoms and improving quality of life, but UAE has the advantage of less infection, shorter hospital stay, quicker recovery time, lower costs, and preservation of reproductive potential[10,13,14]. At one-year, however, 10% of the women treated with UAE require a secondary intervention to treat persistent or recurrent symptoms[15]. Despite the fact that UAE is a safe method, there are some associated risks including post-embolisation syndrome (3%), vaginal fibroid expulsion (2.5%), and non-target ovarian embolisation (7.5%) leading to premature menopause[16-19]. These complications have directed attention to image-guided non-invasive ablation techniques, such as the relatively new technique magnetic resonance-guided HIFU (MR-HIFU). By focusing the ultrasound beam to a focal spot, acoustic energy is converted into heat, resulting in a well-circumscribed necrotic lesion without damaging nearby tissues that the beam passes through[20,21]. This technique does not affect ovarian function[22,23], requires no trans-arterial access, and involves no radiation exposure. Moreover, it can be delivered in an outpatient setting, and patients can usually return to their normal activities the day after treatment. Studies with long-term follow-up after MR-HIFU ablation have reported durable symptom relief for at least 24 months[24-26].

Patient preferences should direct the choice of treatment for symptomatic uterine fibroids. For informed decision-making, data are needed on effectiveness of treatment including symptom alleviation and health-related quality of life (HRQoL)[27,28]. As more long-term follow-up data become available, the efficacy of these techniques can be further compared. The purpose of this historical cohort study was to assess and compare the efficacy of MR-HIFU and UAE for treatment of symptomatic uterine fibroids.

## Materials and methods

**Patients**

Between January 2010 and January 2013, clinical follow-up and MR imaging of premenopausal women treated with volumetric MR-HIFU ablation in an academic hospital (University Medical Center Utrecht, The Netherlands) were compared to patients treated with UAE in a high-volume peripheral center (St. Elisabeth Hospital Tilburg, The Netherlands). All patients included in the UAE group would theoretically also been eligible for MR-HIFU ablation based on size (≤ 12 cm) and number (≤ 5) of fibroids, presence of an accessible superficial dominant uterine fibroid, absence of interposition of bowel loops between the abdominal wall and fibroid, and homogeneous contrast enhancement. Enrolment criteria were established by the investigators at both sites on the basis of current experience with MR-HIFU. All patients had undergone a standardised diagnostic pelvic MRI examination with administration of a gadolinium-based contrast agent at baseline and 3 months' follow-up to assess uterine volume and dominant fibroid volume reductions. Volumetric changes were measured via the prolate ellipsoid formula (length × width × height × [pi/6]). In addition, patients should have completed the uterine fibroid symptom and health-related quality of life (UFS-QoL) questionnaire[27], consisting an 8-item symptom severity score (tSSS) and 29 HRQoL items, obtained at baseline and 3 months' follow-up. Reintervention rates - defined as the need for an additional treatment to control persistent or recurrent fibroid-related symptoms within 12 months after initial treatment - were assessed by the electronic patient documentation (EPD) system and/or by telephone interviewing. Due to the nature of this study, a waiver of requirement for informed consent was obtained by the institutional review board (IRB) of the participating hospitals.

**MR-HIFU treatment**

The volumetric MR-HIFU treatments were performed on a 1.5-T clinical MR-HIFU system (Sonalleve R3, Philips Healthcare, Vantaa, Finland). All procedures were carried out by one interventional radiologist (M.v.d.B.) with 12 years of experience in MR imaging, 7 years of experience in image-guided tumour ablation, but no previous experience in MR-HIFU ablation at the start of the study period. The MR-HIFU platform included a high-intensity phased-array focused ultrasound transducer with 256-channels (emitting at a frequency of 1.2 megahertz [MHz]) incorporated in the MR-HIFU table top, forming a spherical shell with a natural ellipsoidal focus of $1 \times 1 \times 7$ mm$^3$ at 14 cm distance[29]. The procedure typically acquired 2-3 hours, with the patient lying in prone position. This outpatient treatment procedure has been previously described[21]. In short, after depilation of the lower abdomen, infusion of intravenous analgesia (paracetamol 1,000 mg and diclofenac 75 mg) and insertion of a Foley catheter, patients were positioned on top of the acoustic window of the MR-HIFU table top. Before starting treatment, three-dimensional (3D) planning MR images were acquired as shown in *Appendix 1*. T2-weighted MR images were used for anatomical imaging, and T1-weighted MR images were obtained for assuring safety of surrounding critical organs in the near field (nearby skin) and far field (close to vertebral column). The system was capable to execute volumetric ablation using a binary feedback algorithm controlling the duration of the sonication at each sub-trajectory. Treatment cells were available in various sizes by electromechanically steering a single focus along these trajectories (i.e. multiple out-ward moving concentric circles), with an axial diameter of 4,

8, 12, 14, and 16 mm and a length of 10, 20, 30, 35, and 40 mm respectively[30]. To monitor and control the amount of thermal energy at the targeted location, continuous proton resonance frequency (PRF) thermometry was acquired using a segmented gradient echo-echo planar imaging (FFE-EPI) sequence with a resolution of 2.5 × 2.5 mm. As a result, every 3 seconds, two-dimensional (2D) colour temperature maps were displayed on top of the anatomical MR images. When the targeted ablation volume had reached the lethal thermal dose of 240 EM (equivalent minutes at 43°C) or temperatures above 60°C, the sonication was stopped to prevent tissue overheating[31]. The sonication could also be stopped manually by the patient-controlled emergency stop button (PESB), the operator controlled safety device (SB), or the stop button in the user interface. Systematically, the sonication time of each treatment cell persisted 16, 20, 35, 45, and 55 seconds, respectively. At the end of the treatment, contrast-enhanced T1-weighted MRI (gadobutrol, 0.1 mmol/kg, Bayer Schering Pharma) was carried out to visualise the non-perfused volume (NPV), assessed by contour measurements (sum-of-slice method). MR-HIFU treatment was considered successful if a NPV ratio (non-perfused volume divided by fibroid volume) of at least 0.50 was achieved[32-35]. Patients were observed for a short period (approximately two hours) while recovering from the analgesia and discharged home with an escort.

**UAE procedure**

All UAE procedures were performed by two interventional radiologists in a protocolised standard setting with an overnight stay in the hospital. Both radiologists (P.N.M.L. and A.J.S.) had over 15 years of experience in pelvic imaging and UAE. Before treatment, intravenous antibiotic prophylaxis (cefazolin 2 g, EuroCept, The Netherlands) and suppository analgesia (paracetamol 1,000 mg and diclofenac 100 mg) were administered. A fixed periprocedural pain management protocol was used with a piritramide (Dipidolor, 2 mg/5 min bolus

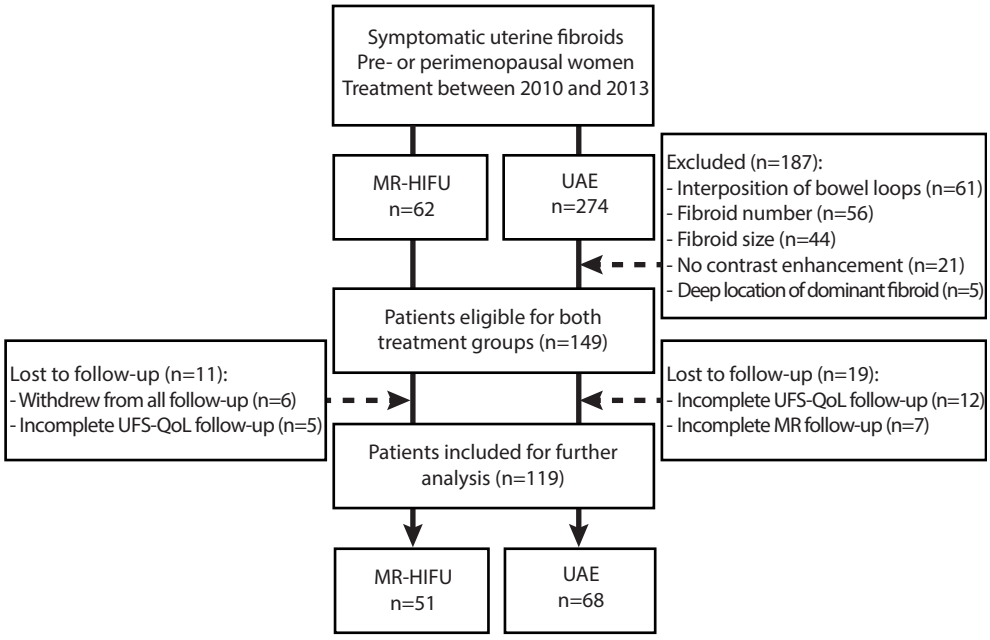


**Figure 1.** Selection of patients for both treatment groups

injection, Janssen-Cilag) and droperidol patient-controlled analgesia (PCA) infusion pump. Under local anaesthesia of the groin, the femoral artery was punctured followed by super-selective catheterisation of both uterine arteries via a right unilateral approach (by A.J.S. in 40%) with a Waltman loop manoeuvre in the aorta[36], or via bilateral femoral approach (by P.N.M.L. in 60%) to avoid extensive ovarian radiation exposure[37]. The tip of either a 4-French Cobra catheter (Cordis Corporation) or coaxial microcatheter (Merit Medical Systems, Inc.) was directed into the horizontal segment of the uterine artery, distal to the origin of the cervicovaginal branches. After proper placement of the catheters in both uterine arteries, contrast angiography (Omnipaque (iohexol) 330, GE Healthcare Inc.) was obtained to guide the treatment and achieve imaging data of the uterine arterial vasculature, including



**Table 1.** Comparison of baseline characteristics for MR-HIFU and UAE

| | MR-HIFU (n=51) | UAE (n=68) | p |
|---|---|---|---|
| PATIENT CHARACTERISTICS | | | |
| Age (years)[a] | 46 (43-49) | 43 (41-46) | 0.001 |
| Ethnicity[b] | | | 0.789 |
| Caucasian | 45 (88%) | 58 (85%) | |
| Non-Caucasian | 6 (12%) | 10 (15%) | |
| Symptoms[b,c] | | | |
| Menorrhagia | 37 (73%) | 63 (93%) | 0.005 |
| Bulky symptoms | 47 (92%) | 50 (74%) | 0.016 |
| Pain | 36 (71%) | 31 (46%) | 0.009 |
| tSSS[a] | 53.1 (40.6-68.8) | 65.3 (56.3-74.2) | 0.001 |
| Total HRQoL[a] | 60.3 (41.4-81.0) | 48.5 (33.8-65.1) | 0.003 |
| LESION CHARACTERISTICS | | | |
| Number of fibroids[b] | | | 0.310 |
| Solitary fibroid | 12 (24%) | 23 (34%) | |
| Multiple fibroids | 39 (76%) | 45 (66%) | |
| 2-5 fibroids | 31 (80%) | 41 (91%) | |
| 6-10 fibroids | 8 (20%) | 4 (9%) | |
| Location of fibroids[b] | | | 0.041 |
| Intramural | 30 (59%) | 38 (56%) | |
| Subserosal | 13 (25%) | 8 (12%) | |
| Submucosal | 8 (16%) | 22 (32%) | |
| Type of fibroid[b,46] | | | 0.013 |
| Type 1 | 29 (57%) | 22 (32%) | 0.008 |
| Type 2 | 16 (31%) | 26 (38%) | 0.440 |
| Type 3 | 6 (12%) | 20 (30%) | 0.022 |
| Maximum fibroid diameter (cm)[a] | 8.5 (6.5-10.7) | 7.2 (5.5-8.4) | 0.005 |
| Dominant fibroid volume ($cm^3$)[a] | 273 (142-478) | 166 (65-236) | <0.001 |
| Uterine volume ($cm^3$)[a] | 792 (454-1,104) | 486 (347-689) | <0.001 |

[a]Median (interquartile range); [b]number (percentage); [c]patients may have multiple symptoms simultaneously; MR-HIFU, magnetic resonance-guided high-intensity focused ultrasound; UAE, uterine artery embolisation; tSSS, transformed symptom severity score (range 0-100) - high scores indicate more severe symptoms; HRQoL, health-related quality of life (range 0-100) - high scores indicate better quality of life; Type 1, low signal intensity on T2-weighted imaging; Type 2, intermediate signal intensity on T2-weighted imaging; Type 3, high signal intensity on T2-weighted imaging

the presence of any anastomoses. Subsequently, flow-directed injection was carried out using hydrogel core Polyzene®-F coated microspheres, sizes 500-1,300 µm (Embozene®, CeloNova BioSciences, San Antonio, Texas), suspended in a solution of contrast agent and saline, to occlude the fibroid vasculature. The angiographic embolisation endpoint was described as a complete cessation of blood flow in the arteries to the peri-fibroid plexus, with preservation of flow in the main uterine artery, cervicovaginal branches, and utero-ovarian anastomoses. After completion of the UAE procedure, manual compression to the punctured femoral arteries was applied until hemostasis was achieved. Accompanying and persistent nausea was treated with ondansetron 4 mg intravenously (Zofran®, GlaxoSmithKline). Almost all patients were discharged the next day after treatment.



**Data collection and statistical analysis**

A retrospective analysis of prospectively collected data was performed. Outcome measures included patient-reported UFS-QoL scores and reintervention rates. Descriptive statistics were used to summarise the patients demographic, clinical, and imaging characteristics of both treatment groups. Frequencies and percentages are reported for categorical data, while continuous data are expressed in median and interquartile range (IQR). Non-parametric tests (Mann-Whitney U test, Fisher's exact test and chi-square test) were used to compare variables between the MR-HIFU group and the UAE group. A multivariable linear regression model was applied to assess the independent correlation between tSSS and total HRQoL improvements and the type of treatment (MR-HIFU versus UAE),

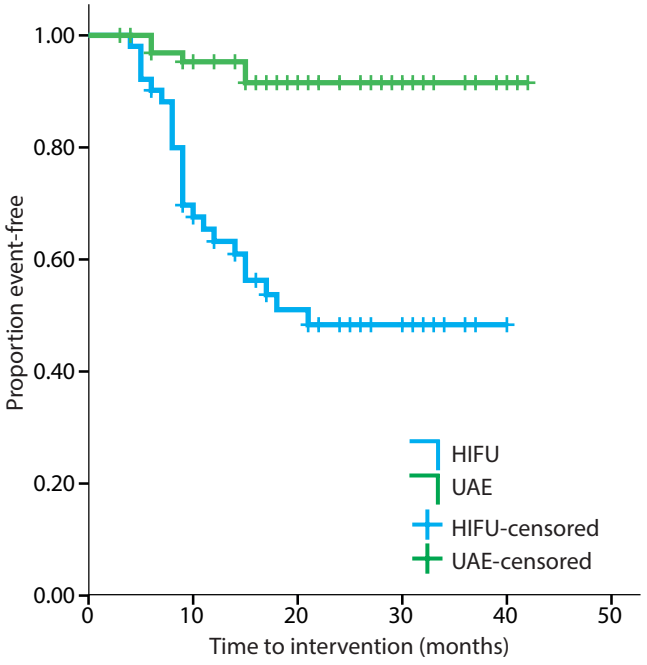


**Figure 2.** The Kaplan-Meier plot illustrates the proportion of event-free patients for a certain length of time after treatment. The green line represents UAE, the blue line represents MR-HIFU ablation. The censored observations are shown as ticks on the line.

corrected for any possible confounding effects such as age, type of fibroid, maximum fibroid diameter, and baseline UFS-QoL scores. To facilitate a meaningful interpretation of the linear model, the continuous data were centred around the mean of the variable. Secondly, logistic regression was performed to calculate the adjusted odds-ratio (OR) of clinically relevant symptom improvement (defined as a 3 months' tSSS ≤ 20 points)[27] of women treated with MR-HIFU versus UAE. A cox regression analysis was performed to calculate the adjusted risk of reintervention between both treatments. A multivariable cox model was constructed, including maximum fibroid diameter, baseline tSSS, and type of treatment. Results are presented as hazard ratios with their corresponding 95% confidence intervals (95% CI). Statistical analyses were executed using IBM SPSS Statistics, version 20.0 (Armonk, New York, USA).



# Results

**Demographics**

During the study period, 336 patients with symptomatic uterine fibroids underwent either volumetric MR-HIFU ablation or UAE in the participating hospitals. Sixty-two women treated with MR-HIFU and 274 women treated with UAE were screened for eligibility. Fifty-one patients (82%) were included in the MR-HIFU group: five patients did not completed the UFS-QoL questionnaires, and six patients withdrew from further follow-up. Sixty-eight patients (25%) in the UAE group fulfilled the inclusion criteria, those who were considered theoretically eligible for MR-HIFU ablation, and included for further analysis (*Figure 1*). Patients with the following conditions were excluded by consensus of two observers: interposition of bowel loops (n=61), unsuitable fibroid number (n=56), too large fibroid size (n=44), inhomogeneous contrast enhancement (n=21), and if the target fibroid was located too deep in the pelvis (n=5). Baseline characteristics of both study populations are presented in *Table 1*. The median baseline tSSS of patients treated with MR-HIFU ablation was significantly lower compared to the group who underwent the UAE procedure (p=0.001). The median age, maximum fibroid diameter, dominant fibroid volume, uterine volume, and baseline total HRQoL score were significantly higher (p<0.005) in the MR-HIFU group.

**Table 2.** Changes in symptom severity (tSSS) and health-related quality of life (HRQoL) scores for MR-HIFU and UAE

| | MR-HIFU (n=51) | | | UAE (n=68) | | | |
|---|---|---|---|---|---|---|---|
| | BL | 3MFU | Δ | BL | 3MFU | Δ | p |
| tSSS[a] | 53.1 (40.6-68.8) | 34.4 (21.9-46.9) | -18.8 (3.1-37.5)* | 65.3 (56.3-74.2) | 21.9 (9.4-34.4) | -43.7 (31.3-53.2)* | <0.001 |
| Total HRQoL[a] | 60.3 (41.4-81.0) | 81.5 (57.6-90.3) | +10.4 (4.5-24.0)* | 48.5 (33.8-65.1) | 85.4 (75.2-94.6) | +33.2 (22.7-49.1)* | <0.001 |

[a]Median (interquartile range); MR-HIFU, magnetic resonance-guided high-intensity focused ultrasound; UAE, uterine artery embolisation; BL, baseline; MFU, months of follow-up; Δ, changes from baseline; tSSS, transformed symptom severity score (range 0-100) - high scores indicate more severe symptoms, HRQoL, health-related quality of life (range 0-100) - high scores indicate better quality of life; * p<0.001

**Outcome measures**

Immediately after MR-HIFU treatment, the median NPV was 100 $cm^3$ (IQR [41-192]), corresponding to a NPV ratio of 0.38 (IQR [0.26-0.62]) of the total fibroid volume. Most patients had limited treatments, with 69% (35/51) of the patients having a NPV ratio of 0.50 or less (median 0.29 (IQR [0.22-0.40]), and 31% (16/51) having a NPV of 0.50 or more (median 0.67 (IQR [0.62-0.83]). Unfortunately, we were not able to acquire these data directly after UAE. At 3 months' follow-up, the UAE group showed a larger fibroid volume reduction (43.3% (IQR [29.9-65.0]) vs. 17.2% (IQR [3.2-34.5]), p<0.001) and a larger uterine volume reduction (35.3% (IQR [25.0-47.1]) vs. 16.3% (IQR [4.2-25.3]), p<0.001) as compared to the MR-HIFU group. The median tSSS in patients treated with MR-HIFU ablation improved significantly (p<0.001) from 53.1 (IQR [40.6-68.8]) at baseline to 34.4 (IQR [21.9-46.9]) at 3 months. After UAE, the median tSSS improved from 65.3 (IQR [56.3-74.2]) to 21.9 (IQR [9.4-34.4]); p<0.001). The median total HRQoL score changed from 60.3 (IQR [41.4-81.0]) to 81.5 (IQR [57.6-90.3]); p<0.001) better quality after MR-HIFU, and improved from 48.5 (IQR [33.8-65.1]) to 85.4 (IQR [75.2-94.6]); p<0.001) in the UAE group. Changes in UFS-QoL scores are shown in *Table 2*. The result of the multivariable

**Table 3.** Crude and adjusted association between treatment and symptom relief and quality of life improvements

| | Symptom severity | | | | Quality of life | | | |
|---|---|---|---|---|---|---|---|---|
| | *B* | 95% CI | | p | *B* | 95% CI | | p |
| | | Lower | Upper | | | Lower | Upper | |
| Step 1 (crude effect) | | | | | | | | |
| Intercept* | -19.9 | -24.7 | -15.1 | | 13.4 | 8.31 | 18.4 | |
| Type of treatment | | | | | | | | |
| MR-HIFU | ref | | | | ref | | | |
| UAE | -21.5 | -27.8 | -15.2 | <0.001 | 21.6 | 15.0 | 28.2 | <0.001 |
| Step 2 (adj. effect) | | | | | | | | |
| Intercept* | -19.1 | -23.6 | -14.6 | | 13.8 | 9.11 | 18.5 | |
| Type of treatment | | | | | | | | |
| MR-HIFU | ref | | | | ref | | | |
| UAE | -13.0 | -19.1 | -7.02 | <0.001 | 14.9 | 8.99 | 20.8 | <0.001 |
| Age | -0.17 | -0.75 | 0.41 | 0.562 | -0.06 | -0.64 | 0.52 | 0.837 |
| Type of fibroid[46] | | | | | | | | |
| Type 1 | ref | | | | ref | | | |
| Type 2 | -1.71 | -7.70 | 4.28 | 0.575 | -0.73 | -6.73 | 5.27 | 0.811 |
| Type 3 | -2.83 | -10.1 | 4.40 | 0.443 | -2.23 | -9.39 | 4.94 | 0.542 |
| Maximum diameter | 1.96 | -0.90 | 3.03 | <0.001 | -0.96 | -2.02 | 0.11 | 0.078 |
| Baseline HRQoL score | | | | | -0.50 | -0.62 | -0.37 | <0.001 |
| Baseline tSSS | -0.52 | -0.69 | -0.36 | <0.001 | | | | |

*B*, regression coefficient; CI, confidence interval; MR-HIFU, magnetic resonance-guided high-intensity focused ultrasound; UAE, uterine artery embolisation; Type 1, low signal intensity on T2-weighted imaging; Type 2, intermediate signal intensity on T2-weighted imaging; Type 3, high signal intensity on T2-weighted imaging; HRQoL, health-related quality of life - high scores indicate better quality of life; tSSS, transformed symptom severity score - high scores indicate more severe symptoms. *Note, linear model was centred around the mean, the intercept represents the variables at the centred values.

linear regression analysis demonstrated that a UAE procedure led to a significantly higher improvement in tSSS (p<0.001) and total HRQoL (p<0.001) than after MR-HIFU ablation. Part of the effect of UAE can be explained by the baseline UFS-QoL score (p<0.001) as shown in *Table 3*: a higher baseline tSSS will result in more symptom relief after 3 months' follow-up, and higher baseline HRQoL scores will result in less quality of life improvement. Secondly, compared to MR-HIFU, patients treated with UAE were more likely to develop adequate symptom improvement (OR=14.9; 95% CI [3.56-62.4]; p<0001).

**Reintervention**

In total, 24 (47%) patients in the MR-HIFU group needed an additional treatment due to insufficient symptom improvement (median follow-up 15 months, IQR [9, 26]): i.e. abdominal hysterectomy (n=10), second MR-HIFU ablation (n=7), UAE (n=5), and hysteroscopic myomectomy (n=2). Patients who needed a reintervention had significantly lower fibroid volume reduction after 3 months' follow-up compared to those who did not require a reintervention (p=0.007). In the UAE group, five patients (7%) needed surgical reintervention (median follow-up 24 months, IQR [14-32]): two patients underwent an abdominal hysterectomy, and three patients a hysteroscopic myomectomy. It is worth taking into consideration that in the UAE group two patients (3%) were treated with antibiotics because of endometritis, two patients (3%) reported an amenorrhea as a result of premature ovarian failure, one patient (1.5%) described an infected hematoma at the arterial puncture site, and one patient (1.5%) developed a vulvar abscess due to non-target embolisation. Seven patients (10%) described a painful spontaneous expulsion of (part of) the treated uterine fibroid, 6 to 12 weeks after UAE. No serious complications or adverse events were described during or after MR-HIFU ablation. At 12 months' follow-up, patients treated with MR-HIFU had a 7.1 (95% CI [2.00-25.3]; p=0.002) times higher risk of a reintervention than the patients treated with UAE (*Figure 2*): e.g. 35% (18/51) versus 4.5% (3/68). In addition, patients who underwent an MR-HIFU ablation were stratified into two groups based on the NPV ratio immediately after treatment. The 12 month reintervention rate was 43% (15/35) of patients with a NPV ratio of < 0.50 versus 19% (3/16) for patients with a NPV ratio of ≥ 0.50.

**Appendix 1 .** Main scan parameters used for screening and treatment planning

| Sequence | T2w MRI | T1w MRI | CE-T1w MRI | MR thermometry |
|---|---|---|---|---|
| Type of scan | 3D TSE<br>Turbo factor 83 | 3D FFE | 3D TFE<br>TFE factor 44 | M2D FFE-EPI<br>EPI factor 11 |
| TE/TR (ms) | 130/1425 | 1.9/3.6 | 2.6/5.4 | 19/41 |
| Flip angle (deg) | 90 | 7 | 10 | 20 |
| Fat suppression | No | No | SPAIR | ProSet |
| FOV (mm × mm) | 250 × 250 | 220 x 240 | 250 x 250 | 400 x 310 |
| ACQ voxel ($mm^3$) | 1.20×1.39×3.00 | 1.25×1.53×2.50 | 1.49×1.89×3.00 | 2.50×2.56×7.00 |
| REC voxel ($mm^3$) | 0.49×0.49×1.50 | 0.47×0.47×1.25 | 0.49×0.49×1.50 | 2.50×2.50×7.00 |
| Scan duration (min:sec) | 3:50.8 | 1:57.3 | 2:14.5 | 00:03.7* |

T2w, T2-weighted imaging; MRI, magnetic resonance imaging; T1w, T1-weighted imaging; CE, contrast-enhanced; 3D, three-dimensional; TSE, turbo spin echo; FFE, spoiled gradient echo; TFE, ultra fast gradient echo; M2D, multiple (sequential) two-dimensional slices; EPI, echo planar imaging; TE/TR, echo time/repetition time; SPAIR, spectral attenuated inversion recovery; ProSet; principle of selective excitation technique; FOV, field of view; ACQ, acquired; REC, reconstructed; *dynamic

## Discussion

During the past decades, minimally or non-invasive treatment has gained popularity and continues to evolve and expand with developments in technology and experience. MR-HIFU and UAE are increasingly advocated and employed as a safe therapy for symptomatic uterine fibroids. As an alternative to surgery, the observed benefits include less tissue trauma, prevention of adhesions, preservation of fertility, less morbidity, less painful recovery, faster return to normal activities, and no cosmetic damage. Our results show that both radiological treatment options lead to significant symptom relief (tSSS) and quality of life improvement (HRQoL). However, the findings also suggest that UAE is to be preferred to MR-HIFU ablation. Compared to UAE, patients treated with MR-HIFU had a significantly higher risk of reintervention after one-year of follow-up. This may be explained by the observed symptom severity after 3 months' follow-up (*Table 2*), this score remained significantly higher after MR-HIFU ablation (median tSSS: 34.4 points) than after UAE (median tSSS: 21.9 points, $p<0.001$). It has been described that women with a tSSS ≤ 20 points, in combination with a total HRQoL score > 80 points, are considered asymptomatic[27] and no longer need additional treatment. These findings in favor of UAE are in accordance with those of a similar German study[38], showing that UAE resulted in a significantly better long-term outcome (tSSS: $p=0.019$; total HRQoL: $p=0.049$) and a significantly lower reintervention rate (12.2% vs. 66.7%; $p<0.001$) as compared to MR-HIFU. However, both studies have some limitations for providing definitive answers. An important issue of a retrospective study design is the possibility of selection bias between comparison groups, that can lead to confounding (by indication). Added to that, retrospective studies are more hampered by missing values than prospective studies, which affects the size and power of the study. Nevertheless, despite the small size, statistically significant differences were observed in both studies. These corroborative data spark further prospective research.

Of course, operator skill and experience affects the success or failure of new techniques. The immediate NPV ratio after MR-HIFU ablation has been shown to be a predictor for the therapeutic outcomes[32,39,40]. LeBlang *et al.*[32] described that larger thermal ablation volumes resulted in greater fibroid volume reduction and more symptom improvement. In order to achieve significantly better results and lower reintervention rates, a minimum NPV of 50% of the total fibroid volume should be pursued[34,35]. It has been claimed that, with accumulating experience and careful patient selection[41,42], an immediate NPV ratio of at least 0.80 can be safely achieved[43]. Moreover, only minor adverse events are described during the MR-HIFU procedure, such as general malaise, mild abdominal tenderness, abnormal vaginal discharge and first-degree skin burns. The treatments in the present study reveal the first three years of experience and did not meet those high standards. Results might have been better with more rigorous MR-HIFU ablation (by covering larger NPVs), as has been done in more recently treated patients in our hospital. In stark contrast, the UAE procedures were performed by an experienced physician with a high peripheral interventional volume (>250 interventions per year) for patients undergoing embolisation for symptomatic uterine fibroids. The past five years, the volumetric MR-HIFU technique has rapidly evolved and treatment protocols have dramatically changed. This as well as growing experience, may contribute to enhancement of the therapeutic effectiveness of MR-HIFU.

The preliminary obstetrical experience after MR-HIFU ablation of uterine fibroids is encouraging, since current studies reassure that fertility can be maintained and term pregnancies can be achieved[22,23,35,38,44,45].

In conclusion, both volumetric MR-HIFU ablation and UAE result in clinically significant symptom relief and improvement of quality of life in patients with symptomatic uterine fibroids. The present findings suggest that - for now - UAE is to be preferred to MR-HIFU. However, it should be noted that in order to deem an MR-HIFU ablation successful, larger NPVs (≥ 50%) should be achieved, which could lead to better treatment results compared to UAE. Given new MR-HIFU protocols and growing experience, the current findings warrant a randomised controlled trial.

# References

1. Rice KE, Secrist JR, Woodrow EL, Hallock LM, Neal JL. Etiology, diagnosis, and management of uterine leiomyomas. *J Midwifery Womens Health.* 2012;57:241-247
2. Parker WH. Etiology, symptomatology, and diagnosis of uterine myomas. *Fertil Steril.* 2007;87:725-736
3. Lippman SA, Warner M, Samuels S, Olive D, Vercellini P, Eskenazi B. Uterine fibroids and gynecologic pain symptoms in a population-based study. *Fertil Steril.* 2003;80:1488-1494
4. Wegienka G, Baird DD, Hertz-Picciotto I, Harlow SD, Steege JF, Hill MC, Schectman JM, Hartmann KE. Self-reported heavy bleeding associated with uterine leiomyomata. *Obstet Gynecol.* 2003;101:431-437
5. van der Kooij SM, Ankum WM, Hehenkamp WJ. Review of nonsurgical/minimally invasive treatments for uterine fibroids. *Curr Opin Obstet Gynecol.* 2012;24:368-375
6. Balasch J, Gratacos E. Delayed childbearing: effects on fertility and the outcome of pregnancy. *Fetal Diagn Ther.* 2011;29:263-273
7. Schmidt L, Sobotka T, Bentzen JG, Nyboe Andersen A. Demographic and medical consequences of the postponement of parenthood. *Hum Reprod Update.* 2012;18:29-43
8. Nevadunsky NS, Bachmann GA, Nosher J, Yu T. Women's decision-making determinants in choosing uterine artery embolization for symptomatic fibroids. *J Reprod Med.* 2001;46:870-874
9. Ravina JH, Herbreteau D, Ciraru-Vigneron N, Bouret JM, Houdart E, Aymard A, Merland JJ. Arterial embolisation to treat uterine myomata. *Lancet.* 1995;346:671-672
10. van der Kooij SM, Hehenkamp WJ, Volkers NA, Birnie E, Ankum WM, Reekers JA. Uterine artery embolization vs hysterectomy in the treatment of symptomatic uterine fibroids: 5-year outcome from the randomized EMMY trial. *Am J Obstet Gynecol.* 2010;203:105 e101-113
11. Hirst A, Dutton S, Wu O, Briggs A, Edwards C, Waldenmaier L, Maresh M, Nicholson A, McPherson K. A multi-centre retrospective cohort study comparing the efficacy, safety and cost-effectiveness of hysterectomy and uterine artery embolisation for the treatment of symptomatic uterine fibroids. The HOPEFUL study. *Health Technol Assess.* 2008;12:1-248, iii
12. Lohle PN, Voogt MJ, De Vries J, Smeets AJ, Vervest HA, Lampmann LE, Boekkooi PF. Long-term outcome of uterine artery embolization for symptomatic uterine leiomyomas. *J Vasc Interv Radiol.* 2008;19:319-326
13. Volkers NA, Hehenkamp WJ, Birnie E, Ankum WM, Reekers JA. Uterine artery embolization versus hysterectomy in the treatment of symptomatic uterine fibroids: 2 years' outcome from the randomized EMMY trial. *Am J Obstet Gynecol.* 2007;196:519 e511-511
14. Hehenkamp WJ, Volkers NA, Donderwinkel PF, de Blok S, Birnie E, Ankum WM, Reekers JA. Uterine artery embolization versus hysterectomy in the treatment of symptomatic uterine fibroids (EMMY trial): peri- and postprocedural results from a randomized controlled trial. *Am J Obstet Gynecol.* 2005;193:1618-1629
15. Edwards RD, Moss JG, Lumsden MA, Wu O, Murray LS, Twaddle S, Murray GD; Committee of the Randomized Trial of Embolization versus Surgical Treatment for Fibroids. Uterine-artery embolization versus surgery for symptomatic uterine fibroids. *N Engl J Med.* 2007;356:360-370
16. Spies JB, Spector A, Roth AR, Baker CM, Mauro L, Murphy-Skrynarz K. Complications after uterine artery embolization for leiomyomas. *Obstet Gynecol.* 2002;100:873-880
17. Walker WJ, Pelage JP. Uterine artery embolisation for symptomatic fibroids: clinical results in 400 women with imaging follow up. *BJOG.* 2002;109:1262-1272
18. Worthington-Kirsch R, Spies JB, Myers ER, Mulgund J, Mauro M, Pron G, Peterson ED, Goodwin S; FIBROID Investigators. The Fibroid Registry for outcomes data (FIBROID) for uterine embolization: short-term outcomes. *Obstet Gynecol.* 2005;106:52-59
19. Martin J, Bhanot K, Athreya S. Complications and reinterventions in uterine artery embolization for symptomatic uterine fibroids: a literature review and meta-analysis. *Cardiovasc Intervent Radiol.* 2013;36:395-402
20. Tempany CM, Stewart EA, McDannold N, Quade BJ, Jolesz FA, Hynynen K. MR imaging-guided focused ultrasound surgery of uterine leiomyomas: a feasibility study. *Radiology.* 2003;226:897-905
21. Ikink ME, Voogt MJ, Verkooijen HM, Lohle PN, Schweitzer KJ, Franx A, Mali WP, Bartels LW, van den Bosch MA. Mid-term clinical efficacy of a volumetric magnetic resonance-guided high-intensity focused ultrasound technique for treatment of symptomatic uterine fibroids. *Eur Radiol.* 2013;23:3054-3061
22. Rabinovici J, David M, Fukunishi H, Morita Y, Gostout BS, Stewart EA. Pregnancy outcome after magnetic resonance-guided focused ultrasound surgery (MRgFUS) for conservative treatment of uterine fibroids. *Fertil Steril.* 2010;93:199-209
23. Bouwsma EV, Gorny KR, Hesley GK, Jensen JR, Peterson LG, Stewart EA. Magnetic resonance-guided focused ultrasound surgery for leiomyoma-associated infertility. *Fertil Steril.* 2011;96:e9-e12

24. Gorny KR, Woodrum DA, Brown DL, Henrichsen TL, Weaver AL, Amrami KK, Hangiandreou NJ, Edmonson HA, Bouwsma EV, Stewart EA, Gostout BS, Ehman DA, Hesley GK. Magnetic resonance-guided focused ultrasound of uterine leiomyomas: review of a 12-month outcome of 130 clinical patients. *J Vasc Interv Radiol.* 2011;22:857-864
25. Kim HS, Baik JH, Pham LD, Jacobs MA. MR-guided high-intensity focused ultrasound treatment for symptomatic uterine leiomyomata: long-term outcomes. *Acad Radiol.* 2011;18:970-976
26. Funaki K, Fukunishi H, Sawada K. Clinical outcomes of magnetic resonance-guided focused ultrasound surgery for uterine myomas: 24-month follow-up. *Ultrasound Obstet Gynecol.* 2009;34:584-589
27. Spies JB, Coyne K, Guaou Guaou N, Boyle D, Skyrnarz-Murphy K, Gonzalves SM. The UFS-QOL, a new disease-specific symptom and health-related quality of life questionnaire for leiomyomata. *Obstet Gynecol.* 2002;99:290-300
28. Harding G, Coyne KS, Thompson CL, Spies JB. The responsiveness of the uterine fibroid symptom and health-related quality of life questionnaire (UFS-QOL). *Health Qual Life Outcomes.* 2008;6:99
29. Kohler MO, Mougenot C, Quesson B, Enholm J, Le Bail B, Laurent C, Moonen CT, Ehnholm GJ. Volumetric HIFU ablation under 3D guidance of rapid MRI thermometry. *Med Phys.* 2009;36:3521-3535
30. Kim YS, Trillaud H, Rhim H, Lim HK, Mali W, Voogt M, Barkhausen J, Eckey T, Köhler MO, Keserci B, Mougenot C, Sokka SD, Soini J, Nieminen HJ. MR thermometry analysis of sonication accuracy and safety margin of volumetric MR imaging-guided high-intensity focused ultrasound ablation of symptomatic uterine fibroids. *Radiology.* 2012;265:627-637
31. Enholm JK, Kohler MO, Quesson B, Mougenot C, Moonen CT, Sokka SD. Improved volumetric MR-HIFU ablation by robust binary feedback control. *IEEE Trans Biomed Eng.* 2010;57:103-113
32. LeBlang SD, Hoctor K, Steinberg FL. Leiomyoma shrinkage after MRI-guided focused ultrasound treatment: report of 80 patients. *AJR Am J Roentgenol.* 2010;194:274-280
33. Park MJ, Kim YS, Keserci B, Rhim H, Lim HK. Volumetric MR-guided high-intensity focused ultrasound ablation of uterine fibroids: treatment speed and factors influencing speed. *Eur Radiol.* 2013;23:943-950
34. Stewart EA, Gostout B, Rabinovici J, Kim HS, Regan L, Tempany CM. Sustained relief of leiomyoma symptoms by using focused ultrasound surgery. *Obstet Gynecol.* 2007;110:279-287
35. Morita Y, Ito N, Hikida H, Takeuchi S, Nakamura K, Ohashi H. Non-invasive magnetic resonance imaging-guided focused ultrasound treatment for uterine fibroids - early experience. *Eur J Obstet Gynecol Reprod Biol.* 2008;139:199-203
36. Waltman AC, Courey WR, Athanasoulis C, Baum S. Technique for left gastric artery catheterization. *Radiology.* 1973;109:732-734
37. Costantino M, Lee J, McCullough M, Nsouli-Maktabi H, Spies JB. Bilateral versus unilateral femoral access for uterine artery embolization: results of a randomized comparative trial. *J Vasc Interv Radiol.* 2010;21:829-835; quiz 835
38. Froeling V, Meckelburg K, Schreiter NF, Scheurig-Muenkler C, Kamp J, Maurer MH, Beck A, Hamm B, Kroencke TJ. Outcome of uterine artery embolization versus MR-guided high-intensity focused ultrasound treatment for uterine fibroids: Long-term results. *Eur J Radiol.* 2013;82:2265-2269
39. Fennessy FM, Tempany CM, McDannold NJ, So MJ, Hesley G, Gostout B, Kim HS, Holland GA, Sarti DA, Hynynen K, Jolesz FA, Stewart EA. Uterine leiomyomas: MR imaging-guided focused ultrasound surgery--results of different treatment protocols. *Radiology.* 2007;243:885-893
40. Al Hilli MM, Stewart EA. Magnetic resonance-guided focused ultrasound surgery. *Semin Reprod Med.* 2010;28:242-249
41. Yoon SW, Lee C, Cha SH, Yu JS, Na YJ, Kim KA, Jung SG, Kim SJ. Patient selection guidelines in MR-guided focused ultrasound surgery of uterine fibroids: a pictorial guide to relevant findings in screening pelvic MRI. *Eur Radiol.* 2008;18:2997-3006
42. Machtinger R, Inbar Y, Cohen-Eylon S, Admon D, Alagem-Mizrachi A, Rabinovici J. MR-guided focus ultrasound (MRgFUS) for symptomatic uterine fibroids: predictors of treatment success. *Hum Reprod.* 2012;27:3425-3431
43. Park MJ, Kim YS, Rhim H, Lim HK. Safety and Therapeutic Efficacy of Complete or Near-Complete Ablation of Symptomatic Uterine Fibroid Tumors by MR Imaging-Guided High-Intensity Focused US Therapy. *J Vasc Interv Radiol.* 2014;2:231-9.
44. Gavrilova-Jordan LP, Rose CH, Traynor KD, Brost BC, Gostout BS. Successful term pregnancy following MR-guided focused ultrasound treatment of uterine leiomyoma. *J Perinatol.* 2007;27:59-61
45. Hanstede MM, Tempany CM, Stewart EA. Focused ultrasound surgery of intramural leiomyomas may facilitate fertility: a case report. *Fertil Steril.* 2007;88:497 e495-497
46. Funaki K, Fukunishi H, Funaki T, Sawada K, Kaji Y, Maruo T. Magnetic resonance-guided focused ultrasound surgery for uterine fibroids: relationship between the therapeutic effects and signal intensity of preexisting T2-weighted magnetic resonance images. *Am J Obstet Gynecol.* 2007;196:184 e181-186

# 4 Volumetric MR-guided high-intensity focused ultrasound with direct skin cooling for the treatment of symptomatic uterine fibroids: proof of concept study

Marlijne E. Ikink
Johanna M.M. van Breugel
Gerald Schubert
Robbert J. Nijenhuis
Lambertus W. Bartels
Chrit T.W. Moonen
Maurice A.A.J. van den Bosch

*Accepted for publication in Biomed Research International*

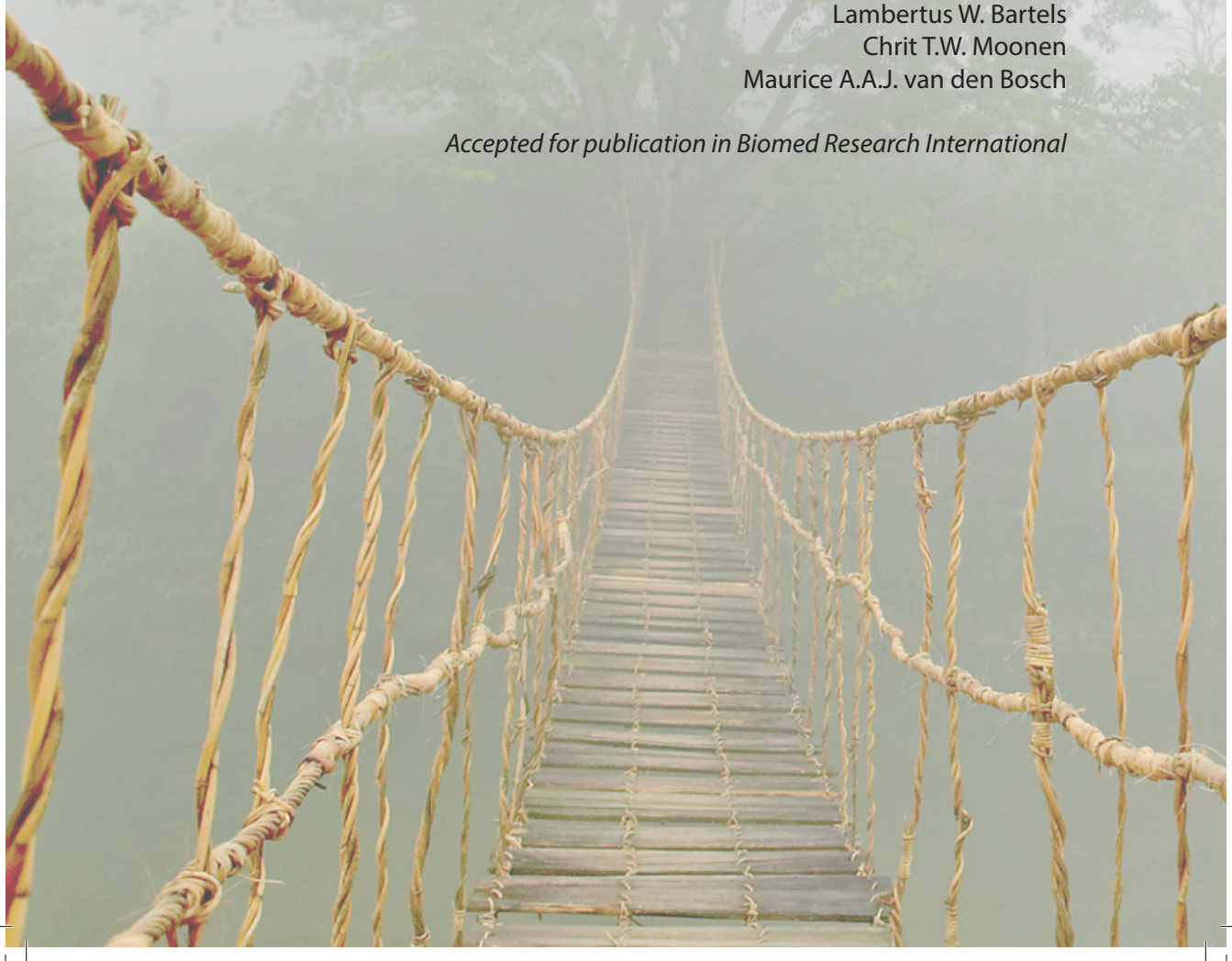

# Abstract

**Objective**

To prospectively assess the safety and technical feasibility of volumetric magnetic resonance-guided high-intensity focused ultrasound (MR-HIFU) ablation with direct skin cooling (DISC) during treatment of uterine fibroids.

**Methods**

In this proof of concept study, eight patients were consecutively selected for clinical MR-HIFU ablation of uterine fibroids with use of an additional DISC device to maintain a constant temperature (T≈20°C) at the interface between the HIFU table top and the patient's skin. Technical feasibility was determined by verification of successful completion of MR-HIFU ablation. Contrast-enhanced T1-weighted MRI was used to measure the treatment effect (i.e. non-perfused volume (NPV) ratio). Safety was evaluated by recording of adverse events (AEs) and their relation to the investigational DISC device within 30 days' follow-up.

**Results**

All MR-HIFU treatments were successfully completed in an outpatient setting. The median NPV ratio was 0.56 (IQR [0.27-0.72]). Immediately after treatment, two patients experienced coldness related discomfort which resolved the same day. No serious (device-related) AEs were reported within 30 days' follow-up. No skin burns, cold injuries or subcutaneous oedema were observed in patients treated with the DISC device.

**Conclusion**

This study showed that it is technically feasible and safe to complete a volumetric MR-HIFU ablation with DISC. This technique may further reduce the risk of thermal injury to the abdominal wall during MR-HIFU ablation of uterine fibroids.

## Introduction

Over the last decade, minimally or non-invasive treatment options have gained popularity and continue to evolve and expand with developments in technology and growing experience. Numerous technological advances have been driven by the observed benefits of the minimally invasive approach, including less side-effects, shorter recovery time, and favourable cosmetic results. Since the first feasibility report in 2003[1], magnetic resonance-guided high-intensity focused ultrasound (MR-HIFU) has been successfully employed to treat symptomatic uterine fibroids in a clinical setting. Although not all uterine fibroids are symptomatic, they are in at least 25% of Caucasian women in their reproductive years associated with significant morbidity, including abnormal menstrual bleeding, pelvic discomfort, and reproductive dysfunction[2,3]. An increasing number of symptomatic patients demands less invasive treatment methods in order to achieve symptom relief and a better quality of life. MR-HIFU offers the advantage to perform completely non-invasive thermal ablation, because the ultrasound transducer is located outside the abdomen and steers high-intensity focused ultrasound energy into the targeted area through the intact skin.

Since 2010, a volumetric MR-HIFU system has been available for routine clinical treatments of uterine fibroids[4]. The volumetric ablation approach utilises the accumulation of heat by electronically steering the focus along outward-moving concentric circles, producing well defined regions of protein denaturation, irreversible cell damage, and coagulative necrosis. However, the treatment of larger ablation volumes requires more thermal energy which may lead to a temperature increase along the ultrasound beam axis in the near field (i.e. intermediate layers located between the ultrasound transducer and the target region, such as epidermis, dermis, subcutaneous tissue and deeper abdominal layers)[5]. During periods of thermal stress, the rate of heat transfer through the skin surface depends primarily on the heat capacity (or ability to absorb heat) and the thermal conductivity (or ability to transfer heat) of the skin to facilitate heat loss[6]. This heat flux may be enhanced through blood circulation by carrying the heat to adjacent tissues[7,8]. Temperature rise within the skin layers will mainly occur in the subcutaneous tissue due to its lower specific heat capacity[6], insulator properties[6,7,9] and its lower blood supply[10-12] than that of other tissues in the abdominal wall. Additionally, reflections at boundaries between different media (e.g. air-skin or skin-fat) can occur because of differences in the acoustic impedance of various media[13]. The transmission losses from reflection at the skin interface and attenuation through the skin layers might lead to hot spots and skin overheating. Although MR-HIFU ablation of uterine fibroids is related to a low complication rate, skin toxicity and abdominal discomfort have been described by several groups[1,14-21]. Undesired heat accumulation in the near field and target area is moderated by enforcing conservative cooling times between the subsequent energy depositions (sonications) to prevent irreversible thermal tissue damage[22,23], such as skin burns, subcutaneous oedema formation or fat necrosis[24]. The cooling time is chosen to ensure return of the heated tissue layers to body temperature, and cooling ranges typically a few minutes per energy delivery. This leads to undesirably long delays between the sonications, which contributes to prolonged overall treatment times. It would therefore be valuable to regulate the temperature of the skin layers at a constant (room) temperature to reduce thermal tissue damage during MR-HIFU ablation, and accordingly, speed-up the treatment procedure.

In this study we demonstrate the concept for the clinical use of a direct skin cooling (DISC) device added to an MR-HIFU system during volumetric ablation of uterine fibroids.

The purpose of this study was to evaluate the feasibility and safety of uterine fibroid treatments using this DISC system as additional buffer against potential adverse events related to skin heating.

## Materials and methods

### Patients and lesions

This prospective non-randomised proof of concept study (NL45458.041.13) was approved by the institutional review board and was conducted in accordance with the rules for international good clinical practice. Patients who participated in this study were already selected for clinical MR-HIFU ablation of uterine fibroids based on their medical history, physical examination and diagnostic pelvic MRI examination. Routine inclusion and exclusion was carried out, eligible patients met the following inclusion criteria[21]: (1) 18 years or older (2) clinically diagnosed with symptomatic uterine fibroids, (3) referred by their gynaecologists with an absolute indication for intervention, (4) premenopausal or perimenopausal, (5) not currently pregnant or breastfeeding, (6) no general contraindications for magnetic resonance imaging (MRI) and MR contrast agents, and (7) able to undergo the MR-HIFU procedure based on diagnostic pelvic MRI examination in prone position (Achieva 1.5-T, Philips Healthcare, Best, The Netherlands). Exclusion criteria were: (1) the presence of other pelvic diseases, (2) unavoidable extensive scar tissue in the lower abdomen (in some cases alternate ultrasound beam paths were possible to avoid scar tissue, e.g. via beam shaping or beam angulation), (3) interposition of the bowel between the anterior abdominal wall and the dominant uterine fibroid, (4) excessive fibroid size (≥ 12 cm), and (5) too many lesions (≥ 10 uterine fibroids). All patients gave written informed consent for conducting an MR-HIFU procedure with the presence of the direct skin cooling (DISC) device.



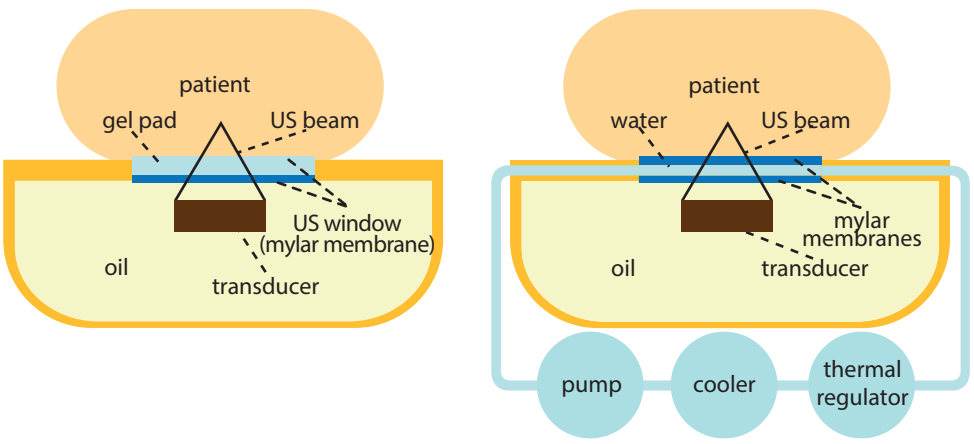


**Figure 1.** Schematic illustration of the differences between the clinical volumetric MR-HIFU system with (right) and without (left) the presence of the investigational DISC device.

**MR-HIFU system**

All treatments were performed on a modified clinical MR-HIFU fibroid therapy system (Sonalleve, Philips Healthcare, Vantaa, Finland) integrated into a 1.5-T MRI scanner (Achieva, Philips Healthcare, Best, The Netherlands). MR images were used for treatment localisation, feedback control (beam guidance), real-time temperature mapping with the proton resonance frequency shift (PRFS) thermometry method, and post-treatment verification of the ablated tissue. The curved patient MR table top incorporated a phased-array 256-channel HIFU transducer (radius of curvature: 14 cm, operating at 1.2 megahertz [MHz]) housed in a electromechanical positioning system to deliver spatially and temporally controlled heating. The DISC device consisted of a liquid (water) cooling reservoir which was mounted on top of the standard clinical MR-HIFU table top, between the degassed liquid (oil) bath - in which the HIFU transducer is immersed - and the patients' skin. A schematic illustration of the clinical volumetric MR-HIFU system with and without the presence of the investigational DISC device is shown in *Figure 1*. The water cooling reservoir was connected to a water pump, cooling element, temperature regulator, degasser and a bubble-trap to assure that air bubbles were extracted from the DISC system. The temperature of the water cooling reservoir was regulated at a constant room temperature (T≈20°C), such that the temperature was well-tolerated on bare skin. The DISC system was filled with degassed water and turned on (10 minutes) before the start of the MR-HIFU treatment to establish the target temperature of the water cooling reservoir. By the active displacement of water through the liquid cooling reservoir (circuit) a stable temperature could be guaranteed. The temperatures in the water cooling reservoir were measured using a fibre-optical temperature sensor (SoftSens, Opsens inc., Quebec, Canada), which was placed in the water between the two Mylar (polyethylene terephthalate) membranes outside the immediate acoustic beam path. Since the skin was in direct contact with the cooled water reservoir (separated only by a 50 µm thick membrane), the measured water temperature directly reflected the patient's skin temperature throughout the MR-HIFU ablation. Local hotspots on skin level that appear during individual sonications are equilibrated on timescales of some tens of seconds. During acquisition of diagnostic MR images, the flow within the water cooling reservoir was stopped to prevent artefacts on the MR data.

**MR-HIFU procedure**

All patients were treated in an outpatient setting. Patient preparation on the day of the MR-HIFU procedure (i.e. hair removal of the lower abdomen; insertion of an intravenous line and Foley catheter), treatment planning, and the volumetric ablation protocol have been described in previous publications[19,21]. Cooling times were enforced as in normal MR-HIFU treatments, so that the DISC device was used as an additional safety buffer against potential adverse events related to skin heating. The required cooling times of at least 90 seconds were respected as suggested by the feedback MR-HIFU system. A standardised preprocedural pain management protocol was used with paracetamol 1,000 mg intravenous (Paracetamol Kabi®, 10 mg/ml, Fresenuis Kabi Nederland B.V., Schelle, Belgium), diclofenac 75 mg intravenous (voltaren®, 25 mg/ml, Novartis Pharma B.V., Arnhem, The Netherlands), and oxycodone 5 mg capsules (OxyNorm®, 5 mg, Mundipharma Pharmaceuticals B.V., Hoevelaken, The Netherlands). In this study, patients were asked to lie down in prone position (feet first) on the patient MR table top with the integrated DISC device. A wetted ultrasound gel pad (7.5 mm) or a thin mixture (10:1) of degassed water and ultrasound gel (gel film) were used as coupling agents to provide adequate

direct contact for the ultrasound waves to penetrate the patient's skin. Two different types of acoustic couplers were evaluated, in order to assess whether treatment could also be carried out without the commonly used gel pad. Standard MR images were acquired to detect any obstacles in the ultrasound beam path and the contact surface to ensure that MR-HIFU ablation was safe with respect to heating in unwanted locations due to the presence of air bubbles, scars, bowel, bone and/or implants. A typical representation of the MR images in the MR-HIFU user interface is shown in *Figure 2*. The following MR sequences were used: coronal membrane bubble scan (three-dimensional (3D) spoiled gradient echo

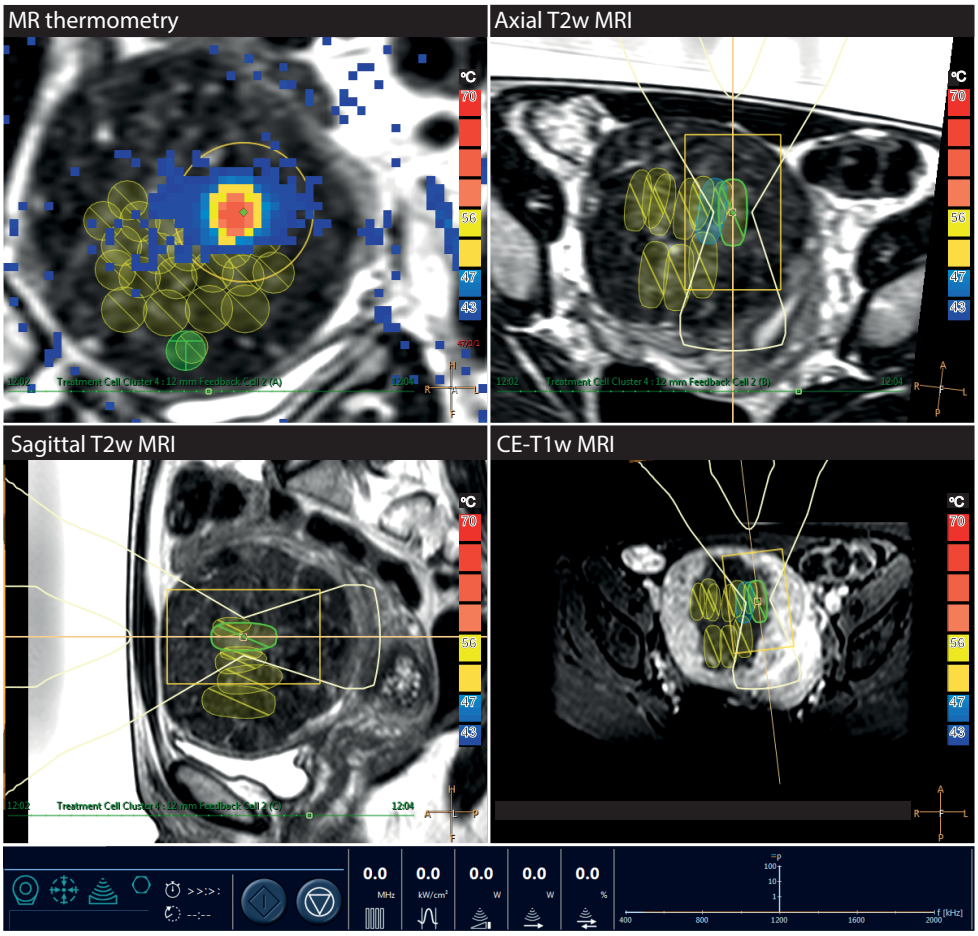


**Figure 2.** Typical representation of the MR images in the MR-HIFU user interface during treatment of uterine fibroids. The patient was lying in prone position (feet first) on the MR table top with the integrated direct skin cooling (DISC) device. The uterine fibroid was positioned directly above the MR-HIFU transducer. The ultrasound beam path was planned using T2-weighted MRI in three orthogonal planes, i.e. coronal (top left), axial (top right) and sagittal (bottom left) plane. During each sonication, colour temperature maps were computed by the MR-HIFU system using the proton resonance frequency shift (PRFS) thermometry method, and shown on top of the anatomical images (top left). Immediately after MR-HIFU treatment, the volume that was successfully treated was defined as the non-enhancing part of the fibroid on contrast-enhanced T1-weighted MRI (bottom right).

(FFE) with repetition time [TR], 5.8 milliseconds [ms]; echo time [TE], 4.0 ms; flip angle [FA], 6°; field of view [FOV], 260 mm × 260 mm; acquired [ACQ] voxel size, 1.00 × 1.00 × 2.00 $mm^3$; reconstructed [REC] voxel size, 0.49 × 0.49 × 1.00 $mm^3$; number of averages [NSA], 6; acquisition time, 00:39 minutes), coronal skin bubble scan (multi-slice single-echo FFE with TR, 150 ms; TE, 15 ms; FA, 55°; FOV, 280 mm × 280 mm; ACQ voxel size, 1.25 × 1.25 × 2.50 $mm^3$; REC voxel size, 0.31 × 0.31 × 2.50 $mm^3$; NSA, 2; acquisition time, 00:38 minutes), coronal scar scan (single-echo 3D FFE with TR, 21 ms; TE, 6.0 ms; FA, 15°; FOV, 200 mm × 200 mm; ACQ voxel size, 0.89 × 0.89 × 2.00 $mm^3$; REC voxel size, 0.31 × 0.31 × 1.00 $mm^3$; NSA, 3; acquisition time, 02:06.5 minutes), anatomical 3D T2-weighted (T2w) turbo spin echo (TSE) with TR, 1425 ms; TE, 130 ms; FA, 90°; FOV, 250 mm × 250 mm; ACQ voxel size, 1.20 × 1.39 × 3.00 $mm^3$; REC voxel size, 0.49 × 0.49 × 1.50 $mm^3$; NSA, 2; acquisition time, 03:50.8 minutes, and 3D T1-weighted (T1w) FFE with TR, 3.6 ms; TE, 1.90 ms; FA, 7°; FOV, 220 mm × 240 mm; ACQ voxel size, 1.25 × 1.53 × 2.50 $mm^3$; REC voxel size, 0.47 × 0.47 × 1.25 $mm^3$; NSA, 8; acquisition time, 01:57.3 minutes. During the treatment procedure, patients received conscious sedation (propofol-ketamine combination) to reduce and control pain or discomfort and involuntary movements. Monitored anaesthesia care was provided by the anaesthesiologist (procedural sedation specialist), which included preprocedural

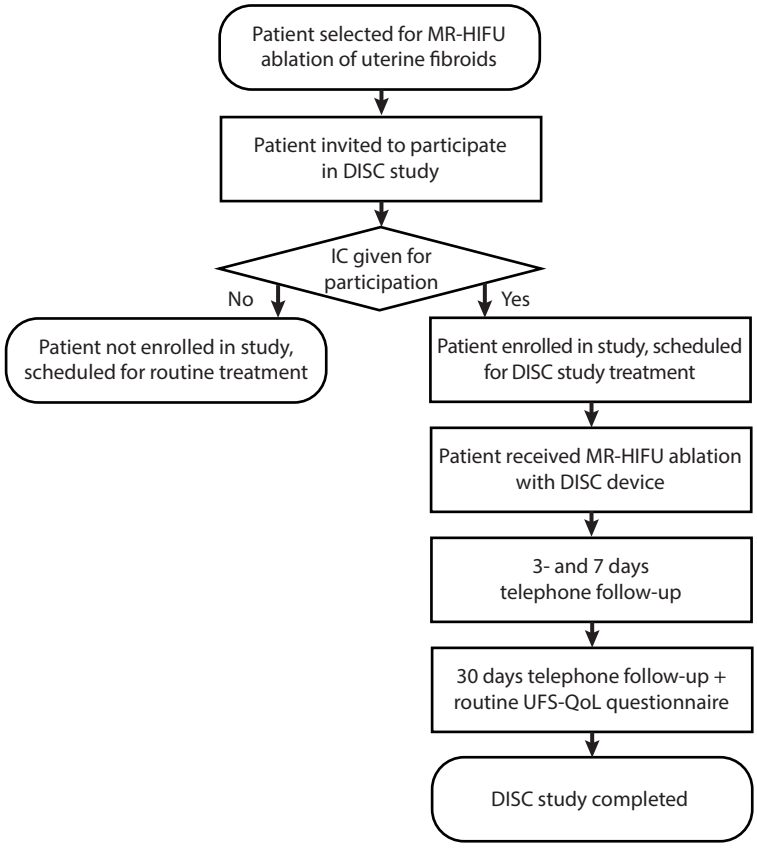


**Figure 3.** Flowchart shows the patients' progress (n=8) through the DISC study. MR-HIFU, magnetic resonance-guided high-intensity focused ultrasound; DISC, direct skin cooling; IC, informed consent; UFS-QoL, uterine fibroid symptom and health-related quality of life

screening, intraprocedural support of vital functions and administration of anaesthetic agents, and post-procedural anaesthesia management. After completion of the MR-HIFU procedure, a set of MR images of the target region was obtained including a contrast-enhanced (gadobutrol, Gadovist®, 0.1 mmol/kg, Bayer Schering Pharma) T1-weighted (CE-T1w) TFE sequence (with TR, 5.4 ms; TE, 2.6 ms; FA, 10°; FOV, 250 mm × 250 mm; ACQ voxel size, 1.49 × 1.89 × 3.00 $mm^3$; REC voxel size, 0.49 × 0.49 × 1.50 $mm^3$; NSA, 4; acquisition time, 02:14.5 minutes) to allow a sum-of-slice measurement of the non-perfused volume (NPV), indicating the volume of fibroid tissue that is non-viable. Following this, patients were conducted to the recovery room for medical supervision before being discharged from the hospital on the same day.



**Data collection**

The primary endpoint of this study was the technical feasibility of clinical MR-HIFU fibroid treatments with direct skin cooling, as determined by recording the successfully completed treatments using the investigational DISC device. Treatment completion was judged by an experienced operating physician (M.v.d.B.). If a treatment was aborted before the desired ablation volume was achieved and the back-up CE-labelled MR-HIFU system had to be used, the treatment was counted as a failure. The extent of treatment was reported by measuring the NPV ratios, defined as the non-enhancing part of the fibroid divided by the fibroid volume. The achieved NPV ratios were compared to data from the literature, to assess whether the performed treatments represent typical MR-HIFU ablations. In order to determine the effectiveness of the MR-HIFU treatments with the DISC device, the energy deposition rate (kilojoule per hour [kJ/h]) was calculated by dividing the deposited treatment energy [kJ] by the total treatment time (1/[h]). The treatment time was defined as the time from the start of the first to the end of the last sonication.

The secondary endpoint of this study was to gain insights into factors influencing the safety. Safety was assessed by recording (serious) adverse events and whether they were related to the investigational DISC device, in particular by inspection of patients' skin immediately after MR-HIFU treatment. All adverse events (AEs) were recorded and classified following the 14155:2011 standard for Good Clinical Practice in clinical investigation of medical devices for human subjects issued by the International Organization for Standardization (ISO). Any AEs observed during or after MR-HIFU treatment were followed and documented until they had abated, or until a stable situation had been reached. Patients were contacted by telephone 3 days, 7 days and 30 days after the MR-HIFU procedure to determine whether any AEs had occurred. A pain assessment scale was obtained using the Visual Analogue Scale (VAS) from 0 (no pain) to 10 (worst pain possible). The flowchart in *Figure 3* shows the patients' progress through the study.

**Statistical analysis**

Data were prospectively collected and analysed to evaluate the safety and feasibility of performing MR-HIFU treatment of uterine fibroids in a volumetric MR-HIFU system equipped with a DISC device. Descriptive statistics were used to describe the distribution of the patients' demographic and lesion characteristics. The treatment data of each patient was subsequently summarised and reported. Categorical data are presented in number and percentage, whereas continuous data are given in median and interquartile range (IQR). Statistical analyses were performed using IBM SPSS Statistics, version 20.0 (Armonk, New York, USA).

## Results

Eight Caucasian patients with nine treatable uterine fibroids were enrolled in this study. One patient was treated for two uterine fibroids during the same MR-HIFU treatment. Three patients had a scar in the lower abdomen: one patient (ID #4) had undergone an abdominal myomectomy (Pfannenstiel incision), one patient (ID #1) underwent an open appendectomy (McBurney incision), and one patient (ID #2) had minor laparoscopic scars after a diagnostic laparoscopy due to chronic abdominal pain. In patient #4, urinary bladder filling (with a saline solution) was used to avoid the surgical scar in the ultrasound beam path. Baseline data collected for each patient at the beginning of the study are presented in *Table 1*. All MR-HIFU treatments were successfully completed using the investigational DISC device, no technical failure was observed. The use of the back-up CE-

**Table 1.** Baseline characteristics and MRI findings (n=8)

| Patient characteristics | Value |
|---|---|
| Age (years)[a] | 42.5 (38.8-47.8) |
| BMI (kg/m$^2$)[a] | 23.1 (19.9-28.1) |
| Symptoms[b] | |
| Menorrhagia | 3 (38%) |
| Bulky symptoms | 4 (50%) |
| Infertility | 1 (12%) |
| tSSS[a] | 57.9 (38.3-79.0) |
| Total HRQoL[a] | 48.7 (28.9-80.4) |
| **Lesion characteristics** | **Value** |
| Number of fibroids[b] | |
| Solitary fibroid | 2 (25%) |
| Multiple fibroids | 6 (75%) |
| 2-5 fibroids | 4 (67%) |
| 6-10 fibroids | 2 (33%) |
| Location of the fibroids[b] | |
| Intramural | 6 (67%) |
| Submucosal | 3 (33%) |
| Type of fibroid[b] | |
| Type 1 | 4 (45%) |
| Type 2 | 3 (33%) |
| Type 3 | 2 (22%) |
| Maximum fibroid diameter (cm)[a] | 7.7 (5.1-8.8) |
| Uterine fibroid volume (cm$^3$)[a] | 147 (49-338) |

[a]Median (interquartile range); [b]number (percentage); BMI, body mass index; tSSS, transformed symptom severity score (range 0-100), high scores indicate more severe symptoms; HRQoL, health-related quality of life (range 0-100), high scores indicate better quality of life; Type 1, low signal intensity on T2-weighted imaging; Type 2, intermediate signal intensity on T2-weighted imaging; Type 3, high signal intensity on T2-weighted imaging; NPV, non-perfused volume

labelled MR-HIFU system was not necessary. The median treatment time was 192 minutes (IQR [180-225]), with a median energy deposition rate of 67 kJ/h (IQR [55-92]). The median volume of the uterine fibroids was 147 $cm^3$ (IQR [49-338]), the median maximum fibroid diameter was 7.7 cm (IQR [5.1-8.8]). A median non-perfused volume of 56 $cm^3$ (IQR [14-91]) was achieved, and a median NPV ratio of 0.56 (IQR [0.27-0.72]) was found. In one patient (ID #7), no NPV could be achieved due to insufficient heating probably as a result of the tissue characteristics of the uterine fibroid (type 3)[25]. *Table 2* shows an overview of the treatment data of each patient treated in this study.

No serious (device-related) adverse events were observed within 30 days' follow-up. No patient required prolonged observation before discharge or readmission after hospital discharge. In particular, no skin burns, cold injuries or subcutaneous oedema (determined by increased signal intensity on T2w images) were observed in patients treated with the DISC device. Several mild AEs were reported, such as abdominal pain or cramping (n=3), back pain (n=3), abdominal tenderness (n=2), ergonomic problems (n=2), viz. fibular compression neuropathy due to external pressure at the right fibular head during a long treatment procedure of 230 minutes (ID #3) and pressure marks due to the curved patient table top, dyspepsia and constipation (n=2), dizziness (n=3), and lethargy (n=4). One mild device-related AE occurred, viz. coldness related discomfort which was rapidly resolved with a hot water bottle on the day of treatment (n=2). At the moment of hospital discharge, the median VAS score was 1.5 (IQR [0.25-3.0], range [0-7]). Typically, AEs resolved within 7 days' follow-up and patients were able to resume their daily activities again. However, after 30 days, two patients were still recovering from ongoing AEs (constipation and lethargy), both probably related to the administration of anaesthetic agents.



**Table 2.** Summary of treatment data of each patient treated with the DISC device

| Patient | | | Patient geometry | | Fibroid | | | | Treatment | | | | Patient condition | |
|---|---|---|---|---|---|---|---|---|---|---|---|---|---|---|
| ID | Age [yrs] | BMI [$kg/m^2$] | Subcut. fat [mm] | Abd. scars | Type | Volume ($cm^3$) | NPV ($cm^3$) | NPV ratio | ener-gy (kJ) | time (min) | Energy dep. rate [kJ/h] | Skin temp [°C] | skin red-ness | sub-cut. edema |
| 1 | 43 | 28.4 | 18-21 | yes | 2 | 408 | 249 | 0.61 | 368 | 223 | 99 | 23.0 | no | no |
| 2 | 48 | 28.1 | 28-33 | yes | 1 | 25 | 15 | 0.60 | 169 | 163 | 62 | 21.5 | no | no |
| 3 | 42 | 22.1 | 8-14 | no | 3 | 268 | 67 | 0.25 | 331 | 230 | 86 | 22.0 | no | no |
| 4 | 48 | 24.2 | 12-14 | yes | 2 | 77 | 56 | 0.72 | 155 | 189 | 49 | 21.5 | no | no |
| 5 | 47 | 19.7 | 8-10 | no | 1 | 73 | 52 | 0.71 | 234 | 191 | 74 | 21.5 | no | no |
| 6 | 38 | 28.0 | 14-20 | no | 1+1 | 17+147 | 14+66 | 0.82+0.45 | 250 | 225 | 64 | 20.5 | no | no |
| 7 | 31 | 20.3 | 7-15 | no | 3 | 200 | 0 | 0.00 | 294 | 177 | 100 | 21.0 | no | no |
| 8 | 41 | 18.4 | 2-4 | no | 2 | 415 | 115 | 0.28 | 183 | 193 | 63 | 20.5 | no | no |

ID, identification number; BMI, body mass index; subcut, subcutaneous; abd, abdominal; dep, deposition; skin temp, equilibrium temperature as measured in the water reservoir; subcut, subcutaneous

## Discussion

During MR-HIFU treatments, undesired heating outside of the targeted ablation area may occur, in particular in the near field region of the HIFU beam. Currently, the risk of near field damage is mitigated by the time-consuming enforcement of cooling periods between ultrasound sonications. Introduction of a cooled interface which allows direct cooling of the patient's skin may further mitigate undesired heating (by shifting the baseline temperature), potentially increasing treatment efficacy and providing an additional buffer. In this proof of concept study we have demonstrated the safety and feasibility of using a direct skin cooling (DISC) device added to a volumetric MR-HIFU system for uterine fibroid treatments. To the best of our knowledge, this concept has not yet been investigated in a clinical setting. Our results showed that it is technically feasible and safe to complete an MR-HIFU treatment with a DISC device. No thermal damage to the near field, due to temperature increase of the ultrasound energy emitted from the HIFU transducer, was observed in this study. All eight patients could be treated as in normal clinical practice, representing a typical case series of uterine fibroid MR-HIFU treatments. No clinical or technical problems have occurred preventing MR-HIFU treatments using the DISC device to be successfully completed. No serious (device-related) AEs occurred after treatment and the achieved median NPV ratio (0.56 (IQR [0.27-0.72]) was comparable to data previously published. Reported NPV ratios ranged from 0.40-0.70 with a median NPV ratio of 0.56[21,26-30]. Specifically, no skin redness and/or irritation of the abdominal wall - either related to skin heating or skin cooling - were seen. As known, cutaneous microvascular reactivity (viz. thermoregulatory reflex) is essential to maintain the human core temperature during challenges to thermal haemostasis[31,32]. Prolonged exposure of direct cooling of the skin will eventually lead to cutaneous vasoconstriction[33-35], which may induce ischaemia. Extended exposure to localised cold-induced vasoconstriction may cause various injuries to the patients' skin that typically fall within the domain termed non-freezing cold injury (NFCI)[36,37]. However, these injuries (e.g. chilblains or immersion foot) are most commonly reported to the body's lower extremities, such as the legs and feet[38,39]. In addition, literature evidence indicates that no serious thermal tissue damage is to be expected within several hours until freezing occurs[40,41]. In general, NFCI occur at temperatures of 0-15°C. Considering the temperatures and exposure times relevant for patients during an MR-HIFU procedure, it can be concluded that the probability of occurrence for this specific low temperature event was indeed very unlikely.

It should be noted that this is a technical feasibility study with a small number of patients (n=8). Despite the promising preliminary results, the current study was not designed to measure the efficacy of the cooling system. Therefore, further research is needed to assess the clinical efficacy of this investigational DISC device as add-on to the volumetric MR-HIFU system. In a future step, a clinical follow-up study will investigate to which extent the DISC system allows for speeding up uterine fibroid MR-HIFU treatments by benefiting from reduced cooling times. After each sonication, the cooling effect in the subcutaneous tissue layers will be systematically monitored using the T2-based thermometry as recently described by Baron *et al.*[42]. The acquired temperature (cool-down) information in the near field can be used to provide thermal feedback to the MR-HIFU system and use this to adjust the cooling periods between the subsequent energy depositions in real-time. This novel technique may result in some advantages for the patient and their treating physician: (1) ablation of larger volumes of (fibroid) tissue in the shortest period of time

that is safely possible, and (2) more efficient treatment of type 3 uterine fibroids with a high signal intensity on T2w imaging[25,43]. The fact that it is technically feasible to produce thermal lesions safely in the present study, highlights the potential of this DISC system in future MR-HIFU ablations of uterine fibroids. Another practical advantage of using DISC is that it seems sufficient to use a gel film (water-gel mixture) for acoustic coupling between the table top membrane and the depilated skin of the patient. Previously, it was easy to trap air bubbles between the commonly used (15 mm) gel pad and the patients' skin in the process of patient positioning. Since air bubbles may reflect the ultrasound energy - due to their low acoustic impedance[44] - they can cause abdominal pain or discomfort and skin burns. This restriction appears alleviated now by the use of a gel film, because we did not observe any air bubbles after positioning. Furthermore, without the insulating gel pad, the patient profits directly from the cooling effect without dissipation. Finally, the DISC system with gel-film has the same thickness as the old gel pads (*Figure1*). This means that it is possible to reach targets as deep in the patient body as before. Consequently, the use of a gel film will potentially reduce risks, and offers opportunities to speed up the patient preparation and overall treatment time.

Several limitations to the present study need to be acknowledged. First, we did not analyse the patient-reported outcomes of symptom severity (tSSS) and health-related quality of life (HRQoL) as measure of the treatment effect. The focus of the current study was to verify that the use of the DISC device did not affect the performance of the volumetric MR-HIFU system. The upcoming studies will require a larger patient cohort, larger ablation volumes, longer follow-up, and careful evaluation of the treatment efficacy using this DISC system. This information could be used to develop targeted interventions aimed at specific subgroups of patients, such as patients with hyper-intense uterine fibroids on pre-treatment T2w MRI[25] with the use of targeted vessel ablation[45]. Another limitation of our study is that we did the post-discharge follow-up by telephone interviewing. While this may not give us always an objective evaluation (due to absence of non-verbal cues), it provided us with the required information about the safety outcome of this study.

In conclusion, in this proof of concept study we successfully performed clinical volumetric MR-HIFU ablation of uterine fibroids using an additional DISC device for reducing the risk of thermal damage to the abdominal wall. On the basis of the small number of patients studied in this trial, using the additional DISC device appears to be safe. No serious (device-related) adverse events occurred.



## Acknowledgements

This work was supported in part by Philips Healthcare (Philips Medical Systems MR Finland). One author (G.S.) is an employee of Philips Healthcare, however the first two authors (M.E.I. and J.M.M.v.B) in control of the study data and data analysis are not employees of Philips Healthcare.

# References

1. Tempany CM, Stewart EA, McDannold N, Quade BJ, Jolesz FA, Hynynen K. MR imaging-guided focused ultrasound surgery of uterine leiomyomas: a feasibility study. *Radiology.* 2003;226:897-905
2. Cramer SF, Patel A. The frequency of uterine leiomyomas. *Am J Clin Pathol.* 1990;94:435-438
3. Buttram VC, Jr., Reiter RC. Uterine leiomyomata: etiology, symptomatology, and management. *Fertil Steril.* 1981;36:433-445
4. Kohler MO, Mougenot C, Quesson B, Enholm J, Le Bail B, Laurent C, Moonen CT, Ehnholm GJ. Volumetric HIFU ablation under 3D guidance of rapid MRI thermometry. *Med Phys.* 2009;36:3521-3535
5. Fan X, Hynynen K. Ultrasound surgery using multiple sonications--treatment time considerations. *Ultrasound Med Biol.* 1996;22:471-482
6. Henriques FC, Moritz AR. Studies of Thermal Injury: I. The Conduction of Heat to and through Skin and the Temperatures Attained Therein. A Theoretical and an Experimental Investigation. *Am J Pathol.* 1947;23:530-549
7. Anderson GS. Human morphology and temperature regulation. *Int J Biometeorol.* 1999;43:99-109
8. Kellogg DL, Pérgola P. Skin responses to exercise and training. In: Garrett WE, Kirkendall DT, ed. Exercise and Sport Science. 1st edn. Philadelphia, USA: Lippincott Williams & Wilkins 2000:239-250
9. Cohen ML. Measurement of the thermal properties of human skin. A review. *J Invest Dermatol.* 1977;69:333-338
10. Rowland M, Tozer TN. Membranes and Distribution Table 4-4. In: Clinical Pharmacokinetics and Pharmacodynamics: Concepts And Applications. 4th edn. Philadelphia, USA: Wolters Kluwer Health/Lippincott William & Wilkins 2010:73-110
11. Heinonen I, Kemppainen J, Kaskinoro K, Knuuti J, Boushel R, Kalliokoski KK. Capacity and hypoxic response of subcutaneous adipose tissue blood flow in humans. *Circ J.* 2014;78:1501-1506
12. Johnson JM, Brengelmann GL, Hales JR, Vanhoutte PM, Wenger CB. Regulation of the cutaneous circulation. *Fed Proc.* 1986;45:2841-2850
13. Williams R. Production and transmission of ultrasound. *Physiotherapy.* 1987;73:113-116
14. Stewart EA, Gedroyc WM, Tempany CM, Quade BJ, Inbar Y, Ehrenstein T, Shushan A, Hindley JT, Goldin RD, David M, Sklair M, Rabinovici J. Focused ultrasound treatment of uterine fibroid tumors: safety and feasibility of a noninvasive thermoablative technique. *Am J Obstet Gynecol.* 2003;189:48-54
15. Stewart EA, Rabinovici J, Tempany CM, Inbar Y, Regan L, Gostout B, Hesley G, Kim HS, Hengst S, Gedroyc WM. Clinical outcomes of focused ultrasound surgery for the treatment of uterine fibroids. *Fertil Steril.* 2006;85:22-29
16. Rabinovici J, Inbar Y, Revel A, Zalel Y, Gomori JM, Itzchak Y, Schiff E, Yagel S. Clinical improvement and shrinkage of uterine fibroids after thermal ablation by magnetic resonance-guided focused ultrasound surgery. *Ultrasound Obstet Gynecol.* 2007;30:771-777
17. Leon-Villapalos J, Kaniorou-Larai M, Dziewulski P. Full thickness abdominal burn following magnetic resonance guided focused ultrasound therapy. *Burns.* 2005;31:1054-1055
18. Hesley GK, Gorny KR, Henrichsen TL, Woodrum DA, Brown DL. A clinical review of focused ultrasound ablation with magnetic resonance guidance: an option for treating uterine fibroids. *Ultrasound Q.* 2008;24:131-139
19. Voogt MJ, Trillaud H, Kim YS, Mali WP, Barkhausen J, Bartels LW, Deckers R, Frulio N, Rhim H, Lim HK, Eckey T, Nieminen HJ, Mougenot C, Keserci B, Soini J, Vaara T, Köhler MO, Sokka S, van den Bosch MA. Volumetric feedback ablation of uterine fibroids using magnetic resonance-guided high intensity focused ultrasound therapy. *Eur Radiol.* 2012;22:411-417
20. Machtinger R, Inbar Y, Cohen-Eylon S, Admon D, Alagem-Mizrachi A, Rabinovici J. MR-guided focus ultrasound (MRgFUS) for symptomatic uterine fibroids: predictors of treatment success. *Hum Reprod.* 2012;27:3425-3431
21. Ikink ME, Voogt MJ, Verkooijen HM, Lohle PN, Schweitzer KJ, Franx A, Mali WP, Bartels LW, van den Bosch MA. Mid-term clinical efficacy of a volumetric magnetic resonance-guided high-intensity focused ultrasound technique for treatment of symptomatic uterine fibroids. *Eur Radiol.* 2013;23:3054-3061
22. Damianou C, Hynynen K. Focal spacing and near-field heating during pulsed high temperature ultrasound therapy. *Ultrasound Med Biol.* 1993;19:777-787
23. Hynynen K, Darkazanli A, Unger E, Schenck JF. MRI-guided noninvasive ultrasound surgery. *Med Phys.* 1993;20:107-115
24. Kim YS, Keserci B, Partanen A, Rhim H, Lim HK, Park MJ, Köhler MO. Volumetric MR-HIFU ablation of uterine fibroids: role of treatment cell size in the improvement of energy efficiency. *Eur J Radiol.* 2012;81:3652-3659

25. Funaki K, Fukunishi H, Funaki T, Sawada K, Kaji Y, Maruo T. Magnetic resonance-guided focused ultrasound surgery for uterine fibroids: relationship between the therapeutic effects and signal intensity of preexisting T2-weighted magnetic resonance images. *Am J Obstet Gynecol.* 2007;196:184 e181-186
26. Park MJ, Kim YS, Rhim H, Lim HK. Safety and therapeutic efficacy of complete or near-complete ablation of symptomatic uterine fibroid tumors by MR imaging-guided high-intensity focused US therapy. *J Vasc Interv Radiol.* 2014;25:231-239
27. Kim YS, Park MJ, Keserci B, Nurmilaukas K, Köhler MO, Rhim H, Lim HK. Uterine fibroids: postsonication temperature decay rate enables prediction of therapeutic responses to MR imaging-guided high-intensity focused ultrasound ablation. *Radiology.* 2014;270:589-600
28. Yoon SW, Cha SH, Ji YG, Kim HC, Lee MH, Cho JH. Magnetic resonance imaging-guided focused ultrasound surgery for symptomatic uterine fibroids: estimation of treatment efficacy using thermal dose calculations. *Eur J Obstet Gynecol Reprod Biol.* 2013;169:304-308
29. Park MJ, Kim YS, Keserci B, Rhim H, Lim HK. Volumetric MR-guided high-intensity focused ultrasound ablation of uterine fibroids: treatment speed and factors influencing speed. *Eur Radiol.* 2013;23:943-950
30. Yoon SW, Seong SJ, Jung SG, Lee SY, Jun HS, Lee JT. Mitigation of abdominal scars during MR-guided focused ultrasound treatment of uterine leiomyomas with the use of an energy-blocking scar patch. *J Vasc Interv Radiol.* 2011;22:1747-1750
31. Charkoudian N. Skin blood flow in adult human thermoregulation: how it works, when it does not, and why. *Mayo Clin Proc.* 2003;78:603-612
32. Johnson JM, Kellogg DL, Jr. Thermoregulatory and thermal control in the human cutaneous circulation. *Front Biosci (Schol Ed).* 2010;2:825-853
33. Khoshnevis S, Craik NK, Diller KR. Cold-induced vasoconstriction may persist long after cooling ends: an evaluation of multiple cryotherapy units. *Knee Surg Sports Traumatol Arthrosc.* 2014 Feb 23
34. Hodges GJ, Zhao K, Kosiba WA, Johnson JM. The involvement of nitric oxide in the cutaneous vasoconstrictor response to local cooling in humans. *J Physiol.* 2006;574:849-857
35. Minson CT. Thermal provocation to evaluate microvascular reactivity in human skin. *J Appl Physiol.* 2010;109:1239-1246
36. Imray CH, Richards P, Greeves J, Castellani JW. Nonfreezing cold-induced injuries. *J R Army Med Corps.* 2011;157:79-84
37. Long WB, 3rd, Edlich RF, Winters KL, Britt LD. Cold injuries. *J Long Term Eff Med Implants.* 2005;15:67-78
38. Ingram BJ, Raymond TJ. Recognition and treatment of freezing and nonfreezing cold injuries. *Curr Sports Med Rep.* 2013;12:125-130
39. Sallis R, Chassay CM. Recognizing and treating common cold-induced injury in outdoor sports. *Med Sci Sports Exerc.* 1999;31:1367-1373
40. McMahon JA, Howe A. Cold weather issues in sideline and event management. *Curr Sports Med Rep.* 2012;11:135-141
41. Tlougan BE, Mancini AJ, Mandell JA, Cohen DE, Sanchez MR. Skin conditions in figure skaters, ice-hockey players and speed skaters: part II - cold-induced, infectious and inflammatory dermatoses. *Sports Med.* 2011;41:967-984
42. Baron P, Ries M, Deckers R, de Greef M, Tanttu J, Köhler M, Viergever MA, Moonen CT, Bartels LW. In vivo T -based MR thermometry in adipose tissue layers for high-intensity focused ultrasound near-field monitoring. *Magn Reson Med.* 2014;72:1057-1064
43. Lenard ZM, McDannold NJ, Fennessy FM, Stewart EA, Jolesz FA, Hynynen K, Tempany CM. Uterine leiomyomas: MR imaging-guided focused ultrasound surgery--imaging predictors of success. *Radiology.* 2008;249:187-194
44. Wells PN. Review: absorption and dispersion of ultrasound in biological tissue. *Ultrasound Med Biol.* 1975;1:369-376
45. Voogt MJ, van Stralen M, Ikink ME, Deckers R, Vincken KL, Bartels LW, Mali WP, van den Bosch MA. Targeted vessel ablation for more efficient magnetic resonance-guided high-intensity focused ultrasound ablation of uterine fibroids. *Cardiovasc Intervent Radiol.* 2012;35:1205-1210

# PART II

# MRI FOR PREDICTION AND MEASUREMENT OF TREATMENT EFFECT

# 5 Diffusion-weighted MRI using different *b*-value combinations for the evaluation of treatment results after volumetric MR-guided high-intensity focused ultrasound ablation of uterine fibroids

Marlijne E. Ikink
Marianne J. Voogt
Maurice A.A.J. van den Bosch
Robbert J. Nijenhuis
Bilgin Keserci
Young-sun Kim
Koen L. Vincken
Lambertus W. Bartels

*Eur Radiol. 2014;24:2118-2127*

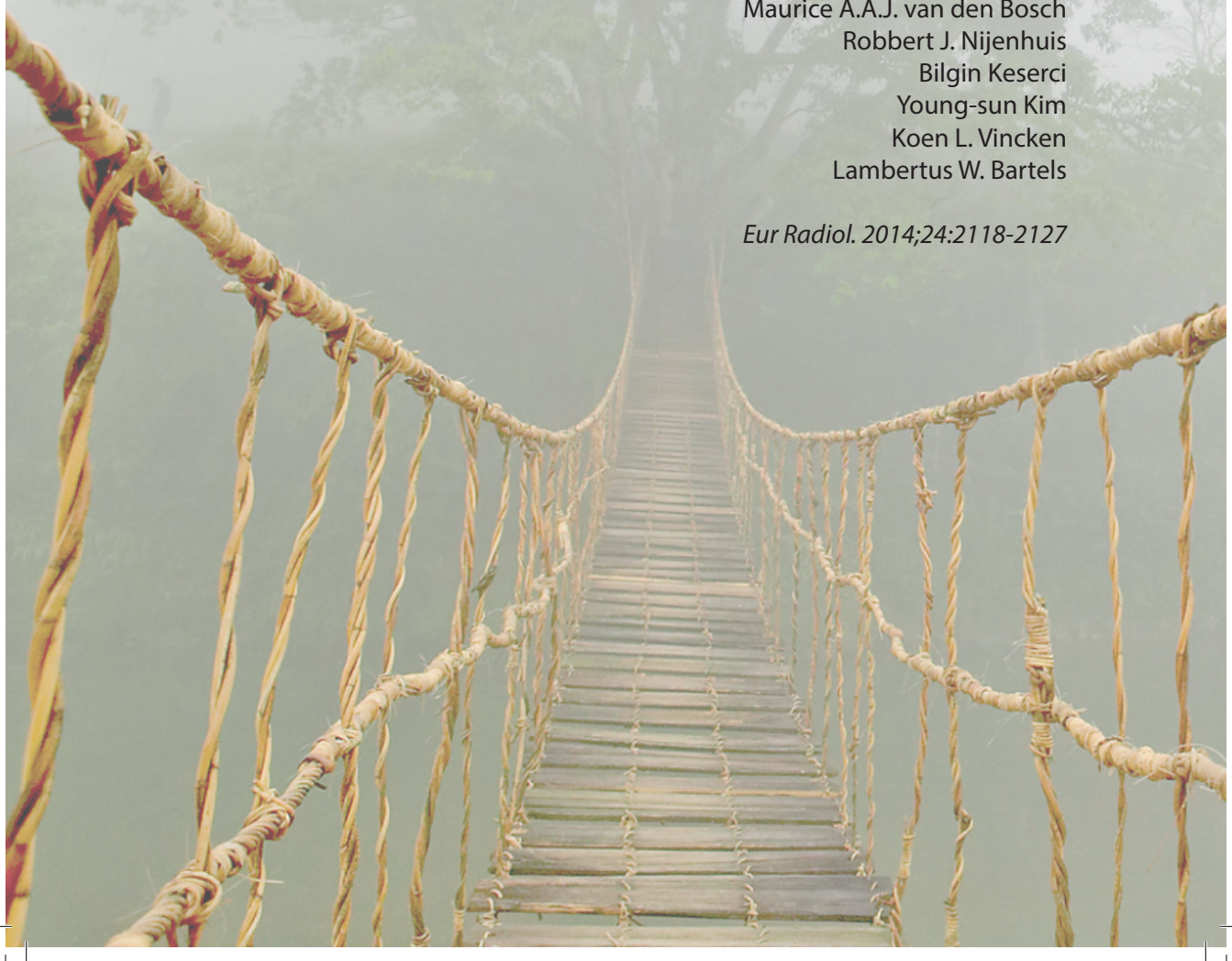

# Abstract

**Objective**

To assess the value of diffusion-weighted magnetic resonance imaging (DWI) and apparent diffusion coefficient (ADC) mapping using different *b*-value combinations for treatment evaluation after magnetic resonance-guided high-intensity focused ultrasound (MR-HIFU) of uterine fibroids.

**Methods**

Fifty-six patients with 67 uterine fibroids were treated with volumetric MR-HIFU. Pre-treatment and post-treatment images were obtained using contrast-enhanced T1-weighted (CE-T1w) MRI and DWI using $b$=0, 200, 400, 600, 800 s/mm$^2$. ADC maps were generated using subsets of *b*-values to investigate the effects of tissue ablation on water diffusion and perfusion in fibroids treated with MR-HIFU. Four combinations of *b*-values were used: (1) all *b*-values; (2) $b$=0, 200 s/mm$^2$; (3) $b$=400, 600, 800 s/mm$^2$; and (4) $b$=0, 800 s/mm$^2$.

**Results**

Using the lowest *b*-values (0 and 200 s/mm$^2$), the mean ADC value in the ablated tissue reduced significantly ($p<0.001$) compared to baseline. Calculating the ADC value with the highest *b*-values (400, 600, 800 s/mm$^2$), the ADC increased significantly ($p<0.001$) post-treatment. ADC maps calculated with the lowest *b*-values resulted in the best visual agreement of non-perfused fibroid tissue detected on CE-T1w MRI. Other *b*-value combinations and normal myometrium showed no difference in ADC after treatment.

**Conclusion**

A decrease in contrast agent uptake within the ablated region on CE-T1w MRI was correlated to a significant decreased ADC when $b$=0 and 200 s/mm$^2$ were used.


## Introduction

Uterine fibroids are common benign gynaecologic tumours, and primarily found in women of reproductive age with a progressive increase above the age of 40 years[1]. Fibroids are the leading indication for hysterectomy, and therefore constitute a major source of public healthcare costs worldwide[2,3]. Symptomatic women typically complain about abnormal uterine bleeding and pelvic discomfort due to mass effect, with a significant negative effect on their quality of life[4,5]. Many therapeutic options are available for treating these symptoms, including drug therapy, surgical interventions, uterine artery embolisation (UAE), and magnetic resonance-guided high-intensity focused ultrasound (MR-HIFU)[6]. The past decade, the demand for conservative treatments has increased. More women wish to preserve their uterus and fertility, and generally avoid invasive procedures associated with a longer recovery, higher morbidity and mortality[7,8]. MR-HIFU is a completely non-invasive outpatient image-guided technique used to thermally treat solid tumours[9,10]. Focused ultrasound energy is used to locally induce tissue heating, resulting in well-defined regions of protein denaturation, irreversible cell damage, and coagulative necrosis, while sparing healthy tissue outside the target area. Magnetic resonance imaging (MRI) offers excellent anatomical resolution for treatment planning, and has the possibility for real-time temperature mapping using MR thermometry techniques[11].

As with other non-invasive techniques, there is a need for methods to evaluate the therapeutic effect during the interventional procedure. Normally, contrast-enhanced T1-weighted (CE-T1w) MRI is used to assess the extent of tissue ablation immediately post-treatment. In such scans, ablated tissue will appear as a non-enhancing region. The sum of all non-perfused areas in the individual images - covering the treated fibroids times the slice thickness - is commonly referred to as the non-perfused volume (NPV). In practice, the NPV is often larger than expected considering the planned ablation volume, i.e. the total volume of treatment cells covering the target area. This effect is likely due to the destruction of blood vessels within the fibroid during treatment resulting in down-stream tissue necrosis[12,13]. For this reason, intraprocedural visualisation of the NPV in between subsequent sonications would be relevant, since the destructed tissue outside the treatment cells does not require further ablation. Identification of the actually treated volume could therefore result in a higher treatment efficiency. The intraprocedural application of contrast-enhanced imaging should be limited, given the possible side effects, the unknown safety profile of the contrast agent after heating, the relatively long clearance time of the agent, and the fact that the acceptable total dose of contrast agent is limited. Gadolinium-based MR contrast agents consists of a stable complex of gadolinium (Gd) with a ligand like diethylenetriaminepentaacetate (DTPA)[14]. Little is known about the stability of the Gd-complexes under MR-HIFU induced temperature elevation. There have been concerns about the entrapment of contrast agent in the ablated tissues, which might result in long-term retention of Gd in the body, followed by potential decomplexation of the Gd-chelate into the toxic components $Gd^{3+}$ and free organic ligand[15-17]. A repeatable method that does not require a gadolinium-based MR contrast agent would therefore be preferred.

An imaging method that has been suggested, for providing the required information for treatment evaluation, is diffusion-weighted magnetic resonance imaging (DWI)[18-22]. DWI provides tissue contrasts based on local differences in the diffusion of water molecules within the intracellular and extracellular space, using strong additional gradient lobes

in the MRI pulse sequence. DWI is based on the notion that the motion of spins in the presence of a heterogeneous magnetic field shall lead to a decrease in signal intensity[23-25]. These field inhomogeneities are created by adding two diffusion sensitizing gradient lobes to a T2-weighted spin echo-based pulse sequence, often with signal read-out using an echo planar imaging (EPI) train to shorten the scan duration. Spins in water molecules with only limited diffusion will show less signal loss than spins in highly mobile water, thereby leading to diffusion-weighting of the MR signal. The strength and timings of the additional gradient lobes determines the amount of diffusion-weighting, which is characterised by the *b*-value[23,26]. It is possible to calculate apparent diffusion coefficient (ADC) maps, by collecting images with at least two different values of the *b*-factor. Especially in well-perfused tissues, like uterine fibroids[27-29], the ADC is known to reflect not only the diffusion of water molecules, but also information about the microcirculation of blood in the capillaries (perfusion). Due to high blood flow velocities, the signal originating from the perfusion fraction inside a voxel will show a much more rapid attenuation as a function of the *b*-value than the true diffusion in the intracellular and extracellular spaces. In ADC maps that are calculated using images obtained at low *b*-values (0, 200 s/mm$^2$), the ADC values are therefore expected to strongly reflect perfusion effects[30,31]. Diffusion effects without perfusion influences would mainly be visible on ADC maps calculated from DWI acquired at multiple higher *b*-values[28,30,32]. Prior studies have already shown that thermal ablation with MR-HIFU is associated with an increased signal intensity on DWI, accompanied by a decreased signal intensity on the ADC map[18,19,21]. However, both groups used only the combination of two different *b*-values to calculate the ADC: 0 and 1000 s/mm$^2$. As the sensitivity of ADC to perfusion effects decreases when higher *b*-values are used, this combination of *b*-values will lead to ADC maps reflecting both real water diffusion and capillary blood flow effects. We hypothesised that by using five different *b*-values (0, 200, 400, 600, and 800 s/mm$^2$), perfusion and diffusion effects could be distinguished.

The aim of our study was to investigate the influence of the choice of *b*-values on the ADC, and to determine what combination of *b*-values allows the best differentiation between ablated fibroid tissue and untreated tissue in the acute phase immediately after volumetric MR-HIFU ablation of uterine fibroids.



## Materials and methods

**Patients**

Patients with symptomatic uterine fibroids who underwent a volumetric MR-HIFU procedure in one of the two hospitals were included in this study. Premenopausal or perimenopausal women with symptomatic uterine fibroids were referred by a general practitioner or gynaecologist and prospectively screened for eligibility. In *Table 1* the most important inclusion and exclusion criteria are summarised. All patients underwent a diagnostic pelvic MR examination to assess fibroid location, fibroid size, number, signal intensity on T2-weighted (T2w) imaging, and contrast enhancement. None of the patients had previously undergone uterine artery embolisation or MR-HIFU ablation. The study was approved by our local institutional review boards. All patients were counselled about the nature of treatment and gave written informed consent for the use of clinical and imaging data.

**Imaging protocol**

MR scans and therapeutic ablation sessions were performed on a clinical MR-HIFU system (Sonalleve, Philips Healthcare, Vantaa, Finland), integrated with a clinical 1.5-T MRI scanner (Achieva, Philips Healthcare, Best, The Netherlands). The patients were treated with a standardised procedure[33], in prone position. For adequate planning of the MR temperature mapping and DWI scans, anatomical three-dimensional (3D) T2w turbo spin echo (TSE) and 3D T1-weighted spoiled gradient echo ($T_1$ TFE) MR images were acquired after localizer scans at the start of the procedure. To facilitate planning, three orthogonal views based on automatically performed multiplanar reconstructions (MPRs) were shown on the HIFU console. The DWI series were additionally performed in the coronal plane using a fat suppressed single-shot spin echo-echo planar imaging (SE-EPI) sequence with *b*-values: 0, 200, 400, 600, and 800 s/mm$^2$. DWI series were acquired pre-treatment and immediately post-treatment, before administration of the contrast agent (Gadovist® 1.0 mmol/ml, gadobutrol, 0.1 mmol/kg, Bayer Schering Pharma). CE-T1w MRI were used to identify devascularised areas, defined as NPV. Dynamic MR temperature imaging was performed using the proton resonance frequency shift (PRFS) method[34,35], thermal dose maps were constructed from phase-difference images obtained from a gradient echo-echo planar imaging (FFE-EPI) sequence. The most relevant scan parameters used in this study are listed in *Table 2*.

**Image analysis**

ADC maps were calculated from the diffusion-weighted images using in-house developed software (imageXplorer, iX 2.0, Image Sciences Institute, Utrecht, The Netherlands), by applying a non-linear least squares method (Marquardt-Levenberg) for a voxel-wise fit of the following function $S(b) = S_0 \bullet e^{-b \bullet ADC}$ to the data, with $S_0$ and ADC as fit parameters. To evaluate to what extent the ADC value varied with the choice of *b*-values, and the diagnostic ability to differentiate between perfusion and diffusion effects, four different combinations of *b*-values were used to calculate the ADC pre-treatment and post-treatment: (1) using all *b*-values (0, 200, 400, 600, and 800 s/mm$^2$); (2) using the lowest two *b*-values to emphasize perfusion effects (0, 200 s/mm$^2$); (3) using the highest *b*-values to emphasize diffusion effects (400, 600, 800 s/mm$^2$); and (4) using lowest and highest *b*-values (0, 800 s/mm$^2$). The agreement between the ADC maps calculated from DWI and the NPV detected on CE-T1w MRI was visually assessed by the investigator. A circular region of interest (ROI) was placed within the fibroid pre-treatment; within the ablated part of the fibroid post-treatment, and in normal myometrium pre-treatment and post-treatment on a single coronal slice of the *b*=0 s/mm$^2$ diffusion-weighted image (i.e. an image without actual diffusion-weighting). The ROI was then copied onto the DWI and ADC maps. ROIs were drawn to include most of the treated fibroid. Care was taken to stay away from parts of the lesion that included adjacent non-lesion pixels to reduce partial volume effects between treated and untreated regions. ROI size was dependent on the size of the fibroid with a mean of 195±175 pixels (interquartile range, 79-243 pixels) and a mean radius of 87±30 mm (interquartile range, 65-109 mm).

**Statistical analysis**

First, we examined the reproducibility of the calculated ADC values by measuring the interrater reliability and interrater agreement. Intra-class correlation coefficient (ICC) was calculated for reliability testing. A correlation coefficient above 0.90 was classified 'good'

**Table 1.** Inclusion and exclusion criteria

| | |
|---|---|
| Inclusion | Women able to give informed consent and willing to attend all study visits |
| | Premenopausal and perimenopausal women, at least 18 years of age |
| | Women diagnosed with symptomatic uterine fibroids |
| Exclusion | Women who desire to become pregnant in the future or currently pregnant |
| | Known with other pelvic diseases, e.g. adenomyosis uteri or PID |
| | Extensive abdominal scar tissue interfering with safe treatment |
| | Uteruses of 24 gestational weeks (navel height) or larger |
| | Presence of all general contraindications for MRI |
| | More than 10 uterine fibroids |
| | Dominant uterine fibroid with a diameter ≤ 3 cm and ≥ 12 cm |
| | Pedunculated fibroids with a stalk base ≤30% of the maximal fibroid diameter |
| | No enhancement of dominant uterine fibroid with gadolinium (Gadovist®) |
| | Evidence of degeneration or calcification in the uterine fibroid |
| | MRI suspicious for malignant (pelvic) disease |

PID = pelvic inflammatory disease; MRI = magnetic resonance imaging



reliability. A Bland-Altman plot was constructed to provide visual information about the distribution of agreement. A paired samples *t*-test was used to calculate the statistical significance of any differences between pre-treatment and post-treatment ADC values of fibroid tissue, and pre-treatment and post-treatment ADC values of normal myometrium. The results are presented as mean ± standard deviation. Tests of the four different *b*-value combinations were conducted using Bonferroni adjusted alpha levels of 0.0125 per test (0.05/4). Statistical analyses were performed using IBM SPSS Statistics, version 20.0 (Armonk, New York, USA).

**Table 2.** Main scan parameters used for screening and treatment planning

| Sequence | T2w MRI | T1w MRI | DWI | CE-T1w MRI | MR thermometry |
|---|---|---|---|---|---|
| Type of scan | 3D TSE Turbo factor 83 | 3D FFE | Multi-slice single-shot SE-EPI | 3D TFE TFE factor 44 | M2D FFE-EPI EPI factor 11 |
| TE/TR (ms) | 130/1425 | 1.9/3.6 | 65/2500 | 2.6/5.4 | 19/41 |
| Flip angle (deg) | 90 | 7 | 90 | 10 | 20 |
| Fat suppression | No | No | SPAIR | SPAIR | ProSet |
| FOV (mm × mm) | 250 × 250 | 220 × 240 | 250 × 188 | 250 × 250 | 400 × 310 |
| ACQ voxel ($mm^3$) | 1.20×1.39×3.00 | 1.25×1.53×2.50 | 2.23×2.26×7.00 | 1.49×1.89×3.00 | 2.50×2.56×7.00 |
| REC voxel ($mm^3$) | 0.49×0.49×1.50 | 0.47×0.47×1.25 | 2.23×2.23×7.00 | 0.49×0.49×1.50 | 2.50×2.50×7.00 |
| Scan duration (min:sec) | 3:50.8 | 1:57.3 | 4:47.5 | 2:14.5 | 00:03.7* |

T2w, T2-weighted imaging; T1w, T1-weighted imaging; DWI, diffusion-weighted magnetic resonance imaging; CE, contrast-enhanced; 3D, three-dimensional; TSE, turbo spin echo; FFE, spoiled gradient echo; SE-EPI, spin echo-echo planar imaging TFE, ultra fast gradient echo; M2D, multiple (sequential) two-dimensional slices; FFE-EPI, gradient echo-echo planar imaging; TE/TR, echo time/repetition time; SPAIR, spectral attenuated inversion recovery; ProSet, principle of selective excitiation technique; FOV, field of view; ACQ, acquired; REC, reconstructed; *dynamic

# Results

**Patients and lesion characteristics**

In total, 56 patients were treated with volumetric MR-HIFU ablation and 67 uterine fibroids were analysed. Of those, 50 patients were included in one centre (The Netherlands). The mean age of the patients was 44.6±4.2 years. Fifteen women (27%) had a solitary fibroid. Most patients had multiple uterine fibroids: 32 women (57%) had 2-5 fibroids, and 9 women (16%) had 6-10 uterine fibroids. The fibroids were predominantly intramurally located (n=41), and the majority of fibroids showed a low-signal intensity on T2w MRI (n=42)[36]. The mean fibroid diameter was 8.8±2.9 cm. Before MR-HIFU treatment, DWI and ADC maps showed no regions of increased or decreased signal intensity, which means that there were no necrotic or degenerated areas in the fibroids that were selected for treatment. After treatment, the NPVs were visualised on CE-T1w MRI. The mean NPV as a percentage of the fibroid volume was 40±20%. An example is shown in *Figure 1a*. All corresponding DWI series showed increased signal intensity in these areas, reflecting restricted diffusion of water in tissue and/or the formation of oedema via the T2-shinethrough effect (*Figure 1b*).

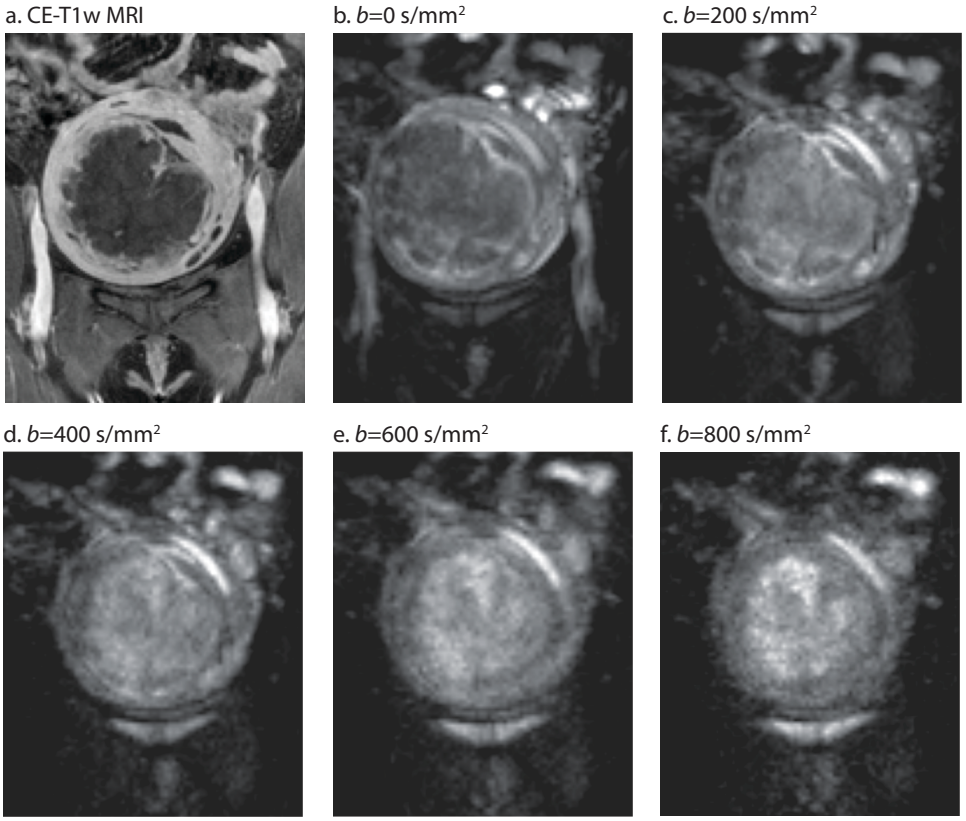


**Figure 1a.** Contrast-enhanced T1-weighted MRI showing the non-perfused volume
**1b-f.** Post-treatment diffusion-weighted MRI acquired using different *b*-values, showing areas of increased signal intensity inside the treated fibroid. Note: images are scaled per *b*-value.

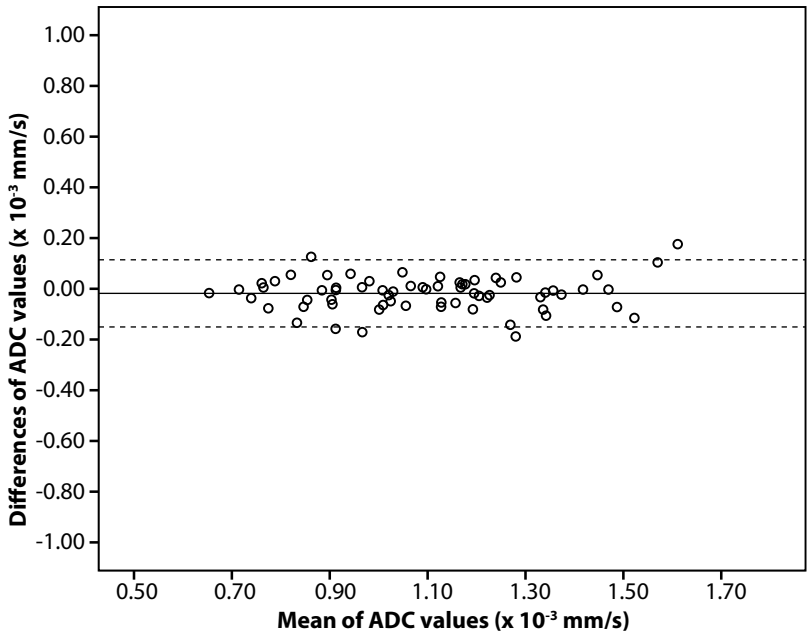


**Figure 2.** Bland-Altman plot shows for each fibroid the difference of the two ADC values (y-axis) plotted against the mean of the two ADC values (x-axis) calculated using *b*=0 and 800 s/mm$^2$, with 95% limits of agreement (LoA). The distance from the solid line to each dot represents the difference between the investigators rating corresponding to the observed mean value on the x-axis for the two raters.

## Reproducibility

A combination of coefficients of reliability and agreement was performed. Based on the average measures of the two raters, the ADC values had good interrater reliability with an ICC of 0.953 (95% CI [0.913, 0.973]; p<0.001) using all *b*-values; 0.936 (95% CI [0.895, 0.961]; p<0.001) using the lowest *b*-values; 0.969 (95% CI [0.949, 0.981]; p<0.001) using the highest *b*-values, and 0.977 (95% CI [0.962, 0.986]; p<0.001) using *b*=0 and 800 s/mm$^2$. The Bland-Altman plot (*Figure 2*) shows that the majority of the differences were less than $0.2\times10^{-3}$ mm$^2$/s.

**Table 3.** ADC values ($10^{-3}$ mm$^2$/s) calculated with different combinations of *b*-values, pre-treatment and post-treatment

| | Treated fibroid tissue | | | Normal myometrium | | |
|---|---|---|---|---|---|---|
| Different *b*-value combinations | Pre-treatment | Post-treatment | p | Pre-treatment | Post-treatment | p |
| 0, 200, 400, 600, 800 s/mm$^2$ | 1.27±0.23 | 1.20±0.25 | 0.034 | 1.85±0.34 | 1.88±0.37 | 0.207 |
| 0, 200 s/mm$^2$ | 2.16±0.33 | 1.53±0.28 | <0.001 | 2.82±0.55 | 2.82±0.58 | 0.918 |
| 400, 600, 800 s/mm$^2$ | 0.76±0.18 | 0.92±0.21 | <0.001 | 1.02±0.19 | 1.07±0.23 | 0.053 |
| 0, 800 s/mm$^2$ | 1.09±0.23 | 1.11±0.24 | 0.492 | 1.55±0.24 | 1.57±0.26 | 0.355 |

Values are expressed in mean ± standard deviation

**Influence of *b*-values on the ADC**

The mean ADC values in the ROIs were calculated using different *b*-value combinations, pre-treatment and immediately post-treatment, and presented in *Table 3*. We observed a significant decrease ($p<0.001$) in the mean ADC value of the ablated fibroid tissue ($1.53\times10^{-3}\pm0.28\times10^{-3}$ mm$^2$/s) compared with baseline ($2.16\times10^{-3}\pm0.33\times10^{-3}$ mm$^2$/s), when low *b*-values (0, 200 s/mm$^2$) were used for ADC mapping. For this *b*-value combination, we found a uniform decrease in the ADC for all individual fibroids. When the highest *b*-values were used (400, 600, and 800 s/mm$^2$), the mean ADC value increased significantly post-treatment ($p<0.001$), although the increase was much lower than the decrease observed at $b=0$ and 200 s/mm$^2$. The other *b*-value combinations did not result in significant ADC changes. The ADC value of the normal myometrium did not change after MR-HIFU treatment, indicating that MR-HIFU treatment does not influence the cellular environment of the myometrium. The ADC changes pre-treatment and post-treatment are depicted in *Figure 3*. *Figure 4* shows an example of data points representing signal intensities at all five *b*-values with the corresponding non-linear fits for the different *b*-value combinations from a typical voxel (ROI radius 0.56 pixels) inside the centre of a uterine fibroid before and after MR-HIFU ablation. The figure shows a steeper signal drop in the low *b*-value

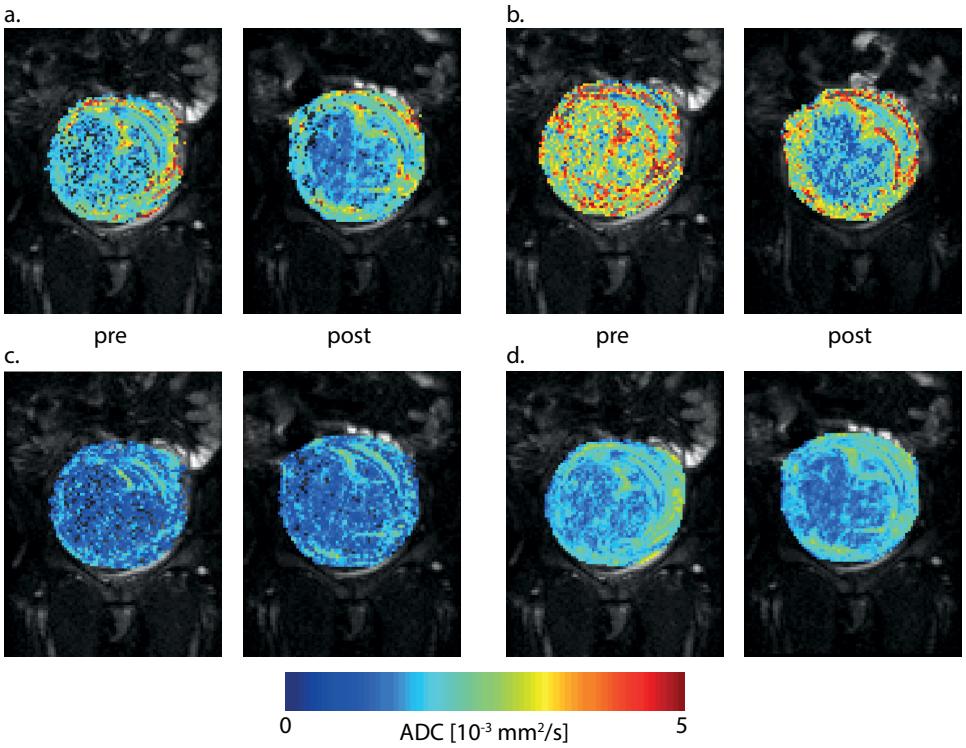


**Figure 3.** A typical example of reconstructed pre-treatment and post-treatment ADC colour maps using four different approaches: (a) ADC maps using all *b*-values (0, 200, 400, 600, and 800 s/mm$^2$); (b) ADC maps using the lowest *b*-values (0, 200 s/mm$^2$), indicating a significant decrease in ADC value; (c) ADC maps using the highest *b*-value combination (400, 600, 800 s/mm$^2$), indicating a significant increase in ADC value; (d) ADC maps using the lowest and the highest *b*-value (0, 800 s/mm$^2$). Note, case is the same as shown in *Figure 1*.

range (0, 200 s/mm$^2$) before ablation, than after MR-HIFU ablation. This corresponds to the observed drop in the ADC at low *b*-values seen in *Table 3* and *Figure 3*. The lowest *b*-value combination (0, 200 s/mm$^2$) resulted in the highest visual contrast between untreated and ablated fibroid tissue in the ADC maps. An evident decrease in contrast agent uptake within the ablated region on CE-T1w MRI, resulted in a uniform increased signal intensity on DWI, characterised by a decreased ADC when *b*=0 and 200 s/mm$^2$ were used for ADC mapping.

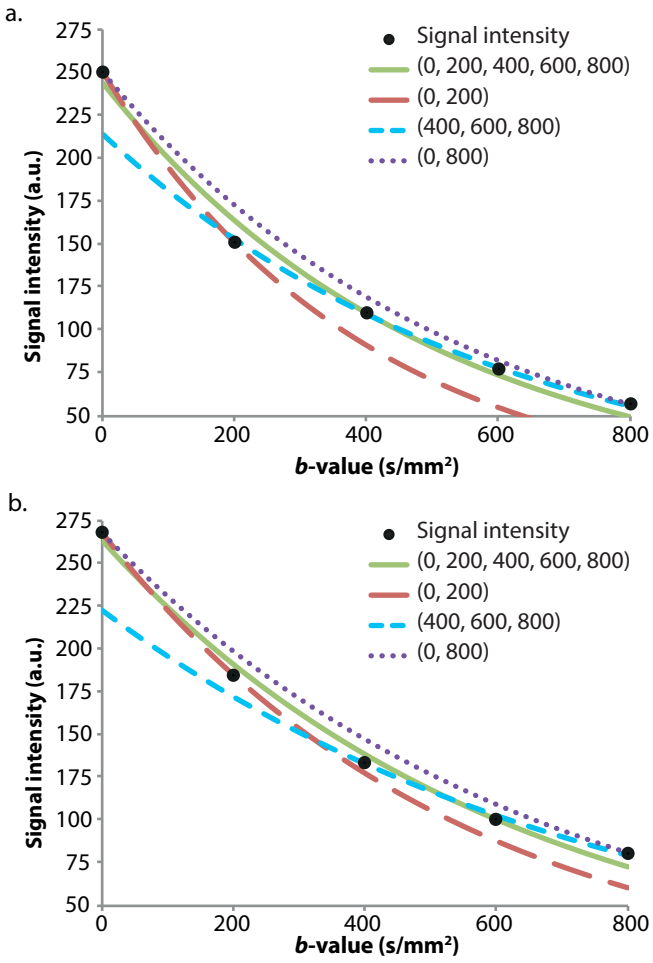


**Figure 4.** These graphs show data points representing signal intensities at all five *b*-values with the corresponding non-linear fits for the different *b*-value combinations from a typical voxel (ROI radius 0.56 pixels) inside the centre of a uterine fibroid before (a) and after (b) MR-HIFU ablation. The solid (green) line represents the fitting function using all *b*-values; the long dashed (red) line represents the fit obtained using the lowest *b*-values (0, 200 s/mm$^2$); the square dotted (blue) line represents the fit with the highest *b*-value combination (400, 600, 800 s/mm$^2$), and the round dotted (purple) line represents the fit for *b*=0 and *b*=800 s/mm$^2$. The signal attenuation is faster at low *b*-values, which supports the hypothesis that the vascular component (perfusion) is responsible for the non-mono-exponential behaviour of the signal decay. This effect is more pronounced pre-treatment than after MR-HIFU ablation. Note, the data is from the same case as shown in *Figure 1*.

## Discussion

The results of this study demonstrate that the measured ADC value in fibroid tissue is influenced by the choice of *b*-values used for ADC calculation. This suggests a non-mono-exponential behaviour of the signal decay as a function of the *b*-value, which supports our hypothesis that DWI in fibroids reflects the effects of both diffusion and perfusion. ADC maps calculated using images obtained at low *b*-values (0, 200 s/mm$^2$) resulted in the best visual agreement with the NPV detected on CE-T1w MRI. Moreover, at baseline, the ADC values measured at these low *b*-values ($2.16\times10^{-3}\pm0.33\times10^{-3}$ mm$^2$/s) were relatively high compared to the ADC-values obtained when also high *b*-values were used (e.g. $1.09\times10^{-3}\pm0.23\times10^{-3}$ mm$^2$/s for *b*-values 0, 800 s/mm$^2$). This could be an indication for the presence of a tissue component with rapid incoherent motion of water molecules, which might be the arterial vascular compartment[28]. Compared to baseline, a significant decrease in the ADC value for *b*=0 and 200 s/mm$^2$ was found post-treatment ($p<0.001$). When only the highest *b*-values (400, 600, and 800 s/mm$^2$) were used, a significant increase in the ADC value was found ($p<0.001$). Other *b*-value combinations showed no significant change in ADC values before and after MR-HIFU treatment.

Jacobs *et al.*[18,19] earlier demonstrated the use of DWI and ADC mapping for treatment monitoring after MR-HIFU. They found a decrease in ADC value of treated fibroid tissue after MR-HIFU using *b*-values 0 and 1000 s/mm$^2$, demonstrating that DWI and ADC mapping could be used for identification of ablated tissue after MR-HIFU. Pilatou *et al.*[21] investigated tissue changes observed in DWI after MR-HIFU treatment of uterine fibroids and studied the relationship between contrast-enhanced imaging, thermal dosimetry, and changes in ADC. They found that the hyper-intense area found on DWI underestimated the NPV on CE-T1w MRI with increasing non-perfused volume. They used two *b*-values (0, 1000 s/mm$^2$) in their study to calculate the ADC. The change in signal intensity on ADC maps was unpredictable: some fibroids showing an increase while others showed a decrease in ADC value immediately post-treatment compared with pre-treatment values. The results we found when we used *b*-values of 0 and 800 s/mm$^2$ for the ADC calculation pre-treatment and post-treatment ($1.09\times10^{-3}\pm0.23\times10^{-3}$ mm$^2$/s and $1.11\times10^{-3}\pm0.24\times10^{-3}$ mm$^2$/s, respectively) are comparable to the results of Pilatou *et al.*[21] ($1.22\times10^{-3}\pm0.22\times10^{-3}$ mm$^2$/s and $1.20\times10^{-3}\pm0.28\times10^{-3}$ mm$^2$/s, respectively). For this combination, no significant change in the ADC value after MR-HIFU treatment was found ($p=0.492$). Our results may be interpreted in the context of the idea that it is possible to separate molecular diffusion effects from capillary perfusion effects using different *b*-value combinations for the calculation of ADC in uterine fibroids[30]. In the presence of perfusion due to randomly oriented capillary flow, the signal attenuation is larger than that caused by diffusion alone[30,37]. Following this line of reasoning, and realising that untreated fibroids are relatively well-perfused, it could be that the apparently restricted diffusion in the NPV, observed immediately post-treatment, is in part related to the reduced perfusion effect. This may be explained by thermal coagulation and by the occlusion of small blood vessels during treatment and compression of blood vessels by oedema[38,39]. The observed change in ADC when the highest *b*-values were used may indicate that the reduced perfusion is actually accompanied by an increase in extracellular fluid volume directly after ablation, which may be due to direct thermal and/or mechanical damage to the cell membranes caused by the HIFU ablation. The corresponding increased permeability of capillary endothelial cells to macromolecular serum proteins (e.g. albumin) is associated with an

increased diffusion, characterised by an increased ADC. This is in correspondence to the findings published by Luo *et al.*[39], and Solomon *et al.*[40] who investigated the pathologic changes after thermal ablation of uterine fibroids. The most prominent acute finding was the obliterated interstitial vessels in the necrotic zone, with contracted smooth-muscle cells and dilated interstitial spaces in the surrounding area.

There are some technical limitations to our study. Although the usefulness of DWI has already been proven for intracranial imaging, abdominal MRI involves many challenges and is susceptible to a variety of artefacts related to physiologic motion (e.g. respiratory, gastrointestinal, and voluntary movement), and susceptibility effects[41-43]. However, DWI is an evolving technology. Stronger gradient pulses, echo planar imaging readout, and parallel imaging techniques[44], allow faster data acquisition and fewer artefacts, resulting in better image quality. In addition, the examination was performed in patients who were lying in prone position, and who were receiving benzodiazepines in combination with intravenous administration of an opioid analgesic. These factors allowed the examination to be completed with less breathing and abdominal motion. Furthermore, there is a possible variability in ADC values as a result of hardware, human or biologic factors, even when using the same MR-system and protocol. Another limitation of the current study was the small non-randomised design, 57 patients with 67 uterine fibroids were treated with volumetric MR-HIFU ablation and included for statistical analysis. In spite of the relatively small sample size, significant differences have been found. Since no treat-and-resect study has been performed, there was no correlation to immediate histopathology. Because of the non-invasive nature of MR-HIFU ablation, there was no justification to perform invasive surgery in these patients. Finally, our data does not prove that the suggested reasons for the observed changes in DWI signal and ADC are true, as there is no reference standard which measures the motion of water molecules. Considering that the ADC maps calculated using the combination of lowest *b*-values, i.e. *b*=0 and 200 s/mm$^2$, may still be presenting a mixture of diffusion and perfusion effects, it would be interesting to perform measurements at even lower *b*-values and to perform intravoxel incoherent motion (IVIM) analyses on such data.

In conclusion, our results may suggest that there is a substantial change in perfusion after MR-HIFU treatment due to vessel destruction, and that using low *b*-values might be the best choice to emphasise such perfusion changes in ADC maps. The results we found confirm that DWI can become a helpful tool to assess the NPV, especially for periprocedural treatment monitoring, since this is a non-invasive technique without the use of an intravenous contrast agent. In addition to previous studies published[18,19,21], we demonstrated that the choice of *b*-values used for ADC mapping influences the absolute ADC values and contrasts in the ADC maps. Our data suggest that the shutdown of perfusion may partly explain the observed reduction in the apparent diffusion coefficient immediately post-treatment.



## Acknowledgements

Philips Healthcare provided financial support for the expenses of the first 10 patients, including treatment and follow-up. One author (B.K.) is an employee of Philips Healthcare, however the first two authors (M.E.I., and M.J.V.) in control of the study data and data analysis are not employees of Philips Healthcare.

# References

1. Merrill RM. Hysterectomy surveillance in the United States, 1997 through 2005. *Med Sci Monit.* 2008;14:CR24-31
2. Cramer SF, Patel A. The frequency of uterine leiomyomas. *Am J Clin Pathol.* 1990;94:435-438
3. Stewart EA. Uterine fibroids. *Lancet.* 2001;357:293-298
4. Gupta S, Jose J, Manyonda I. Clinical presentation of fibroids. *Best Pract Res Clin Obstet Gynaecol.* 2008;22:615-626
5. Zimmermann A, Bernuit D, Gerlinger C, Schaefers M, Geppert K. Prevalence, symptoms and management of uterine fibroids: an international internet-based survey of 21,746 women. *BMC Womens Health.* 2012;12:6
6. Parker WH. Uterine myomas: management. *Fertil Steril.* 2007;88:255-271
7. Behera MA, Leong M, Johnson L, Brown H. Eligibility and accessibility of magnetic resonance-guided focused ultrasound (MRgFUS) for the treatment of uterine leiomyomas. *Fertil Steril.* 2010;94:1864-1868
8. Zowall H, Cairns JA, Brewer C, Lamping DL, Gedroyc WM, Regan L. Cost-effectiveness of magnetic resonance-guided focused ultrasound surgery for treatment of uterine fibroids. *BJOG.* 2008;115:653-662
9. Tempany CM, Stewart EA, McDannold NJ, Quade BJ, Jolesz FA, Hynynen K. MR imaging-guided focused ultrasound surgery of uterine leiomyomas: a feasibility study. *Radiology.* 2003;226:897-905
10. Voogt MJ, Trillaud H, Kim YS, Mali WP, Barkhausen J, Bartels LW, Deckers R, Frulio N, Rhim H, Lim HK, Eckey T, Nieminen HJ, Mougenot C, Keserci B, Soini J, Vaara T, Köhler MO, Sokka S, van den Bosch MA. Volumetric feedback ablation of uterine fibroids using magnetic resonance-guided high intensity focused ultrasound therapy. *Eur Radiol.* 2012;22:411-417
11. Jolesz FA. MRI-guided focused ultrasound surgery. *Annu Rev Med.* 2009;60:417-430
12. Hindley J, Gedroyc WM, Regan L, Stewart EA, Tempany CM, Hynyen K, McDannold NJ, Inbar Y, Itzchak Y, Rabinovici J, Kim HS, Geschwind JF, Hesley G, Gostout B, Ehrenstein T, Hengst S, Sklair-Levy M, Shushan A, Jolesz F. MRI guidance of focused ultrasound therapy of uterine fibroids: early results. *AJR Am J Roentgenol.* 2004;183:1713-1719
13. Stewart EA, Gedroyc WM, Tempany CM, Quade BJ, Inbar Y, Ehrenstein T, Shushan A, Hindley JT, Goldin RD, David M, Sklair M, Rabinovici J. Focused ultrasound treatment of uterine fibroid tumors: safety and feasibility of a noninvasive thermoablative technique. *Am J Obstet Gynecol.* 2003;189:48-54
14. Weinmann HJ, Brasch RC, Press WR, Wesbey GE. Characteristics of gadolinium-DTPA complex: a potential NMR contrast agent. *AJR Am J Roentgenol.* 1984;142:619-624
15. Hijnen NM, Elevelt A, Grull H. Stability and trapping of magnetic resonance imaging contrast agents during high-intensity focused ultrasound ablation therapy. *Invest Radiol.* 2013;48:517-524
16. Merckel LG, Bartels LW, Kohler MO, van den Bongard HJ, Deckers R, Mali WP, Binkert CA, Moonen CT, Gilhuijs KG, van den Bosch MA. MR-guided high-intensity focused ultrasound ablation of breast cancer with a dedicated breast platform. *Cardiovasc Intervent Radiol.* 2013;36:292-301
17. Laurent S, Elst LV, Copoix F, Muller RN. Stability of MRI paramagnetic contrast media: a proton relaxometric protocol for transmetallation assessment. *Invest Radiol.* 2001;36:115-122
18. Jacobs MA, Herskovits EH, Kim HS. Uterine fibroids: diffusion-weighted MR imaging for monitoring therapy with focused ultrasound surgery--preliminary study. *Radiology.* 2005;236:196-203
19. Jacobs MA, Gultekin DH, Kim HS. Comparison between diffusion-weighted imaging, T2-weighted, and postcontrast T1-weighted imaging after MR-guided, high intensity, focused ultrasound treatment of uterine leiomyomata: preliminary results. *Med Phys.* 2010;37:4768-4776
20. Liapi E, Kamel IR, Bluemke DA, Jacobs MA, Kim HS. Assessment of response of uterine fibroids and myometrium to embolization using diffusion-weighted echoplanar MR imaging. *J Comput Assist Tomogr.* 2005;29:83-86
21. Pilatou MC, Stewart EA, Maier SE, Fennessy FM, Hynynen K, Tempany CM, McDannold N. MRI-based thermal dosimetry and diffusion-weighted imaging of MRI-guided focused ultrasound thermal ablation of uterine fibroids. *J Magn Reson Imaging.* 2009;29:404-411
22. Faye N, Pellerin O, Thiam R Chammings F, Brisa M, Marques E, Cuénod CA, Sapoval M, Fournier LS. Diffusion-weighted imaging for evaluation of uterine arterial embolization of fibroids. *Magn Reson Med.* 2013;70:1739-1747
23. Bammer R. Basic principles of diffusion-weighted imaging. *Eur J Radiol.* 2003;45:169-184
24. Le Bihan D, Breton E, Lallemand D, Grenier P, Cabanis E, Laval-Jeantet M. MR imaging of intravoxel incoherent motions: application to diffusion and perfusion in neurologic disorders. *Radiology.* 1986;161:401-407
25. Stejskal EO. Use of Spin Echoes in a Pulsed Magnetic-Field Gradient to Study Anisotropic, Restricted Diffusion and Flow. *J Chem Phys.* 1965;43:3597-3603

26. Hagmann P, Jonasson L, Maeder P, Thiran JP, Wedeen VJ, Meuli R. Understanding diffusion MR imaging techniques: from scalar diffusion-weighted imaging to diffusion tensor imaging and beyond. *Radiographics.* 2006;26 Suppl 1:S205-223
27. Farrer-Brown G, Beilby JO, Tarbit MH. The vascular patterns in myomatous uteri. *J Obstet Gynaecol Br Commonw.* 1970;77:967-975
28. Lemke A, Laun FB, Simon D, Stieltjes B, Schad LR. An in vivo verification of the intravoxel incoherent motion effect in diffusion-weighted imaging of the abdomen. *Magn Reson Med.* 2010;64:1580-1585
29. Walocha JA, Litwin JA, Miodonski. Vascular system of intramural leiomyomata revealed by corrosion casting and scanning electron microscopy. *Hum Reprod AJ.* 2003;18:1088-1093
30. Le Bihan D, Breton E, Lallemand D, Aubin ML, Vignaud J, Laval-Jeantet M. Separation of diffusion and perfusion in intravoxel incoherent motion MR imaging. *Radiology.* 1988;168:497-505
31. Thoeny HC, De Keyzer F, Boesch C, Hermans R. Diffusion-weighted imaging of the parotid gland: Influence of the choice of b-values on the apparent diffusion coefficient value. *J Magn Reson Imaging.* 2004;20:786-790
32. Yamada I, Aung W, Himeno Y, Nakagawa T, Shibuya H. Diffusion coefficients in abdominal organs and hepatic lesions: evaluation with intravoxel incoherent motion echo-planar MR imaging. *Radiology.* 1999;210:617-623
33. Ikink ME, Voogt MJ, Verkooijen HM, Lohle PN, Schweitzer KJ, Franx A, Mali WP, Bartels LW, van den Bosch MA. Mid-term clinical efficacy of a volumetric magnetic resonance-guided high-intensity focused ultrasound technique for treatment of symptomatic uterine fibroids. *Eur Radiol.* 2013;23:3054-3061
34. Mougenot C, Quesson B, de Senneville BD, de Oliveira PL, Sprinkhuizen S, Palussière J, Grenier N, Moonen CT. Three-dimensional spatial and temporal temperature control with MR thermometry-guided focused ultrasound (MRgHIFU). *Magn Reson Med.* 2009;61:603-614
35. Ishihara Y, Calderon A, Watanabe H, Okamoto K, Suzuki Y, Kuroda K. A precise and fast temperature mapping using water proton chemical shift. *Magn Reson Med.* 1995;34:814-823
36. Funaki K, Fukunishi H, Funaki T, Sawada K, Kaji Y, Maruo T. Magnetic resonance-guided focused ultrasound surgery for uterine fibroids: relationship between the therapeutic effects and signal intensity of preexisting T2-weighted magnetic resonance images. *Am J Obstet Gynecol.* 2007;196:184 e181-186
37. Turner R, Le Bihan D, Maier J, Vavrek R, Hedges LK, Pekar J. Echo-planar imaging of intravoxel incoherent motion. *Radiology.* 1990;177:407-414
38. Hynynen K, Colucci V, Chung A, Jolesz F. Noninvasive arterial occlusion using MRI-guided focused ultrasound. *Ultrasound Med Biol.* 1996;22:1071-1077
39. Luo X, Shen Y, Song WX, Chen PW, Xie XM, Wang XY. Pathologic evaluation of uterine leiomyoma treated with radiofrequency ablation. *Int J Gynaecol Obstet.* 2007;99:9-13
40. Solomon SB, Nicol TL, Chan DY, Fjield T, Fried N, Kavoussi LR. Histologic evolution of high-intensity focused ultrasound in rabbit muscle. *Invest Radiol.* 2003;38:293-301
41. Koh DM, Takahara T, Imai Y, Collins DJ. Practical aspects of assessing tumors using clinical diffusion-weighted imaging in the body. *Magn Reson Med Sci.* 2007;6:211-224
42. Le Bihan D, Poupon C, Amadon A, Lethimonnier F. Artifacts and pitfalls in diffusion MRI. *J Magn Reson Imaging.* 2006;24:478-488
43. Yang RK, Roth CG, Ward RJ, deJesus JO, Mitchell DG. Optimizing abdominal MR imaging: approaches to common problems. *Radiographics.* 2010;30:185-199
44. Glockner JF, Hu HH, Stanley DW, Angelos L, King K. Parallel MR imaging: a user's guide. *Radiographics.* 2005;25:1279-1297

# 6 Intravoxel incoherent motion MRI for tissue characterisation of uterine fibroids before MR-guided high-intensity focused ultrasound ablation

Marlijne E. Ikink
Marijn van Stralen
Johanna M.M. van Breugel
Marissa Frijlingh
Koen L. Vincken
Maurice A.A.J. van den Bosch
Lambertus W. Bartels

*Manuscript in preparation*

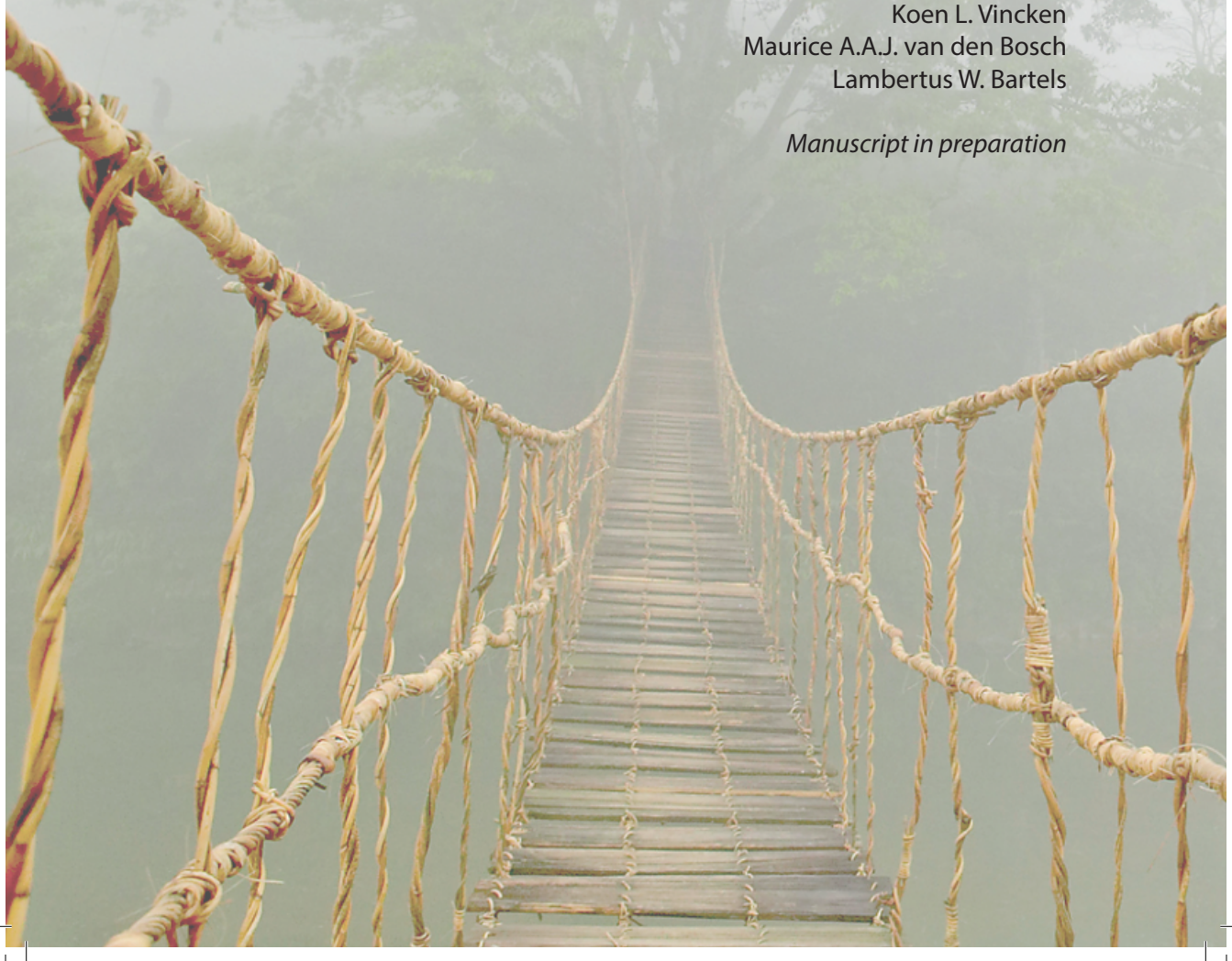

# Abstract

**Objective**

To investigate the tissue characteristics of uterine fibroids based on a pre-treatment intravoxel incoherent motion (IVIM) model and to assess whether the IVIM parameters could predict the heating effectiveness of magnetic resonance-guided high-intensity focused ultrasound (MR-HIFU) ablation.

**Methods**

Thirty-five uterine fibroids in 31 patients were treated with volumetric MR-HIFU ablation and included in this study. Pre-treatment anatomical T2-weighted (T2w) and contrast-enhanced T1-weighted (CE-T1w) MRI scans were acquired, and diffusion-weighted MRI series were performed with $b$=0, $b$=200, $b$=400, $b$=600, and $b$=800 s/mm$^2$. An apparent diffusion coefficient (ADC) map was calculated from the images $b_0$=0 s/mm$^2$ and $b_1$=200 s/mm$^2$, the perfusion-free diffusion parameter $D$ was determined from the images $b_1$=400 s/mm$^2$, $b_2$=600 s/mm$^2$ and $b_3$=800 s/mm$^2$. Subsequently, the voxel-wise perfusion fraction $f$ was calculated. In addition, semi-quantitative fibroid tissue characterisation was based on the normalised T2w signal intensity $S'$, using reference values of the rectus abdominis muscle and uterine myometrium. Analysis of the anatomical (T2w and CE-T1w MRI), functional (IVIM MRI) and temperature curves derived from MR thermometry data was performed in cell-based ellipsoidal ($4 \times 4 \times 10$ mm$^3$) volumes of interest (VOIs). Thermal ablation was classified successful if the VOI was completely devascularised as visualised on CE-T1w MRI. Univariable linear regression analysis was used to assess whether there was a relationship between the pre-treatment cell-based IVIM parameters, pre-treatment normalised T2w signal $S'$ and the temperature curves.

**Results**

Within the cell-based VOIs (n=724), the mean perfusion fraction $f$ was 0.41±0.17 and the mean diffusion coefficient $D$ was $0.73\times10^{-3}\pm0.31\times10^{-3}$ mm$^2$/s. We found a positive correlation ($B$=0.671, p<0.001, $R^2$=0.269) between the mean pre-treatment diffusion coefficient $D$ and pre-treatment normalised T2w signal intensity $S'$, but we were not able to show correlations between the pre-treatment IVIM parameters and any of the temperature parameters ($R^2$ ranged from 0.002 to 0.032). A significant higher (p<0.001) pre-treatment flow-related pseudodiffusion coefficient $D^*$ was found in the suboptimally treated VOIs compared to successfully ablated treatment cells ($2.37\times10^{-3} \pm 0.80\times10^{-3}$ mm$^2$/s vs $2.19\times10^{-3} \pm 0.69\times10^{-3}$ mm$^2$/s, respectively).

**Conclusion**

The extent of non-perfused volume may be related to the perfusion coefficient $D^*$ rather than the normalised T2w signal intensity. However, further research with MRI-based blood flow measurement techniques is needed to explore the relationship between perfusion and thermal response of MR-HIFU ablation.

## Introduction

In the past decade, magnetic resonance-guided high-intensity focused ultrasound (MR-HIFU) has evolved as an attractive alternative to conventional treatments for symptomatic uterine fibroids. MR-HIFU is a completely non-invasive ablation method that combines the high-resolution anatomical images and thermometry capabilities of MR imaging, with the therapeutic application of high-intensity focused ultrasound[1,2]. The thermal effect of MR-HIFU is caused by the absorption of acoustic energy, which results in a rapid temperature elevation in a focal point. It has been reported that elevation of the tissue temperature to above 60 degrees Celsius (°C) for at least 1 second will generally induce localised irreversible cell damage due to coagulation necrosis[3-5]. The maximum thermal effect will be achieved across the focal zone, while surrounding normal tissues are spared. Multiple clinical and anatomical factors influence patient eligibility for MR-HIFU treatment of uterine fibroids, which must be taken into account to ensure patient safety and treatment efficacy[6-8]. The success of ablation is highly dependent on the characteristics of the ultrasound beam (e.g. frequency, intensity, accuracy and exposure duration), and the targeted tissue (e.g. ultrasound absorption coefficient, thermal conductivity and blood perfusion) through which the ultrasound waves travels[9]. Uterine fibroids are benign monoclonal tumours of the uterine smooth muscle cells, enriched in abnormal extracellular matrix that contains collagen, fibronectin, and proteoglycan[10,11]. Tissues that are high in collagen or protein content (e.g. muscle) are known to show a high absorption of ultrasound, whereas those with high water content show lower absorption and higher penetration[12,13].

Magnetic resonance imaging (MRI) is the preferred imaging modality for accurate visualisation and characterisation of uterine fibroids, and therefore provides clinically important information regarding assessment of treatment response prior to MR-HIFU ablation. Non-degenerated uterine fibroids typically appear as well-circumscribed homogeneous masses of low signal intensity on T2-weighted (T2w) MRI[14]. At histopathological examination, those hypo-intense uterine fibroids are predominantly composed of uniform spindles of smooth muscle cells with intervening collagen[15]. Hyper-intense uterine fibroids (on T2w imaging) can be categorised in two main varieties: (1) cellular and (2) degenerated fibroids. Cellular lesions typically show densely packed cellular fascicles of smooth muscle cells with little intervening collagen, while degenerated lesions will demonstrate various histopathological patterns of degeneration, such as hyaline (65%), myxomatous (15%), calcific (10%), cystic, fatty, or carneous (red) degeneration[16]. Nevertheless, in some cases, it seems difficult to differentiate between these histopathological backgrounds that are reflected in the signal intensity on T2w MRI. Diffusion-weighted MRI (DWI) with subsequent mapping of the apparent diffusion coefficient (ADC) allows tissue characterisation based upon differences in the microscopic motion of water molecules[17,18]. In biologic tissues, this motion includes both molecular diffusion of water and microcirculation of blood in the capillary (perfusion). DWI may provide information about the biophysical properties of tissues such as cell organisation, cell density, microstructure, microcirculation, cellular oedema, and necrosis[19-22]. The ADC is generally estimated by voxel-wise fitting of the signal decay over a series of diffusion weighted images obtained with different diffusion-weighting factors (*b*-values) using a simple mono-exponential model, thereby ignoring the fact that the signal decay in the presence of multiple compartments, i.e. one with diffusion and one with perfusion, will

generally not be mono-exponential. The extent to which perfusion contributes to the ADC varies depending on the combination of *b*-values used to extract the ADC from the fitting process. The signal attenuation ascribed to the vascular compartment occurs predominantly in the range of low *b*-values. On the contrary, the ADC sensitivity to perfusion can be neglected for large *b*-values[23]. The intravoxel incoherent motion (IVIM) analysis technique uses a signal model with two separate compartments with a mono-exponential decay per compartment to extract perfusion-related information from multi-*b*-value DWI data[23]. Tissue is assumed to incorporate a perfusion compartment of water flowing in randomly oriented capillaries. In the signal decay model, this compartment contributes to the DWI signal with a perfusion fraction *f*. In addition, a fraction (1-*f*) of static perfusion-free diffusion (*D*) of intracellular and extracellular water is assumed to be present. The faster component (*D**) is thought to represent the microcirculation of blood through the capillaries, with the relatively high blood velocities causing a sharper decrease in signal with diffusion-weighting[24]. Although the application of IVIM to tissues with small perfusion fractions, like the brain, has been a subject of controversy[25,26], the IVIM theory has recently been found to be applicable in (abdominal) organs with much higher values of the perfusion fraction *f*[27]. Based upon previous literature[28,29-31], we expect that uterine fibroids are similarly characterised by a high vascular component, and that IVIM MRI can be useful for tissue characterisation of uterine fibroids before MR-HIFU ablation.

Funaki *et al*.[32] have previously reported a correlation between the appearance of uterine fibroids on T2w MR images and the efficacy of MR-HIFU ablation. According to the signal intensity on T2w images, fibroids were classified as type 1 (very low signal intensity - comparable with the abdominal muscle), type 2 (intermediate signal intensity), and type 3 (very high signal intensity - equal or higher than the outer myometrium). They found that type 3 uterine fibroids were the least receptive to MR-HIFU ablation with regards to the non-perfused volume (NPV) ratio (i.e. NPV divided by fibroid volume) and the fibroid volume reduction after 6 months' follow-up. The hypothesis is that morphological and functional features, such as cellularity, vascularity, perfusion, haemorrhage, necrosis, oedema, and calcification that are reflected in the signal intensity on T2w MRI[33,34], could influence the clinical outcome. However, what exactly causes the differences in signal intensity on T2w MRI and why an MR-HIFU ablation fails in certain patients with uterine fibroids has not been extensively studied. Several groups have already tried to identify important predictors associated with treatment efficacy of MR-HIFU ablation for symptomatic uterine fibroids, including dynamic contrast-enhanced (DCE) MRI parameters[35] and semi-quantitative perfusion MR imaging parameters[36]. The purpose of our study was to determine whether pre-treatment IVIM diffusion and perfusion characteristics of uterine fibroids could predict the heating effectiveness of MR-HIFU ablation on treatment cell level and to investigate whether these DWI characteristics differ for fibroids with different signal intensities on T2w MRI.

## Materials and methods

This study was approved by our local institutional review board, and all patients gave written informed consent for the use of clinical and imaging data. Patients were consecutively included for this study if they underwent a volumetric MR-HIFU ablation in our hospital. The eligibility criteria for treatment have been previously described[37,38]. We included adult premenopausal women with symptomatic uterine fibroids with at least one large uterine fibroid of maximum 12 cm in diameter. The presence of (1) bowel loops (small or large intestine) between the uterus and the outer abdominal wall, (2) more than 10 uterine fibroids, (3) extensive scar tissue in the lower abdomen, and (4) inhomogeneous contrast enhancement before MR-HIFU treatment resulted in exclusion from the study.



**Data acquisition**

All MR examinations were performed on a clinical MR-HIFU system (Sonalleve, Philips Healthcare, Finland) integrated into a 1.5-T MRI scanner (Achieva, Philips Healthcare, The Netherlands). The routine pelvic imaging protocol consisted of anatomical sagittal three-dimensional (3D) T2w turbo spin-echo (TSE) (repetition time [TR], 1425 milliseconds [ms]; echo time [TE], 130 ms; flip angle [FA], 90°; field of view [FOV], 250 mm × 250 mm; acquired [ACQ] voxel size, 1.20 × 1.39 × 3.00 $mm^3$; reconstructed [REC] voxel size, 0.49 × 0.49 × 1.50 $mm^3$; number of signal averages [NSA], 2; acquisition time, 3 min 50 seconds [s]), and 3D T1-weighted (T1w) spoiled gradient echo (FFE) sequences (TR, 3.6 ms; TE, 1.9 ms; FA, 7°; FOV, 220 mm × 240 mm; ACQ voxel size, 1.25 × 1.53 × 2.50 $mm^3$; REC voxel size, 0.47 × 0.47 × 1.25 $mm^3$; NSA, 8; acquisition time, 1 min 57 s). DWI was obtained in the coronal plane using a fat suppressed multi-slice single shot spin-echo echo planar imaging (SE-EPI) sequence (TR, 2500 ms; TE, 65 ms; ACQ matrix size, 112 × 83; FA, 90°; FOV, 250 mm × 187.5 mm; ACQ voxel size, 2.23 × 2.26 × 7.00 $mm^3$; REC voxel size, 2.23 × 2.23 × 7.00 $mm^3$; NSA, 6; acquisition time, 4 min 47 s) with $b$=0, $b$=200, $b$=400, $b$=600, and $b$=800 $s/mm^2$ [39].

**MR-HIFU treatment**

Patients were admitted to our day care unit, where pre-treatment patient preparation was carried out. A Foley catheter was inserted in order to minimise displacement of the uterus (as a result of the natural filling of the bladder) during MR-HIFU treatment. Accordingly, a peripheral intravenous line was placed to provide anaesthetic care for administration of minimal sedation (anxiolytics) or procedural sedation. The applicable degree of sedation was determined by the experience of the anaesthesiologist and radiologist. After depilation of the hair between the umbilicus and the pubic bone, patients were asked to lie down in prone position with the targeted uterine fibroid in the centre of the transducer window in the MR table top. Volumetric ablations with treatment cells of 4, 8, 12, 14, or 16 mm in axial dimension and 10, 20, 30, 35, or 40 mm in longitudinal dimension were performed[40,41]. The selection of treatment cell size, location, frequency (1.2 or 1.45 megahertz [MHz]), power levels (80-280 Watt [W]), and cooling times (without overriding the predefined cooling time) were determined by the treating physician. During each sonication (i.e. energy delivery), the system measured temperature changes using the proton resonance frequency shift (PRFS) MR temperature mapping method using 2D FFE segmented echo planar imaging (EPI) (TR, 41 ms; TE, 19 ms; FA, 20°; EPI-factor, 11; FOV, 400 mm × 310 mm; REC voxel size, 2.50 mm; NSA, 1; temporal resolution, 3.7 s per dynamic)[42,43]. Colour temperature maps were computed by the system software

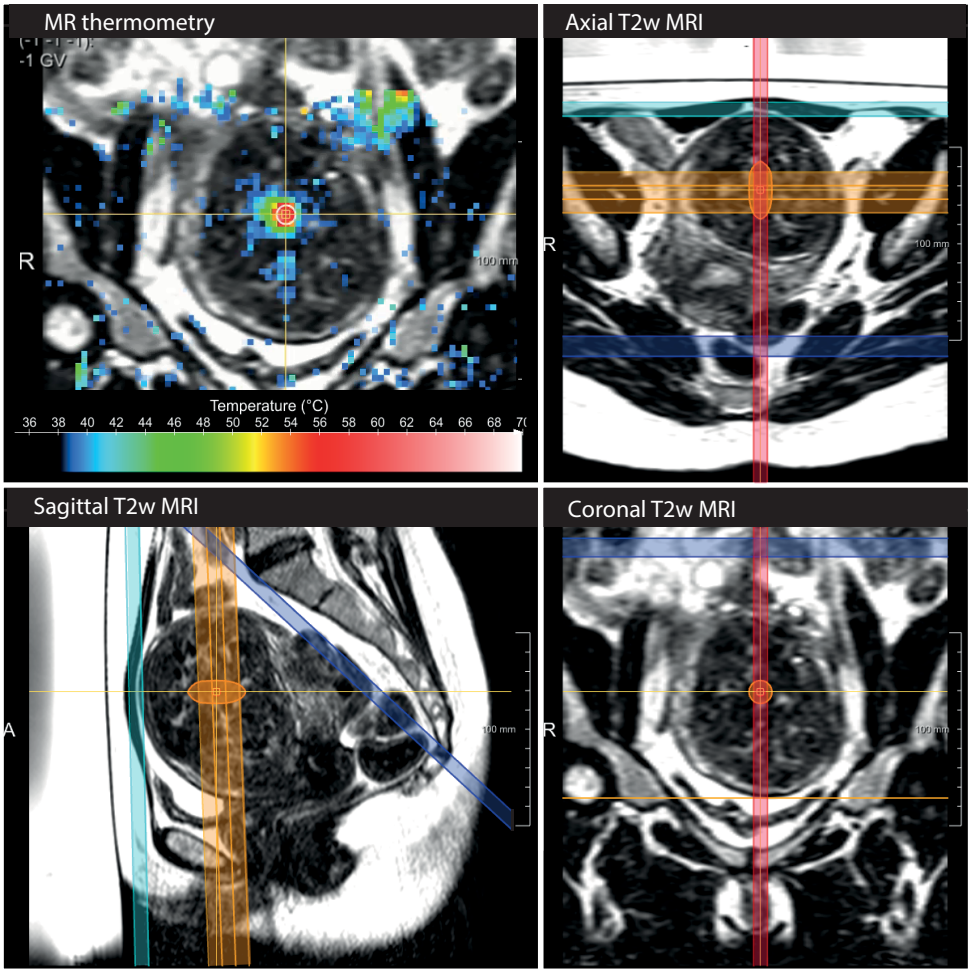


**Figure 1.** For real-time MR thermometry, the MR-HIFU system acquires multiplane (i.e. sagittal, axial, and coronal) temperature images. Temperature increase was monitored in the focal region by three adjacent coronal slices (yellow) and one sagittal slice (red). The near field slice is typically positioned in the rectus abdominis muscle (light blue), the far field slice in the bowel or close to the spine (dark blue). Colour temperature maps were automatically computed using the proton resonance frequency shift (PRFS) method, and shown as overlay on top of the anatomical images (top left).

from temperature difference measurements obtained from MR signal phase differences of subsequent dynamic images, and shown as overlay on top of the anatomical images. Temperature increase was monitored in the focal point, near field area (near the skin) and far field area (in the retro-rectal (presacral) area) as shown in *Figure 1*. Using the concept of thermal dose as proposed by Sapareto and Dewey[44], volumetric thermal dose maps were automatically estimated from the acquired time-temperature information. Thermal dose was expressed in cumulative equivalent minutes (EM) at 43°C. A thermal dose of 240 EM or more can be expected to cause ischaemic coagulative necrosis in the targeted tissue[45-47]. Immediately post-treatment, the ablated area was verified by determining the extent of non-perfused volume (NPV), as visualised on the coronal 3D contrast-enhanced (gadobutrol, Gadovist®, 0.1 mmol/kg, Bayer Schering Pharma) T1-weighted (CE-T1w) FFE MRI (TR, 5.4 ms; TE, 2.6 ms; FA, 10°; FOV, 250 mm × 250 mm; ACQ voxel size, 1.49 × 1.89 × 3.00 $mm^3$; REC voxel size, 0.49 × 0.49 × 1.50 $mm^3$; NSA, 4; acquisition time, 2 min 14 sec).

**Image analysis**

Assessment of the anatomical (T2w and CE-T1w MRI), functional (DWI) and MR thermometry data, in relation to the target fibroid and treatment cell geometry, was done using in-house developed software based on MeVisLab (2.6, MeVis Medical Solutions AG, Bremen, Germany). The targeted uterine fibroids and the NPV were semi-automatically segmented by manually contouring a randomly chosen subset of slices on the T2w and CE-T1w MRI, respectively. A three-dimensional (3D) surface was reconstructed[48] to find the complete volumetric segmentation of the structure. This was done in an iterative fashion, allowing correction or addition of the 2D contours until the 3D surface fit was visually accurate. Per ablation cell, ellipsoidal volumes of interest (VOIs) corresponding to the individual treatment cells were derived from meta data logged by the MR-HIFU system. The cell-based VOIs had a size of 4 × 4 × 10 $mm^3$. A cell-based analysis was chosen to be able to deal with heterogeneity in the fibroid tissue and vascular distribution.

On the basis of the IVIM theory proposed by Le Bihan *et al.*[23], we calculated an ADC map (denoted *D**) from the diffusion-weighted images $b_0$=0 s/$mm^2$ and $b_1$=200 s/$mm^2$ by voxel-wise analytically solving of the signal decay function: $S(b) = S_0 \cdot e^{-b \cdot ADC}$ to the DWI data. The perfusion-free diffusion coefficient *D* was fitted by nonlinear least squares curve fitting (Levenberg-Marquardt algorithm) to the signal intensities at *b*-values 400, 600 and 800 s/$mm^2$. Subsequently, the perfusion fraction *f* was calculated for each voxel from the ADC and *D* maps using the following equation: $f = 1 - \exp[-b_1 \cdot (ADC - D)]$[23]. In addition, semi-quantitative tissue characterisation, similar to the Funaki classification[32], was based on the T2w signal intensity. The measured T2w signal *S* was normalised using scan specific reference values of the rectus abdominis muscle ($S_r$) and the uterine myometrium ($S_m$). These scan specific reference values were taken from manually drawn ROIs in these tissues. The normalised intensity was calculated as follows: $S' = (S-S_r)/(S_m-S_r)$.

For every targeted uterine fibroid and individual treatment cell, the pre-treatment normalised T2w signal intensity *S'*, mean diffusion coefficient *D*, mean pseudodiffusion coefficient *D** and mean perfusion fraction *f* were measured for statistical analysis. Per treatment cell individually, the perfusion defect (NPV divided by cell-based VOI), the mean temperature curves, and the resulting lethal (thermal) dose index within the VOIs were analysed. The lethal dose index per cell was represented as the volumetric fraction of the VOI that had reached the lethal thermal dose of 240 EM at 43°C. The following cell-specific temperature parameters were extracted from the temperature curves: maximum average

temperature within the VOI (°C), time to maximum average temperature (s), average temperature at t=10 s, t=20 s, and t=30 s (°C), time to lethal temperature of 60°C (s), and time to lethal thermal dose (s). All temperature-related parameters were computed as the average of the coronal slice stack and sagittal slice intersecting the corresponding treatment cell.

**Statistical analysis**

Descriptive statistics were used to summarise the patient, lesion and temperature characteristics. Continuous data are presented as mean ± standard deviation (SD), while categorical variables are expressed in frequency and percentage. A one-way analysis of variance (ANOVA) with post-hoc multiple comparisons (Bonferroni) was used to determine whether there were any significant differences between the means of two or more groups. After confirmation of a normal distribution, a univariable linear regression analysis was applied to measure and describe the correlation between the mean pre-treatment IVIM perfusion parameters (i.e. perfusion-free diffusion coefficient *D*, flow-related pseudodiffusion coefficient *D**, and perfusion fraction *f*) and the normalised T2w signal intensity *S'* and any of the parameters describing the temperature evolution over time. An independent sample t-test was used to determine whether the IVIM parameters and cell-specific temperature parameters were significantly different between successfully and suboptimally sonicated treatment cells. A sonication was classified successful if the treatment cell was completely ablated within the drawn ellipsoidal VOI (perfusion defect = 1), a suboptimal ablation was equal to a perfusion defect less than 1. All statistical analyses were conducted by using IBM SPSS Statistics, version 20.0 (Armonk, NY, USA).



**Table 1.** Features of the therapeutic sonications, analysed in a cell-based ellipsoidal volume of 4 × 4 × 10 $mm^3$ (n=724)

| Characteristics | Value |
|---|---|
| Cell type | |
| Feedback | 720 (99%) |
| Non-feedback | 4 (1%) |
| Frequency | |
| 1.2 MHz | 704 (97%) |
| 1.45 MHz | 20 (3%) |
| Acoustic power (W) | 160±45 |
| T max (°C) | 58.2±5.0 |
| Time to T max (s) | 44.4±18.3 |
| T (°C) | |
| t=10 s | 45.8±4.0 |
| t=20 s | 52.3±5.3 |
| t=30 s | 54.6±5.1 |
| Time to lethal dose (s) | 54.6±23.4 |

Values are expressed in mean ± standard deviation (SD) and number (percentage); T, temperature; t, time. Note: all temperature-related parameters were computed as the average of the coronal slice stack and sagittal slice intersecting the corresponding treatment cell.

# Results

**Patient and lesions**

Between April 2010 and April 2014, in total, 73 premenopausal women with symptomatic uterine fibroids underwent a clinical MR-HIFU treatment in our hospital. After evaluation of the anatomical (T2w MRI and CE-T1w MRI), functional (DWI) and MR thermometry data, 31 patients (42%) with 35 uterine fibroids were selected for analyses. The reasons for exclusion (n=42) were: an incomplete dataset (n=11) or an unusable dataset (n=31) caused by motion through for instance pain, repositioning or intra-procedural urinary bladder filling (with saline in order to affect the range of the ultrasound beam path). The mean age of the included patients was 44.0±4.2 years with a mean body mass index (BMI) of 23.6±3.0 kg/m$^2$. The mean baseline fibroid volume was 401±278 cm$^3$, the mean achieved NPV was 152±151 cm$^3$ which corresponds to a NPV ratio of 0.38±0.21.

The mean pre-treatment perfusion fraction *f* in the contour segmentations of the uterine fibroids was 0.45±0.07, the mean diffusion coefficient *D* was $0.77\times10^{-3}\pm0.17\times10^{-3}$ mm$^2$/s and the flow-related pseudodiffusion coefficient *D** was $2.51\times10^{-3}\pm0.38\times10^{-3}$ mm$^2$/s. According to the Funaki classification[32], the uterine fibroids were classified into type 1 (n=18), type 2 (n=10), and type 3 (n=7). The mean pre-treatment normalised T2w signal intensity *S'* was, respectively, 0.16±0.19, 0.47±0.44 and 0.72±0.42 (p<0.001). When these IVIM parameters were categorised into the three types of uterine fibroids[32], we found a significantly (p<0.001) higher diffusion coefficient *D* in the high-intensity type 3 uterine fibroids ($0.91\times10^{-3}\pm0.21\times10^{-3}$ mm$^2$/s) when compared to low-intensity type 1 fibroids ($0.69\times10^{-3}\pm0.12\times10^{-3}$ mm$^2$/s). No significant difference in the perfusion fraction *f* was observed between the three groups (p=0.818).

**Treatment cell analyses using the cell-based VOIs**

A total of 833 therapeutic sonications were used to treat 35 uterine fibroids in 31 patients. After evaluation of the HIFU focal point position, 109 therapeutic sonications were excluded due to a displaced focal point (n=70) or motion-related MR thermometry artefacts (n=39). The remaining 724 therapeutic sonications (87%) were included for further statistical analysis (*Figure 2*). The main treatment cell characteristics, as analysed in the cell-based VOIs, are presented in *Table 1*.

The mean pre-treatment perfusion fraction *f* over the cell-based VOIs was 0.41±0.17, the mean diffusion coefficient *D* was $0.73\times10^{-3}\pm0.31\times10^{-3}$ mm$^2$/s and the flow-related pseudodiffusion coefficient *D** was $2.26\times10^{-3}\pm0.74\times10^{-3}$ mm$^2$/s. The univariable linear regression analysis showed a positive correlation (*B*=0.671, p<0.001, $R^2$=0.269) between the mean pre-treatment diffusion coefficient *D* and the baseline normalised T2w signal intensity *S'* (*Table 2*). Accordingly, 27% of the variability in the T2w signal intensity *S'* can

**Table 2.** Pre-treatment intravoxel incoherent motion (IVIM) parameters in relation to pre-treatment normalised T2w signal intensity *S'* (n=724)

| IVIM parameter | Normalised T2w SI (*S'*) | |
|---|---|---|
| | *B* | $R^2$ |
| Diffusion coefficient (*D*) | 0.671 (p<0.001) | 0.269 |
| Perfusion coefficient (*D**) | 0.082 (p<0.001) | 0.023 |
| Perfusion fraction (*f*) | -0.147 (p=0.098) | 0.004 |

T2w SI, T2-weighted signal intensity; *B*, regression coefficient; $R^2$, coefficient of determination

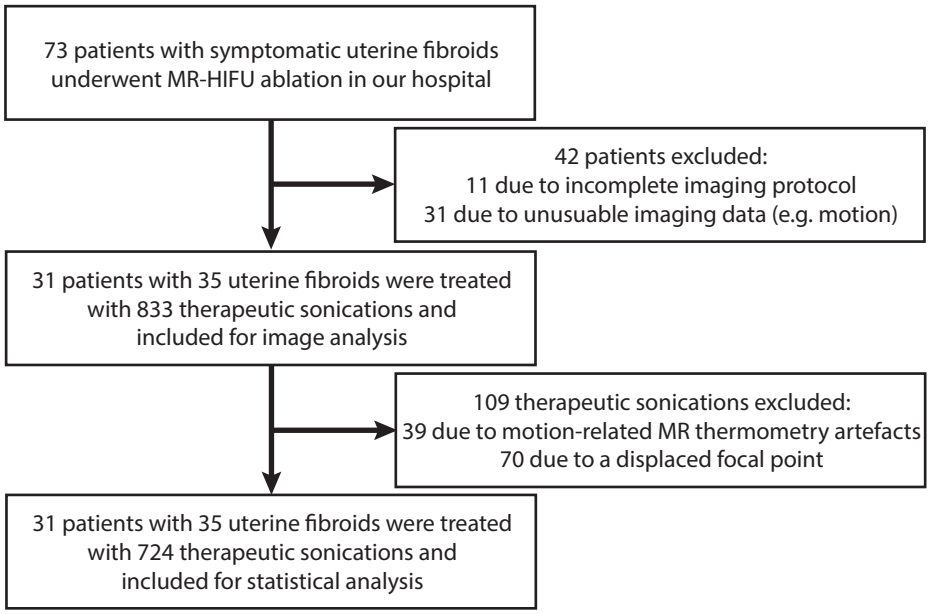


**Figure 2.** Flowchart for selection of anatomical, functional and MR thermometry data collected in patients undergoing MR-HIFU ablation of uterine fibroids.

be explained by the diffusion coefficient *D*. *Figure 3* shows a scatter plot of the relationship between the mean pre-treatment diffusion coefficient *D* and the pre-treatment normalised T2w signal intensity *S'*. As shown in *Table 3*, we found no linear relationship between the pre-treatment normalised T2w signal intensity *S'* and any of the parameters describing

**Table 3.** Pre-treatment intravoxel incoherent motion (IVIM) parameters and normalised T2w signal intensity S' in relation to the any of the parameters describing the temperature evolution over time (n=724)

| | Max ΔT (°C) | | Time to max ΔT (s) | | ΔT (°C) t=20 s | | ΔT (°C) t=30 s | | Time to T=60°C (s)[a,b] | | Time to lethal dose (s)[b] | |
|---|---|---|---|---|---|---|---|---|---|---|---|---|
| | *B* | $R^2$ | *B* | $R^2$ | *B* | $R^2$ | *B* | $R^2$ | *B* | $R^2$ | *B* | $R^2$ |
| *D* | -1.182 (p=0.045) | 0.006 | -2.344 (p=0.282) | 0.002 | -0.681 (p=0.279) | 0.002 | -0.907 (p=0.133) | 0.003 | 0.105 (p=0.207) | 0.006 | 0.099 (p=0.065) | 0.005 |
| *D** | -1.198 (p<0.001) | 0.032 | -2.107 (p=0.022) | 0.007 | -0.619 (p=0.019) | 0.008 | -0.655 (p=0.010) | 0.009 | -0.027 (p=0.482) | 0.002 | -0.032 (p=0.155) | 0.003 |
| *f* | -4.056 (p<0.001) | 0.019 | -6.759 (p=0.093) | 0.004 | -1.465 (p=0.208) | 0.002 | -1.839 (p=0.100) | 0.004 | -0.189 (p=0.239) | 0.005 | -0.221 (p=0.027) | 0.007 |
| *S'* | -0.659 (p=0.149) | 0.003 | 3.791 (p=0.024) | 0.007 | -0.958 (p=0.048) | 0.005 | -0.926 (p=0.047) | 0.005 | 0.057 (p=0.423) | 0.002 | 0.092 (p=0.025) | 0.007 |

*D*, perfusion-free diffusion coefficient; *D**, flow-related pseudodiffusion coefficient; *f*, perfusion fraction; S', normalised T2-weighted signal intensity; *B*, regression coefficient; $R^2$, coefficient of determination; ΔT, temperature increase, calculated from an assumed baseline temperature of 37°C; t, time; T, temperature; [a], only the treatment cells which have reached a temperature of ≥60°C are shown (n=282); [b], Logarithmic transformation was applied to obtain a normal distribution of the variables. Note: all temperature-related parameters were computed as the average of the coronal slice stack and sagittal slice intersecting the corresponding treatment cell.

**Table 4.** Differences in pre-treatment intravoxel incoherent motion (IVIM) parameters and normalised T2w signal intensity *S'* between successfully and suboptimally ablated ellipsoidal treatment cells ($4 \times 4 \times 10$ mm$^3$)

| IVIM parameter | Perfusion defect < 1 (n=307) | Perfusion defect = 1 (n=417) | p | MD (SE) |
|---|---|---|---|---|
| Diffusion coefficient (*D*) | 0.74±0.29 | 0.72±0.33 | 0.283 | 0.03 (0.02) |
| Perfusion coefficient (*D**) | 2.37±0.80 | 2.19±0.69 | 0.001 | 0.19 (0.06) |
| Perfusion fraction (*f*) | 0.43±0.17 | 0.40±0.17 | 0.005 | 0.04 (0.01) |
| Normalised T2w SI (*S'*) | 0.39±0.42 | 0.35±0.39 | 0.248 | 0.04 (0.03) |

Values are expressed in mean ± standard deviation; Perfusion defect, non-perfused volume divided by cell-based volume of interest, MD, mean difference; SE, standard error of difference; T2w SI, T2-weighted signal intensity



the temperature evolution over time ($R^2$ ranged from 0.002 to 0.007). Moreover, there was no linear relation found ($R^2$ ranged from 0.002 to 0.032) between the mean pre-treatment IVIM parameters and any of the parameters describing the temperature evolution over time.

We observed a significantly higher (p=0.001) mean pre-treatment pseudodiffusion coefficient *D** in the suboptimally sonicated treatment cells ($2.37\times10^{-3}\pm0.80\times10^{-3}$ mm$^2$/s) as compared with the successfully sonicated treatment cells ($2.19\times10^{-3}\pm0.69\times10^{-3}$ mm$^2$/s). No significant difference in the mean pre-treatment diffusion coefficient *D* (p=0.283) and normalised T2w signal intensity *S'* (p=0.248) was found between the successfully and suboptimally sonicated treatment cells (*Table 4*).

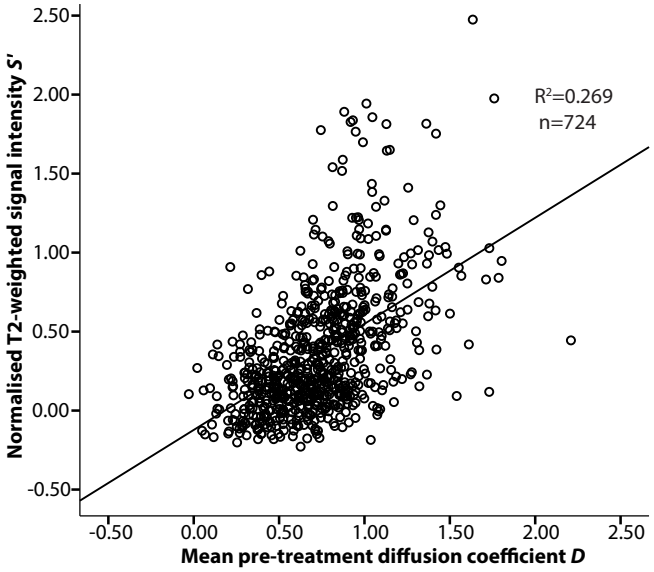


**Figure 2.** Scatter plot shows a positive correlation ($R^2$=0.269) between the mean pre-treatment diffusion coefficient *D* and the normalised T2-weighted signal intensity *S'*. A higher pre-treatment diffusion coefficient *D* is related to a higher normalised T2w signal intensity *S'*, most probably indicating lower restriction of water molecule motion in more fluid-rich tissue.

## Discussion

Several studies[8,32,49-53] have shown that the NPV ratio is an important indicator for success of MR-HIFU ablation. A higher NPV ratio corresponds to a higher fibroid volume reduction and more symptom relief and quality of life improvement. The primary mechanism involved in developing an appropriate NPV ratio with MR-HIFU ablation is the generation of heat due to absorption of acoustic energy leading to a cytotoxic temperature increase in the targeted tissue[54,55]. The tolerance of tissues to temperature elevation is dependent on the type of tissue and the magnitude and duration of temperature rise. Assuming that the tissue-specific thermal conductivity is less variable among uterine fibroids, it is expected that the maximum rates of temperature change are largely dependent on the specific heat capacity and the blood perfusion state of the uterine fibroids[36,56]. Since the specific heat capacity of water - by a given amount of thermal energy - is higher than that of any other tissue component (e.g. collagen), the abundance of interstitial water likely plays an important role in the temperature elevation with MR-HIFU. Knowledge of the perfusion state of uterine fibroids is important as blood flow can have a direct quantitative effect on the rate and distribution of heating. Therefore, we have investigated whether IVIM MRI could be used for tissue characterisation of uterine fibroids and whether IVIM diffusion and perfusion parameters could predict the temperature rise during an MR-HIFU ablation. Using linear regression, we were not able to find a relation between the IVIM parameters and the temperature curves. This may be the result of a number of factors. First, the success of an MR-HIFU ablation is not only influenced by the observed biologic tissue characteristics of the uterine fibroid. Other variables may have influenced the amount of thermal energy which has actually reached the targeted region. For instance, the amount of acoustic energy applied, the sonication frequency and treatment cell size used[57], acoustic attenuation of ultrasound while travelling through different tissue layers, accumulated heating in subsequent treatment cells (although the prescribed cooling times were obeyed), or the presence of a large blood vessel. Second, for an adequate separation of the perfusion and diffusion effects using IVIM analysis[23,24,58], the use of multiple *b*-values in a lower range would be preferable[59,60]. The lowest non-zero *b*-value (200 s/mm$^2$) is relatively high, limiting the capability of measuring the rapid perfusion component. Especially in highly-perfused tissues[20,27,61-63] like uterine fibroids, the importance of acquiring low *b*-values becomes paramount. Using the ADC maps from the signal intensities at *b*-values 0 and 200 s/mm$^2$ might have led to an underestimation of the true perfusion effect[64]. An optimisation of the DWI acquisition scheme, by adding more *b*-values in the lower range, would therefore be interesting to improve the image quality of the IVIM maps. However, the necessity to embed the DWI scans in the clinical workflow without causing unacceptable acquisition times has forced us to use to the current protocol. Third, IVIM MRI does not measure the volume blood flow within the uterine fibroids, which would be the parameter governing the cooling effect due to perfusion. The IVIM theory has been proposed to describe the presence of two water compartments: the slow extravascular molecular movement of water (diffusion coefficient *D*) and the faster randomly-orientated motion of water through the capillaries (pseudodiffusion coefficient *D**). The calculated perfusion fraction *f* is therefore merely a representation of the volume fraction of incoherently flowing blood in tissues. Future research with MRI-based perfusion measurement techniques[65,66], such as dynamic contrast-enhanced (DCE) MRI or arterial spin labelling (ASL) are warranted to measure the blood perfusion flow rate that deprives the tissues of heat due to

heat-sink[67,68]. Recently, Kim *et al*.[35,69,70] have reported the use of DCE MRI in the prediction of the immediate treatment efficacy of MR-HIFU ablation. They found that a higher pre-treatment volume transfer constant (i.e. $K^{trans}$) will lead to a significantly lower NPV ratio. However, $K^{trans}$ characterises the diffusive transport (kinetics) of gadolinium-based contrast agent across the capillary endothelium[71] to determine the vascular permeability (transendothelial leakage from the capillaries). It is not well-known to what extent $K^{trans}$ determines the blood flow[35,71], therefore, measurements of blood volume (BV) and blood flow (BF) are indicated for an accurate assessment of perfusion. Finally, several other limitations have to be acknowledged. The study population consisted of only patients who fulfilled the eligibility criteria for treatment and who had undergone the complete set of MR examinations (*Figure 2*). This could have induced a selection bias, because less heterogeneous T2w hyper-intense uterine fibroids (type 3)[32] were included in this study. In addition, we did not use histological analyses to confirm treatment success. There is a possibility that measurement errors have occurred in the MR thermometry data, even a slight motion will significantly degrade the accuracy of the temperature map[72,73]. Considering that our study dealt with non-invasive clinical MR-HIFU data, there was no justification to perform such invasive measurements.



In conclusion, our results show a high pre-treatment perfusion fraction (*f*) of more than 0.4 in the targeted uterine fibroids. We found a significantly positive correlation between the cell-based mean pre-treatment diffusion coefficient *D* and normalised T2w signal intensity *S'* ($B$=0.671, $p<0.001$, $R^2$=0.269), but we were not able to show correlations between the IVIM parameters and the heating effectiveness of MR-HIFU ablation, as determined from the MR thermometry data. However, we did find a significant higher pre-treatment pseudodiffusion coefficient *D** in the suboptimally sonicated treatment cells, as determined with CE-T1w MRI data, which may suggest that the extent of non-perfused volume is related to the perfusion coefficient *D** rather than the normalised T2w signal intensity. For an absolute quantification of perfusion, further studies with MRI-based perfusion measurement techniques are indicated to measure the volume blood flow within the uterine fibroids to validate our findings.

# References


1. Hynynen K. MRIgHIFU: a tool for image-guided therapeutics. *J Magn Reson Imaging.* 2011;34:482-493
2. Zhou YF. High intensity focused ultrasound in clinical tumor ablation. *World J Clin Oncol.* 2011;2:8-27
3. Diller KR, Ryan TP. Heat transfer in living systems: Current opportunities. *ASME J Heat Transf.* 1998;120:810-829
4. Lepock JR. How do cells respond to their thermal environment? *Int J Hyperthermia.* 2005;21:681-687
5. Simanovskii DM, Mackanos MA, Irani AR, O'Connell-Rodwell CE, Contag CH, Schwettman HA, Palanker DV. Cellular tolerance to pulsed hyperthermia. *Phys Rev E Stat Nonlin Soft Matter Phys.* 2006;74:011915
6. Arleo EK, Khilnani NM, Ng A, Min RJ. Features influencing patient selection for fibroid treatment with magnetic resonance-guided focused ultrasound. *J Vasc Interv Radiol.* 2007;18:681-685
7. Behera MA, Leong M, Johnson L, Brown H. Eligibility and accessibility of magnetic resonance-guided focused ultrasound (MRgFUS) for the treatment of uterine leiomyomas. *Fertil Steril.* 2010;94:1864-1868
8. Lenard ZM, McDannold NJ, Fennessy FM, Stewart EA, Jolesz FA, Hynynen K, Tempany CM. Uterine leiomyomas: MR imaging-guided focused ultrasound surgery-imaging predictors of success. *Radiology.* 2008;249:187-194
9. Zhang J, Mougenot C, Partanen A, Muthupillai R, Hor PH. Volumetric MRI-guided high-intensity focused ultrasound for noninvasive, in vivo determination of tissue thermal conductivity: initial experience in a pig model. *J Magn Reson Imaging.* 2013;37:950-957
10. Stewart EA, Friedman AJ, Peck K, Nowak RA. Relative overexpression of collagen type I and collagen type III messenger ribonucleic acids by uterine leiomyomas during the proliferative phase of the menstrual cycle. *J Clin Endocrinol Metab.* 1994;79:900-906
11. Leppert PC, Baginski T, Prupas C, Catherino WH, Pletcher S, Segars JH. Comparative ultrastructure of collagen fibrils in uterine leiomyomas and normal myometrium. *Fertil Steril.* 2004; 82 Suppl 3:1182-1187
12. Wells PN. Review: absorption and dispersion of ultrasound in biological tissue. *Ultrasound Med Biol.* 1975;1:369-376
13. Dyson M. Mechanisms involved in therapeutic ultrasound. *Physiotherapy.* 1987;73:116-120
14. Hricak H, Tscholakoff D, Heinrichs L, Fisher MR, Dooms GC, Reinhold C, Jaffe RB. Uterine leiomyomas: correlation of MR, histopathologic findings, and symptoms. *Radiology.* 1986;158:385-391
15. Yamashita Y, Torashima M, Takahashi M, Tanaka N, Katabuchi H, Miyazaki K, Ito M, Okamura H. Hyperintense uterine leiomyoma at T2-weighted MR imaging: differentiation with dynamic enhanced MR imaging and clinical implications. *Radiology.* 1993;189:721-725
16. Ueda H, Togashi K, Konishi I, Kataoka ML, Koyama T, Fujiwara T, Kobayashi H, Fujii S, Konishi J. Unusual appearances of uterine leiomyomas: MR imaging findings and their histopathologic backgrounds. *Radiographics.* 1999;19 Spec No:S131-145
17. Bammer R. Basic principles of diffusion-weighted imaging. *Eur J Radiol.* 2003;45:169-184
18. Hagmann P, Jonasson L, Maeder P, Thiran JP, Wedeen VJ, Meuli R. Understanding diffusion MR imaging techniques: from scalar diffusion-weighted imaging to diffusion tensor imaging and beyond. *Radiographics.* 2006;26 Suppl 1:S205-223
19. Le Bihan D. Molecular diffusion, tissue microdynamics and microstructure. *NMR Biomed.* 1995;8:375-386
20. Yamada I, Aung W, Himeno Y, Nakagawa T, Shibuya H. Diffusion coefficients in abdominal organs and hepatic lesions: evaluation with intravoxel incoherent motion echo-planar MR imaging. *Radiology.* 1999;210:617-623
21. Basser PJ. Inferring microstructural features and the physiological state of tissues from diffusion-weighted images. *NMR Biomed.* 1995;8:333-344
22. Yoshida S, Masuda H, Ishii C, Saito K, Kawakami S, Kihara K. Initial experience of functional imaging of upper urinary tract neoplasm by diffusion-weighted magnetic resonance imaging. *Int J Urol.* 2008;15:140-143
23. Le Bihan D, Breton E, Lallemand D, Aubin ML, Vignaud J, Laval-Jeantet M. Separation of diffusion and perfusion in intravoxel incoherent motion MR imaging. *Radiology.* 1988;168:497-505
24. Le Bihan D, Turner R, MacFall JR. Effects of intravoxel incoherent motions (IVIM) in steady-state free precession (SSFP) imaging: application to molecular diffusion imaging. *Magn Reson Med.* 1989;10:324-337
25. Le Bihan D, Breton E, Lallemand D, Grenier P, Cabanis E, Laval-Jeantet M. MR imaging of intravoxel incoherent motions: application to diffusion and perfusion in neurologic disorders. *Radiology.* 1986;161:401-407

26. Federau C, Maeder P, O'Brien K, Browaeys P, Meuli R, Hagmann P. Quantitative measurement of brain perfusion with intravoxel incoherent motion MR imaging. *Radiology.* 2012;265:874-881
27. Lemke A, Laun FB, Simon D, Stieltjes B, Schad LR. An in vivo verification of the intravoxel incoherent motion effect in diffusion-weighted imaging of the abdomen. *Magn Reson Med.* 2010;64:1580-1585
28. Muniz CJ, Fleischer AC, Donnelly EF, Mazer MJ. Three-dimensional color Doppler sonography and uterine artery arteriography of fibroids: assessment of changes in vascularity before and after embolization. *J Ultrasound Med.* 2002;21:129-133
29. Chen CL, Xu YJ, Liu P, Zhu JH, Ma B, Zeng BL, Zhou Y, Wang L, Tang YX, Guo CJ. Characteristics of vascular supply to uterine leiomyoma: an analysis of digital subtraction angiography imaging in 518 cases. *Eur Radiol.* 2013;23:774-779
30. Lethaby A, Vollenhoven B, Sowter M. Pre-operative GnRH analogue therapy before hysterectomy or myomectomy for uterine fibroids. *Cochrane Database Syst Rev.* 2001;2:CD000547
31. Kröncke TJ. Benign uterine lesions. In: Hamm B, Forstner R, ed. MRI and CT of the Female Pelvis. 1st edn. Berlin Heidelberg, Germany: Springer-Verlag 2007:61-100
32. Funaki K, Fukunishi H, Funaki T, Sawada K, Kaji Y, Maruo T. Magnetic resonance-guided focused ultrasound surgery for uterine fibroids: relationship between the therapeutic effects and signal intensity of preexisting T2-weighted magnetic resonance images. *Am J Obstet Gynecol.* 2007;96:184 e181-186
33. Swe TT, Onitsuka H, Kawamoto K, Ueyama T, Tsuruchi N, Masuda K. Uterine leiomyoma: correlation between signal intensity on magnetic resonance imaging and pathologic characteristics. *Radiat Med.* 1992;10:235-242
34. Ha HK, Jee MK, Lee HJ, Choe BY, Park JS, Lee JM, Nam-Koong SE. MR imaging analysis of heterogeneous leiomyomas of the uterus. *Front Biosci.* 1997;2:f4-12
35. Kim YS, Lim HK, Kim JH, Rhim H, Park BK, Keserci B, Köhler MO, Bae DS, Kim BG, Lee JW, Kim TJ, Sokka S, Lee JH. Dynamic contrast-enhanced magnetic resonance imaging predicts immediate therapeutic response of magnetic resonance-guided high-intensity focused ultrasound ablation of symptomatic uterine fibroids. *Invest Radiol.* 2011;46:639-647
36. Kim YS, Kim BG, Rhim H, Bae DS, Lee JW, Kim TJ, Choi CH, Lee YY, Lim HK. Uterine Fibroids: Semiquantitative Perfusion MR Imaging Parameters Associated with the Intraprocedural and Immediate Postprocedural Treatment Efficiencies of MR Imaging-guided High-Intensity Focused Ultrasound Ablation. *Radiology.* 2014 Jul 1:132719
37. Ikink ME, Voogt MJ, Verkooijen HM, Lohle PN, Schweitzer KJ, Franx A, Mali WP, Bartels LW, van den Bosch MA. Mid-term clinical efficacy of a volumetric magnetic resonance-guided high-intensity focused ultrasound technique for treatment of symptomatic uterine fibroids. *Eur Radiol.* 2013;23:3054-3061
38. Voogt MJ, Trillaud H, Kim YS, Mali WP, Barkhausen J, Bartels LW, Deckers R, Frulio N, Rhim H, Lim HK, Eckey T, Nieminen HJ, Mougenot C, Keserci B, Soini J, Vaara T, Köhler MO, Sokka S, van den Bosch MA. Volumetric feedback ablation of uterine fibroids using magnetic resonance-guided high intensity focused ultrasound therapy. *Eur Radiol.* 2012;22:411-417
39. Ikink ME, Voogt MJ, van den Bosch MA, Nijenhuis RJ, Keserci B, Kim YS, Vincken KL, Bartels LW. Diffusion-weighted magnetic resonance imaging using different b-value combinations for the evaluation of treatment results after volumetric MR-guided high-intensity focused ultrasound ablation of uterine fibroids. *Eur Radiol.* 2014;24:2118-2127
40. Kohler MO, Mougenot C, Quesson B, Enholm J, Le Bail B, Laurent C, Moonen CT, Ehnholm GJ. Volumetric HIFU ablation under 3D guidance of rapid MRI thermometry. *Med Phys.* 2009;36:3521-3535
41. Enholm JK, Kohler MO, Quesson B, Mougenot C, Moonen CT, Sokka SD. Improved volumetric MR-HIFU ablation by robust binary feedback control. *IEEE Trans Biomed Eng.* 2010;57:103-113
42. Ishihara Y, Calderon A, Watanabe H, Okamoto K, Suzuki Y, Kuroda K. A precise and fast temperature mapping using water proton chemical shift. *Magn Reson Med.* 1995;34:814-823
43. Mougenot C, Quesson B, de Senneville BD, de Oliveira PL, Sprinkhuizen S, Palussière J, Grenier N, Moonen CT. Three-dimensional spatial and temporal temperature control with MR thermometry-guided focused ultrasound (MRgHIFU). *Magn Reson Med.* 2009;61:603-614
44. Sapareto SA, Dewey W. Thermal dose determination in cancer therapy. *Int J Radiat Oncol Biol Phys.* 1984;10:787-800
45. Chung AH, Jolesz FA, Hynynen K. Thermal dosimetry of a focused ultrasound beam in vivo by magnetic resonance imaging. *Med Phys.* 1999;26:2017-2026
46. Yarmolenko PS, Moon EJ, Landon C, Manzoor A, Hochman DW, Viglianti BL, Dewhirst MW. Thresholds for thermal damage to normal tissues: an update. *Int J Hyperthermia.* 2011;27:320-343
47. Dewhirst MW, Viglianti BL, Lora-Michiels M, Hanson M, Hoopes PJ. Basic principles of thermal dosimetry and thermal thresholds for tissue damage from hyperthermia. *Int J Hyperthermia.* 2003;19:267-294
48. Heckel F, Konrad O, Karl Hahn H, Peitgen H-O. Interactive 3D medical image segmentation with energy-minimizing implicit functions. *Computers & Graphics.* 2011;35:275-287

49. Stewart EA, Gostout B, Rabinovici J, Kim HS, Regan L, Tempany CM. Sustained relief of leiomyoma symptoms by using focused ultrasound surgery. *Obstet Gynecol.* 2007;110:279-287
50. LeBlang SD, Hoctor K, Steinberg FL. Leiomyoma shrinkage after MRI-guided focused ultrasound treatment: report of 80 patients. *AJR Am J Roentgenol.* 2010;194:274-280
51. Okada A, Morita Y, Fukunishi H, Takeichi K, Murakami T. Non-invasive magnetic resonance-guided focused ultrasound treatment of uterine fibroids in a large Japanese population: impact of the learning curve on patient outcome. *Ultrasound Obstet Gynecol.* 2009;34:579-583
52. Machtinger R, Inbar Y, Cohen-Eylon S, Admon D, Alagem-Mizrachi A, Rabinovici J. MR-guided focus ultrasound (MRgFUS) for symptomatic uterine fibroids: predictors of treatment success. *Hum Reprod.* 2012;27:3425-3431
53. Morita Y, Ito N, Hikida H, Takeuchi S, Nakamura K, Ohashi H. Non-invasive magnetic resonance imaging-guided focused ultrasound treatment for uterine fibroids - early experience. *Eur J Obstet Gynecol Reprod Biol.* 2008;139:199-203
54. O'Brien WD Jr. Ultrasound-biophysics mechanisms. *Prog Biophys Mol Biol.* 2007;93:212-255
55. Whittingham TA. The purpose and techniques of acoustic output measurement. In: Duck FA, Baker AC, Starritt HC, ed. Ultrasound in Medicine. 1st edn. Bristol, UK: Taylor & Francis 1998:129-132
56. Pennes HH. Analysis of tissue and arterial blood temperatures in the resting human forearm. *J Appl Physiol.* 1948;1:93-122
57. Kim YS, Keserci B, Partanen A, Rhim H, Lim HK, Park MJ, Köhler MO. Volumetric MR-HIFU ablation of uterine fibroids: role of treatment cell size in the improvement of energy efficiency. *Eur J Radiol.* 2012;81:3652-3659
58. Le Bihan D. Intravoxel incoherent motion perfusion MR imaging: a wake-up call. *Radiology.* 2008;249:748-752
59. Lemke A, Stieltjes B, Schad LR, Laun FB. Toward an optimal distribution of b values for intravoxel incoherent motion imaging. *Magn Reson Imaging.* 2011;29:766-776
60. Freiman M, Voss SD, Mulkern RV, Perez-Rossello JM, Callahan MJ, Warfield SK. In vivo assessment of optimal b-value range for perfusion-insensitive apparent diffusion coefficient imaging. *Med Phys.* 2012;39:4832-4839
61. Luciani A, Vignaud A, Cavet M, Nhieu JT, Mallat A, Ruel L, Laurent A, Deux JF, Brugieres P, Rahmouni A. Liver cirrhosis: intravoxel incoherent motion MR imaging--pilot study. *Radiology.* 2008;249:891-899
62. Muller MF, Prasad P, Siewert B, Nissenbaum MA, Raptopoulos V, Edelman RR. Abdominal diffusion mapping with use of a whole-body echo-planar system. *Radiology.* 1994;190:475-478
63. Dyvorne HA, Galea N, Nevers T, Fiel MI, Carpenter D, Wong E, Orton M, de Oliveira A, Feiweier T, Vachon ML, Babb JS, Taouli B. Diffusion-weighted imaging of the liver with multiple b values: effect of diffusion gradient polarity and breathing acquisition on image quality and intravoxel incoherent motion parameters-a pilot study. *Radiology.* 2013;266:920-929
64. Cohen AD, Schieke MC, Hohenwalter MD, Schmainda KM. The effect of low b-values on the intravoxel incoherent motion derived pseudodiffusion parameter in liver. *Magn Reson Med.* 2014;Jan 29:25109
65. Essig M, Shiroishi MS, Nguyen TB, Saake M, Provenzale JM, Enterline D, Anzalone N, Dörfler A, Rovira A, Wintermark M, Law M. Perfusion MRI: the five most frequently asked technical questions. *AJR Am J Roentgenol.* 2013;200:24-34
66. Sandrasegaran K. Functional MR imaging of the abdomen. *Radiol Clin North Am.* 2014;52:883-903
67. Kolios MC, Sherar MD, Hunt JW. Large blood vessel cooling in heated tissues: a numerical study. *Phys Med Biol.* 1995;40:477-494
68. Jiang F, He M, Liu YJ, Wang ZB, Zhang L, Bai J. High intensity focused ultrasound ablation of goat liver in vivo: Pathologic changes of portal vein and the "heat-sink" effect. *Ultrasonics.* 2013;53:77-83
69. Kim YS, Kim JH, Rhim H, Lim HK, Keserci B, Bae DS, Kim BG, Lee JW, Kim TJ, Choi CH. Volumetric MR-guided high-intensity focused ultrasound ablation with a one-layer strategy to treat large uterine fibroids: initial clinical outcomes. *Radiology.* 2012;263:600-609
70. Kim YS, Park MJ, Keserci B, Nurmilaukas K, Köhler MO, Rhim H, Lim HK. Uterine fibroids: postsonication temperature decay rate enables prediction of therapeutic responses to MR imaging-guided high-intensity focused ultrasound ablation. *Radiology.* 2014;270:589-600
71. Tofts PS, Brix G, Buckley DL, Evelhoch JL, Henderson E, Knopp MV, Larsson HB, Lee TY, Mayr NA, Parker GJ, Port RE, Taylor J, Weisskoff RM. Estimating kinetic parameters from dynamic contrast-enhanced T(1)-weighted MRI of a diffusable tracer: standardized quantities and symbols. *J Magn Reson Imaging.* 1999;10:223-232
72. Roujol S, Ries M, Quesson B, Moonen C, Denis de Senneville B. Real-time MR-thermometry and dosimetry for interventional guidance on abdominal organs. *Magn Reson Med.* 2010;63:1080-1087
73. Rieke V, Butts Pauly K. MR thermometry. *J Magn Reson Imaging.* 2008;27:376-390

# 7 General discussion

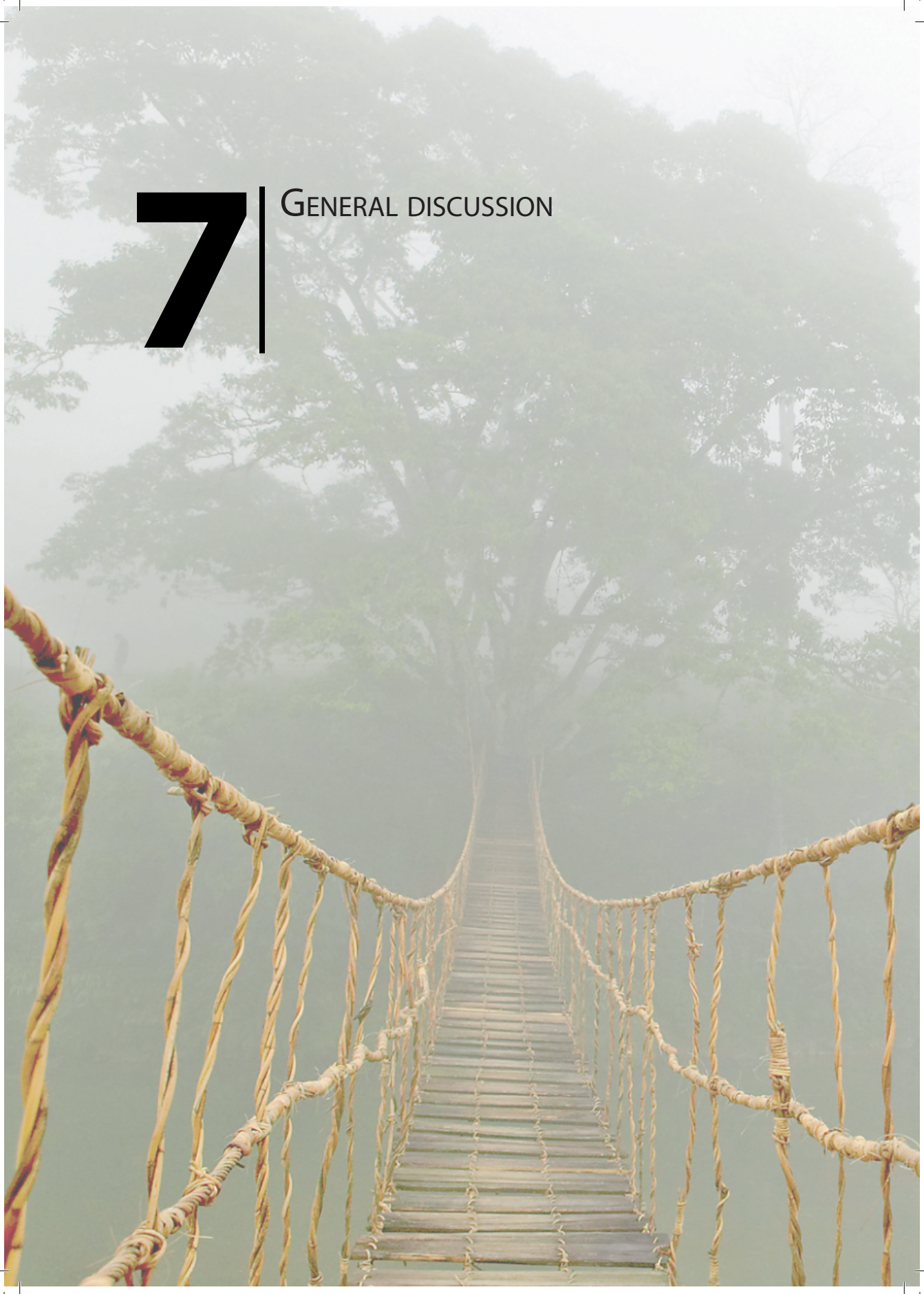

Magnetic resonance-guided high-intensity focused ultrasound (MR-HIFU) ablation has been increasingly used for the treatment of symptomatic uterine fibroids. Previously, treatment of uterine fibroids was merely the domain of the gynaecologist. However, over the past two decades, minimally or non-invasive treatment techniques in the field of interventional radiology have been introduced to treat uterine fibroids: uterine artery embolisation (UAE) and MR-HIFU (*Figure 1*). Development of these radiological techniques has significantly expanded the range of treatment options. Both UAE and MR-HIFU provide alternative treatments for patients suffering from uterine fibroids and avoid invasive procedures with the preservation of the uterus[1]. In 2009, a novel volumetric MR-HIFU system was approved by the European Union for the treatment of uterine fibroids[2]. Ever since, extensive research has been performed in order to demonstrate the safety and clinical efficacy of using this system. A prospective multicentre study has already proven that it is technically feasible and safe to perform a volumetric MR-HIFU ablation for the treatment of uterine fibroids[3].

The aim of the studies described in this thesis is to investigate the clinical implementation of volumetric MR-HIFU ablation for uterine fibroids. For this purpose, the mid-term clinical efficacy of volumetric MR-HIFU ablation was studied first (*Chapter 2*)[4]. Subsequently, the efficacy of this technique was compared with that of UAE (*Chapter 3*)[5]. Both volumetric MR-HIFU ablation and UAE resulted in significant symptom relief and improvement of quality of life in patients with symptomatic uterine fibroids. Although initial results suggest that UAE is to be preferred over MR-HIFU ablation, with expanding knowledge and experience it will likely be possible to treat increasingly aggressively with persistence of patient safety and comfort. Within this framework, a direct skin cooling (DISC) device was developed to provide an additional buffer against potential adverse events related to skin heating and to enhance the safety and efficacy of MR-HIFU treatments for uterine fibroids (*Chapter 4*). In the second part of this thesis, MR imaging techniques were explored for the measurement (*Chapter 5*)[6] and prediction (*Chapter 6*) of the treatment effect, which may also lead to higher non-perfused volume (NPV) ratios (i.e. NPV divided by fibroid volume) to be ablated more quickly. Currently, the lengthy procedure time (typically 2-3 hours) to perform an effective MR-HIFU ablation in patients with uterine fibroids remains a large obstacle to its widespread clinical implementation. Therefore, knowledge of important predictors of success is crucial in determining how to optimise and modify the treatment strategy of an MR-HIFU ablation with regards to the aggressiveness of treatment.

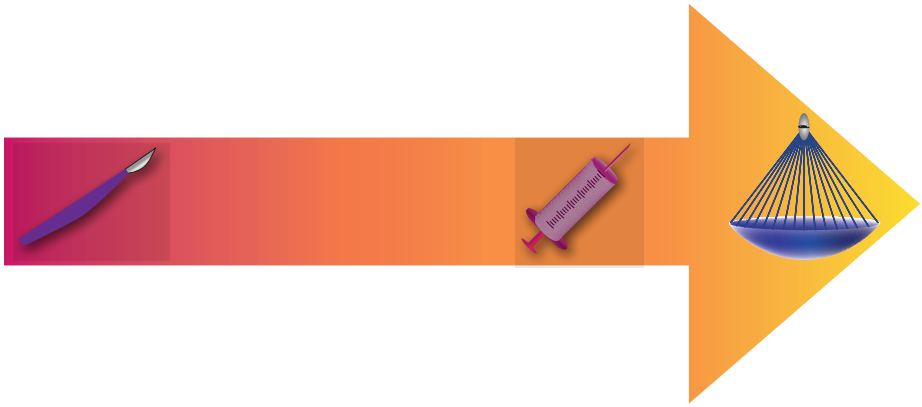

**Figure 1.** Shift towards non-invasive treatments for patients with symptomatic uterine fibroids.

Below, we will discuss the clinical importance of our study results and provide future considerations to improve volumetric MR-HIFU ablation of uterine fibroids. The key findings resulting from the research described in this thesis are as follows:

**Part I. Clinical treatment evaluation**

- A prospective evaluation of the outcome of volumetric MR-HIFU ablation for symptomatic uterine fibroids showed that volumetric MR-HIFU results in an effective treatment for uterine fibroids.
- We retrospectively compared outcomes between volumetric MR-HIFU ablation and UAE for treatment of uterine fibroids to find that both MR-HIFU ablation and UAE result in significant symptom relief and health-related quality of life improvement.
- It was found that UAE had a stronger positive effect on symptom relief and quality of life improvement.
- The reintervention rates after MR-HIFU ablation were significantly higher than after UAE.
- It was found to be technically feasible and safe to use a direct skin cooling (DISC) device added to a volumetric MR-HIFU system for uterine fibroid treatments.
- DISC may reduce the risk of thermal injury to the abdominal wall during MR-HIFU ablation of uterine fibroids, which allows for further improvement of clinical outcomes and speeding up treatment.

**Part II. MRI for prediction and measurement of treatment effect**

- Diffusion-weighted MRI (DWI) can become a useful tool for treatment evaluation of MR-HIFU ablation for uterine fibroids.
- We were able to show that the apparent diffusion coefficient (ADC) in fibroid tissue is influenced by the choice of *b*-values used for ADC calculation, suggesting that a multi-compartment model is needed to describe the diffusivity in uterine fibroid tissue.
- Post-treatment ADC maps calculated using images obtained at low *b*-values (0, 200 s/mm$^2$) resulted in the best visual agreement with the NPV on contrast-enhanced MRI as opposed to using higher *b*-values (400, 600 and 800 s/mm$^2$).
- Our results show that it is feasible to measure diffusion and perfusion coefficients in uterine fibroids using the intravoxel incoherent motion (IVIM) approach.
- A higher T2-weighted signal intensity is correlated to a higher diffusion coefficient, most probably indicating lower restriction of water molecule motion in more fluid-rich tissue.

**Part I. Clinical treatment evaluation**

A number of non-surgical alternatives to the traditional hysterectomy have become available as treatment options for symptomatic uterine fibroids. These alternative treatments do not have a curative intent and may therefore not relieve all symptoms. Consequently, a disease-specific uterine fibroid symptom and health-related quality of life (UFS-QoL) questionnaire has been developed[7] to systematically assess the patient function and well-being in women who choose these alternative treatments. Several pioneering studies have evaluated the responsiveness of UFS-QoL as a measure for the clinical therapeutic effect of MR-HIFU ablation for uterine fibroids[8-10], where a 10-point reduction in the transformed symptom severity score (tSSS) was considered to be

clinically relevant. Six month clinical follow-up studies after therapy using the point-by-point ablation technique (ExAblate® 2000 system, Insightec Ltd, Haifa, Israel) showed that 73-91% of the patients with uterine fibroids reported a significant symptom relief. In *Chapter 2* we have used this 10-point reduction in tSSS as primary endpoint to assess the 6 month efficacy of volumetric MR-HIFU ablation[4]. In 54% of the patients, a significant symptom improvement was observed. Because the treatments in the present study[4] reveal the first two years of experience with volumetric MR-HIFU ablation, including the first treatments where just small NPV ratios were ablated, our results did not (yet) meet the results obtained with the point-by-point ablation technique. After the treatment efficacy was compared with the results obtained in patients who had undergone a UAE procedure (*Chapter 3*), we demonstrated that UAE led to significantly more symptom relief ($p<0.001$) and better health-related quality of life ($p<0.001$) than MR-HIFU ablation did[5]. In addition, patients treated with MR-HIFU had a significantly higher risk of reintervention after one-year of follow-up. These findings in favour of UAE are in line with the results presented by previous work of Froeling *et al.*[11]. The immediate NPV ratio has been shown to be a surrogate marker for treatment success of MR-HIFU ablation[10,12,13]. LeBlang *et al.*[12] described that the immediate NPV ratio is positively linearly related to fibroid shrinkage and symptom relief. Data from UAE treatment studies also clearly demonstrated the impact of the achieved fibroid devascularisation on patient outcome[14-17]. Therefore, we believe that the differences found in clinical efficacy can be primarily explained by the relatively small NPV ratios (0.40) achieved with MR-HIFU ablation in our study.

MR-HIFU ablation has a relatively short history and the adopted clinical protocol and guidelines, which were mainly influenced by the safety aspect of treatment, may have likely contributed to less favourable results. Nevertheless, in order to achieve significantly better results and lower reintervention rates after MR-HIFU ablation, larger NPV ratios should be pursued[18-21] without compromising said safety aspects. A recently published study[22] confirms that complete or near-complete ablation of symptomatic uterine fibroids can be safely achieved with MR-HIFU. As such, several limiting factors that might have restricted complete fibroid ablation with MR-HIFU need to be acknowledged. First, MR-HIFU has a learning curve. Based on our clinical experience, we note that manual operator skills and experience substantially affect treatment speed and success of treatment. Studies have shown[23,24] that treatment outcomes, as measured by the immediate NPV ratios, fibroid volume reduction rate and probability of reintervention-free survival at one-year of follow-up significantly improved over time. In order to treat as much non-perfused volume as possible, it is essential to obtain an adequate acoustic window covering the outer-most peripheral areas of the uterine fibroid as well as the more central tissues which are easier to reach. As bone and scar tissue absorb acoustic energy, and air in bowel loops causes reflection of the ultrasound beam, these structures would interfere with the propagation of ultrasound waves and therefore obscure targeted tissue behind these interfaces. Anatomy manipulation and mitigation techniques may help to avoid bone, abdominal scars and bowel loops in the ultrasound beam path and should therefore be used to gain maximum access to the uterine fibroid[25,26]. Techniques that have been described are, for example, electronic beam shaping (by adjusting the electronic signals to the elements of the phased array HIFU transducer), angulation of the ultrasound beam path, displacement of bowel loops out of the pelvic area with a degassed water balloon[27], or the use of urinary bladder filling (with saline) or rectal filling (with ultrasound gel) to push the uterus away from sensitive structures that obstruct the ultrasound beam path[28].

Ideally, the treatment should be terminated only when the entire device-accessible fibroid area has been ablated. For large uterine fibroids this leads to a time-consuming process which may require more than one session to be completed. To overcome this drawback, an innovative application of MR-HIFU ablation was presented by Voogt *et al*.[29]. This approach, called targeted uterine vessel ablation, aims to combine the advantages of two interventional techniques: the efficacy of UAE mixed with the minor complications associated with MR-HIFU ablation. The concept of targeted vessel ablation is that selective ablation of supplying arteries at the periphery of the uterine fibroids will result in vascular compression and thermal endothelial damage leading to occlusive thrombus formation within the lumen[30,31]. This, in turn, may cause cessation of blood flow resulting in downsteam tissue necrosis of non-treated tissue in the region which is fed by the targeted vessel with subsequently larger near-complete areas of devascularised fibroid tissue[32]. However, the resultant non-perfused volume cannot be increased indefinitely because of the developing steady state between the amount of energy deposition and the perfusion-mediated tissue cooling (i.e. heat-sink effect) by local blood flow[33-35]. The rate of heat loss from highly-perfused targeted areas causes either undertreatment - with insufficient results close to large blood vessels - or overtreatment by the use of a higher thermal energy with higher complication rates due to elevated energy densities in the near field area (close to the skin). The risk of cumulative temperature increase in the near field area is currently mitigated by accommodating time-consuming cooling intervals between the individual therapeutic sonications. This allows the heated interstitial and subcutaneous tissue layers to cool down, but increases the procedure time of MR-HIFU ablation to an undesirable duration. Since the main objective of the volumetric treatment approach was to reduce treatment time, a different form of cooling must be applied to effectively reduce the duration of the procedure. As such, in *Chapter 4* we presented a direct skin cooling (DISC) device as a possible method. The concept of introducing a cooled interface that allows for direct cooling of the patient's skin at a constant temperature (T≈20°C) may increase the treatment efficacy (by allowing the use of higher acoustic powers) and shorten treatment time (by benefiting from reduced cooling intervals). The results of our study showed that it is technically feasible and safe to complete a volumetric MR-HIFU ablation with DISC during treatment of symptomatic uterine fibroids. No serious DISC-related adverse events occurred in the present study. Now the safety has been assessed, an upcoming study will investigate whether DISC can actually improve the clinical efficacy of MR-HIFU ablation. Our hypothesis is that with the use of the DISC device together with a previously published one-layer strategy[36], significantly higher NPV ratios can be ablated more quickly. The one-layer strategy takes advantage of the near field heat accumulation and the resulting lethal thermal dose that occurs in the anterior part of the uterine fibroid. With this method, treatment cells are planned in a coronal plane placed at two-thirds of the anteroposterior axis of the targeted uterine fibroid aiming to create larger NPVs than the actually planned targeted volume (i.e. total volume of treatment cells placed within the uterine fibroid). Although the heat accumulation garnered with this strategy may result in higher NPV ratios within uterine fibroids, temperature monitoring of the subcutaneous skin layers and rectus abdominis muscles has to be controlled adequately to prevent irreversible thermal damage[37]. Our forthcoming study hypothesises that the DISC device may positively affect temperature control in these near field areas.

**Part II. MRI for prediction and measurement of treatment effect**

Promising advances in the application of imaging techniques will contribute to improvements in the visualisation of the MR-HIFU treatment effect. Currently, contrast-enhanced T1-weighted (CE-T1w) MRI is used to assess the non-enhancing region, commonly referred to as the NPV, immediately after MR-HIFU treatment. However, intraprocedural visualisation of the NPV in between the subsequent sonications is also important as a complete coverage of the targeted area is critical for a successful treatment, and previously destructed tissue outside the treatment cells does not require further ablation. Therefore, guidance and monitoring of the actually treated fibroid volume could potentially enhance treatment efficacy and reduce treatment time. A repeatable contrast method that does not require a gadolinium-based MR contrast agent is preferred, since the presence of paramagnetic material such as gadolinium MRI contrast agents may influence the accuracy of the commonly used proton resonance frequency shift (PRFS) method for real-time temperature monitoring[38]. Other reasons against the use of gadolinium-based contrast agents during MR-HIFU ablation are the unknown safety profile of the contrast agent after heating, the relatively long clearance time of the agent, and the fact that the acceptable total dose of the contrast agent is limited. In *Chapter 5*, we investigated the use of diffusion-weighted magnetic resonance imaging (DWI) and apparent diffusion coefficient (ADC) mapping as a tool for treatment evaluation of MR-HIFU ablation[6]. DWI provides tissue contrasts based on local differences in the diffusion of water molecules within the extracellular space, using strong additional gradient lobes in the MRI pulse sequence[39,40]. The strength and timing of the additional gradient lobes determine the amount of diffusion-weighting, which is characterised by the *b*-value. In the presence of perfusion due to randomly oriented capillary flow, the signal originating from the perfusion fraction inside a voxel will show a much more rapid attenuation as a function of the *b*-value than the true diffusion in the intracellular- and extracellular spaces. In ADC maps that are calculated using images obtained at low *b*-values, the ADC values are therefore expected to more strongly reflect perfusion effects[41]. Diffusion effects without perfusion influences would mainly be visible on ADC maps calculated from DWI acquired at multiple higher *b*-values. Our results showed that a decreased contrast agent uptake in the ablated volume on CE-T1w MRI best corresponded to the ADC maps calculated when only the lowest *b*-values (0, 200 s/mm$^2$) were used. These findings seem to confirm the idea that DWI can become a helpful non-invasive tool to assess the NPV with an aim to improve the treatment efficacy of MR-HIFU ablation. Considering that the lowest non-zero *b*-value is relatively high, leading to problems with respect to measuring the rapid perfusion component, it would still be interesting to perform measurements at even lower *b*-values[42], and to perform intravoxel incoherent motion (IVIM) analyses[41,43] on such data.

Multiple study groups[44-47] have tried to identify important predictors of treatment failure, such as patient characteristics or baseline uterine morphology, to allow for better patient selection and clinical risk stratification prior to MR-HIFU ablation. It has been found that the baseline fibroid T2w signal intensity appears to have a negative correlation with the NPV ratio and fibroid volume reduction[44,45,47]. The appearance of uterine fibroids on T2w MRI may be associated with the amount of blood flow and fluid content of tissue[26,46,48], what causes hyper-intense uterine fibroids more difficult to heat. In *Chapter 6*, the IVIM theory as proposed by Le Bihan *et al.*[41] was applied to see whether it can be used to predict the success of MR-HIFU ablation. We investigated whether baseline

IVIM diffusion and perfusion characteristics of uterine fibroids could predict the heating effectiveness of MR-HIFU ablation on a treatment cell level. The IVIM analysis technique uses a signal model with two separate compartments with a mono-exponential decay per compartment to extract perfusion-related information from multi-*b*-value DWI data[41]. In the signal decay model, the perfusion compartment of incoherently flowing blood in tissues contributes to the DWI signal with a perfusion fraction *f*. Overall, we found a high perfusion fraction *f* of over 0.4, but were not able to show correlations between the IVIM parameters and the thermal response and ablation efficacy. Further studies with MRI-based blood flow measurement techniques are indicated, since IVIM MRI does not measure the volume blood flow within the uterine fibroids which would be the parameter governing the cooling effect due to perfusion.



**Future prospects of MR-HIFU ablation**

Although quite some research has been performed aimed at demonstrating the safety and clinical efficacy of MR-HIFU ablation for the treatment of uterine fibroids, a direct comparison or randomised controlled trial (RCT) between MR-HIFU ablation and other uterine-sparing treatments for symptomatic uterine fibroids has not yet been made. Bouwsma *et al.*[49] presented a study design of the FIRSTT (Fibroid Interventions: Reducing Symptoms Today and Tomorrow) trial, whose results can provide important information for patients and health professionals regarding the clinical efficacy of MR-HIFU and UAE. The FIRSTT study was designed to find out how these two minimally invasive treatments compare with respect to the need for any additional intervention to control fibroid-related symptoms after initial treatment, health-related quality of life improvement, adverse events on ovarian function, and cost-effectiveness. To the best of our knowledge, no previous studies have assessed the impact of MR-HIFU ablation on the ovarian and uterine function[50]. For this reason, initial studies excluded patients who were interested in preserving their fertility even though the non-invasive and non-ionizing nature of MR-HIFU ablation offers opportunities to treat uterine fibroids in women who wish to become pregnant in the future. A number of recent studies and case reports[50-58] have reported encouraging results with uncomplicated pregnancies, deliveries and postpartum periods in patients conceiving after undergoing MR-HIFU treatment of uterine fibroids. While additional evidence from large-scale prospective clinical studies is needed, available results suggest that the highly localised treatment of uterine fibroids with MR-HIFU ablation could be a well-tolerated approach for patients who desire future fertility. In addition, MR-HIFU ablation may even be an appropriate alternative for women suffering from (non-hysteroscopically resectable) fibroid-related infertility, since MR-HIFU is associated with a low complication rate and able to reduce fibroid volume and restore the size and shape of the endometrial cavity[53,58-60]. Yet, the number of cases currently is too small to detect any rare obstetric adverse event (such as placentation disorders or uterine rupture) or to draw conclusions about fertility and outcomes after MR-HIFU ablation. In the meantime, patients should be informed that there are potential risks to MR-HIFU for future pregnancies.

Although the interest in MR-HIFU ablation for symptomatic uterine fibroids is high and continues to grow, obtaining reimbursement to secure health insurance coverage remains complicated. In order to prevent MR-HIFU from becoming a niche modality, it must be demonstrated that MR-HIFU is at least as effective as currently offered treatment options. To date, in several economic studies[61-63] the projected cost-effectiveness was calculated

and concluded that MR-HIFU can be a cost-effective treatment for symptomatic uterine fibroids. Increased experience and further advances in technological developments may allow for treatment of uterine fibroids in previously disadvantageous locations and create room for further improvements in clinical efficacy and costs.

# References


1. Pron G, Cohen M, Soucie J, Garvin G, Vanderburgh L, Bell S. The Ontario Uterine Fibroid Embolization Trial. Part 1. Baseline patient characteristics, fibroid burden, and impact on life. *Fertil Steril.* 2003;79:112-119
2. Kohler MO, Mougenot C, Quesson B, Enholm J, Le Bail B, Laurent C, Moonen CT, Ehnholm GJ. Volumetric HIFU ablation under 3D guidance of rapid MRI thermometry. *Med Phys.* 2009;36:3521-3535
3. Voogt MJ, Trillaud H, Kim YS, Mali WP, Barkhausen J, Bartels LW, Deckers R, Frulio N, Rhim H, Lim HK, Eckey T, Nieminen HJ, Mougenot C, Keserci B, Soini J, Vaara T, Köhler MO, Sokka S, van den Bosch MA. Volumetric feedback ablation of uterine fibroids using magnetic resonance-guided high intensity focused ultrasound therapy. *Eur Radiol.* 2012;22:411-417
4. Ikink ME, Voogt MJ, Verkooijen HM, Lohle PN, Schweitzer KJ, Franx A, Mali WP, Bartels LW, van den Bosch MA. Mid-term clinical efficacy of a volumetric magnetic resonance-guided high-intensity focused ultrasound technique for treatment of symptomatic uterine fibroids. *Eur Radiol.* 2013;23:3054-3061
5. Ikink ME, Nijenhuis RJ, Verkooijen HM, Voogt MJ, Reuwer PJ, Smeets AJ, Lohle PN, van den Bosch MA. Volumetric MR-guided high-intensity focused ultrasound versus uterine artery embolisation for treatment of symptomatic uterine fibroids: comparison of symptom improvement and reintervention rates. *Eur Radiol. 2014; 24:2649-2657*
6. Ikink ME, Voogt MJ, van den Bosch MA, Nijenhuis RJ, Keserci B, Kim YS, Vincken KL, Bartels LW. Diffusion-weighted magnetic resonance imaging using different b-value combinations for the evaluation of treatment results after volumetric MR-guided high-intensity focused ultrasound ablation of uterine fibroids. *Eur Radiol.* 2014;24:2118-2127
7. Spies JB, Coyne K, Guaou Guaou N, Boyle D, Skyrnarz-Murphy K, Gonzalves SM. The UFS-QOL, a new disease-specific symptom and health-related quality of life questionnaire for leiomyomata. *Obstet Gynecol.* 2002;99:290-300
8. Hindley J, Gedroyc WM, Regan L, Stewart E, Tempany C, Hynyen K, Mcdannold N, Inbar Y, Itzchak Y, Rabinovici J, Kim HS, Geschwind JF, Hesley G, Gostout B, Ehrenstein T, Hengst S, Sklair-Levy M, Shushan A, Jolesz F. MRI guidance of focused ultrasound therapy of uterine fibroids: early results. *AJR Am J Roentgenol.* 2004;183:1713-1719
9. Stewart EA, Rabinovici J, Tempany CM, Inbar Y, Regan L, Gostout B, Hesley G, Kim HS, Hengst S, Gedroyc WM. Clinical outcomes of focused ultrasound surgery for the treatment of uterine fibroids. *Fertil Steril.* 2006;85:22-29
10. Fennessy FM, Tempany CM, McDannold NJ, So MJ, Hesley G, Gostout B, Kim HS, Holland GA, Sarti DA, Hynynen K, Jolesz FA, Stewart EA. Uterine leiomyomas: MR imaging-guided focused ultrasound surgery--results of different treatment protocols. *Radiology.* 2007;243:885-893
11. Froeling V, Meckelburg K, Schreiter NF, Scheurig-Muenkler C, Kamp J, Maurer MH, Beck A, Hamm B, Kroencke TJ. Outcome of uterine artery embolization versus MR-guided high-intensity focused ultrasound treatment for uterine fibroids: long-term results. *Eur J Radiol.* 2013;82:2265-2269
12. LeBlang SD, Hoctor K, Steinberg FL. Leiomyoma shrinkage after MRI-guided focused ultrasound treatment: report of 80 patients. *AJR Am J Roentgenol.* 2010;194:274-280
13. Al Hilli MM, Stewart EA. Magnetic resonance-guided focused ultrasound surgery. *Semin Reprod Med.* 2010;28:242-249
14. Lohle PN, Voogt MJ, De Vries J, Smeets AJ, Vervest HA, Lampmann LE, Boekkooi PF. Long-term outcome of uterine artery embolization for symptomatic uterine leiomyomas. *J Vasc Interv Radiol.* 2008;19:319-326
15. Scheurig-Muenkler C, Koesters C, Grieser C, Hamm B, Kroencke TJ. Treatment failure after uterine artery embolization: prospective cohort study with multifactorial analysis of possible predictors of long-term outcome. *Eur J Radiol.* 2012;81:e727-731
16. Katsumori T, Kasahara T, Kin Y, Nozaki T. Infarction of uterine fibroids after embolization: relationship between postprocedural enhanced MRI findings and long-term clinical outcomes. *Cardiovasc Intervent Radiol.* 2008;31:66-72
17. Kroencke TJ, Scheurig C, Poellinger A, Gronewold M, Hamm B. Uterine artery embolization for leiomyomas: percentage of infarction predicts clinical outcome. *Radiology.* 2010;255:834-841
18. Stewart EA, Gostout B, Rabinovici J, Kim HS, Regan L, Tempany CM. Sustained relief of leiomyoma symptoms by using focused ultrasound surgery. *Obstet Gynecol.* 2007;110:279-287
19. Morita Y, Ito N, Hikida H, Takeuchi S, Nakamura K, Ohashi H. Non-invasive magnetic resonance imaging-guided focused ultrasound treatment for uterine fibroids - early experience. *Eur J Obstet Gynecol Reprod Biol.* 2008;139:199-203

20. Trumm CG, Stahl R, Clevert DA, Herzog P, Mindjuk I, Kornprobst S, Schwarz C, Hoffmann RT, Reiser MF, Matzko M. Magnetic resonance imaging-guided focused ultrasound treatment of symptomatic uterine fibroids: impact of technology advancement on ablation volumes in 115 patients. *Invest Radiol.* 2013;48:359-365
21. Rabinovici J, Inbar Y, Revel A, Zalel Y, Gomori JM, Itzchak Y, Schiff E, Yagel S. Clinical improvement and shrinkage of uterine fibroids after thermal ablation by magnetic resonance-guided focused ultrasound surgery. *Ultrasound Obstet Gynecol.* 2007;30:771-777
22. Park MJ, Kim YS, Rhim H, Lim HK. Safety and therapeutic efficacy of complete or near-complete ablation of symptomatic uterine fibroid tumors by MR imaging-guided high-intensity focused US therapy. *J Vasc Interv Radiol.* 2014;25:231-239
23. Park MJ, Kim YS, Keserci B, Rhim H, Lim HK. Volumetric MR-guided high-intensity focused ultrasound ablation of uterine fibroids: treatment speed and factors influencing speed. *Eur Radiol.* 2013;23:943-950
24. Okada A, Morita Y, Fukunishi H, Takeichi K, Murakami T. Non-invasive magnetic resonance-guided focused ultrasound treatment of uterine fibroids in a large Japanese population: impact of the learning curve on patient outcome. *Ultrasound Obstet Gynecol.* 2009;34:579-583
25. Kim YS, Bae DS, Park MJ, Viitala A, Keserci B, Rhim H, Lim HK. Techniques to expand patient selection for MRI-guided high-intensity focused ultrasound ablation of uterine fibroids. *AJR Am J Roentgenol.* 2014;202:443-451
26. Yoon SW, Lee C, Cha SH, Yu JS, Na YJ, Kim KA, Jung SG, Kim SJ. Patient selection guidelines in MR-guided focused ultrasound surgery of uterine fibroids: a pictorial guide to relevant findings in screening pelvic MRI. *Eur Radiol.* 2008;18:2997-3006
27. Zhang L, Chen WZ, Liu YJ, Hu X, Zhou K, Chen L, Peng S, Zhu H, Zou HL, Bai J, Wang ZB. Feasibility of magnetic resonance imaging-guided high intensity focused ultrasound therapy for ablating uterine fibroids in patients with bowel lies anterior to uterus. *Eur J Radiol.* 2010;73:396-403
28. Park MJ, Kim YS, Rhim H, Lim HK. Technique to displace bowel loops in MRI-guided high-intensity focused ultrasound ablation of fibroids in the anteverted or anteflexed uterus. *AJR Am J Roentgenol.* 2013;201:W761-764
29. Voogt MJ, van Stralen M, Ikink ME, Deckers R, Vincken KL, Bartels LW, Mali WP, van den Bosch MA. Targeted vessel ablation for more efficient magnetic resonance-guided high-intensity focused ultrasound ablation of uterine fibroids. *Cardiovasc Intervent Radiol.* 2012;35:1205-1210
30. Shaw CJ, ter Haar GR, Rivens IH, Giussani DA, Lees CC. Pathophysiological mechanisms of high-intensity focused ultrasound-mediated vascular occlusion and relevance to non-invasive fetal surgery. *J R Soc Interface.* 2014;11:20140029
31. Hynynen K, Colucci V, Chung A, Jolesz F. Noninvasive arterial occlusion using MRI-guided focused ultrasound. *Ultrasound Med Biol.* 1996;22:1071-1077
32. de Melo FC, Diacoyannis L, Moll A, Tovar-Moll F. Reduction by 98% in uterine myoma volume associated with significant symptom relief after peripheral treatment with magnetic resonance imaging-guided focused ultrasound surgery. *J Minim Invasive Gynecol.* 2009;16:501-503
33. Lu DS, Raman SS, Vodopich DJ, Wang M, Sayre J, Lassman C. Effect of vessel size on creation of hepatic radiofrequency lesions in pigs: assessment of the "heat sink" effect. *AJR Am J Roentgenol.* 2002;178:47-51
34. Patterson EJ, Scudamore CH, Owen DA, Nagy AG, Buczkowski AK. Radiofrequency ablation of porcine liver in vivo: effects of blood flow and treatment time on lesion size. *Ann Surg.* 1998;227:559-565
35. Shih TC, Liu HL, Horng ATL. Cooling effect of thermally significant blood vessels in perfused tumor tissue during thermal therapy. *International Communications in Heat and Mass Transfer.* 2006;33:135-141
36. Kim YS, Kim JH, Rhim H, Lim HK, Keserci B, Bae DS, Kim BG, Lee JW, Kim TJ, Choi CH. Volumetric MR-guided high-intensity focused ultrasound ablation with a one-layer strategy to treat large uterine fibroids: initial clinical outcomes. *Radiology.* 2012;263:600-609
37. Baron P, Ries M, Deckers R, de Greef M, Tanttu J, Köhler M, Viergever MA, Moonen CT, Bartels LW. In vivo T -based MR thermometry in adipose tissue layers for high-intensity focused ultrasound near-field monitoring. *Magn Reson Med.* 2014;72:1057-1064
38. Hijnen NM, Elevelt A, Grull H. Stability and trapping of magnetic resonance imaging contrast agents during high-intensity focused ultrasound ablation therapy. *Invest Radiol.* 2013;48:517-524
39. Bammer R. Basic principles of diffusion-weighted imaging. *Eur J Radiol.* 2003;45:169-184
40. Hagmann P, Jonasson L, Maeder P, Thiran JP, Wedeen VJ, Meuli R. Understanding diffusion MR imaging techniques: from scalar diffusion-weighted imaging to diffusion tensor imaging and beyond. *Radiographics.* 2006;26 Suppl 1:S205-223
41. Le Bihan D, Breton E, Lallemand D, Aubin ML, Vignaud J, Laval-Jeantet M. Separation of diffusion and perfusion in intravoxel incoherent motion MR imaging. *Radiology.* 1988;168:497-505

42. Qayyum A. Diffusion-weighted imaging in the abdomen and pelvis: concepts and applications. *Radiographics.* 2009;29:1797-1810
43. Lemke A, Laun FB, Simon D, Stieltjes B, Schad LR. An in vivo verification of the intravoxel incoherent motion effect in diffusion-weighted imaging of the abdomen. *Magn Reson Med.* 2010;64:1580-1585
44. Machtinger R, Inbar Y, Cohen-Eylon S, Admon D, Alagem-Mizrachi A, Rabinovici J. MR-guided focus ultrasound (MRgFUS) for symptomatic uterine fibroids: predictors of treatment success. *Hum Reprod.* 2012;27:3425-3431
45. Lenard ZM, McDannold NJ, Fennessy FM, Stewart EA, Jolesz FA, Hynynen K, Tempany CM. Uterine leiomyomas: MR imaging-guided focused ultrasound surgery-imaging predictors of success. *Radiology.* 2008;249:187-194
46. Kim YS, Lim HK, Kim JH, Rhim H, Park BK, Keserci B, Köhler MO, Bae DS, Kim BG, Lee JW, Kim TJ, Sokka S, Lee JH. Dynamic contrast-enhanced magnetic resonance imaging predicts immediate therapeutic response of magnetic resonance-guided high-intensity focused ultrasound ablation of symptomatic uterine fibroids. *Invest Radiol.* 2011;46:639-647
47. Funaki K, Fukunishi H, Funaki T, Sawada K, Kaji Y, Maruo T. Magnetic resonance-guided focused ultrasound surgery for uterine fibroids: relationship between the therapeutic effects and signal intensity of preexisting T2-weighted magnetic resonance images. *Am J Obstet Gynecol.* 2007;196:184 e181-186
48. Huang J, Holt RG, Cleveland RO, Roy RA. Experimental validation of a tractable numerical model for focused ultrasound heating in flow-through tissue phantoms. *J Acoust Soc Am.* 2004;116:2451-2458
49. Bouwsma EV, Hesley GK, Woodrum DA, Weaver AL, Leppert PC, Peterson LG, Stewart EA. Comparing focused ultrasound and uterine artery embolization for uterine fibroids-rationale and design of the Fibroid Interventions: reducing symptoms today and tomorrow (FIRSTT) trial. *Fertil Steril.* 2011;96:704-710
50. Bohlmann MK, Hoellen F, Hunold P, David M. High-Intensity Focused Ultrasound Ablation of Uterine Fibroids - Potential Impact on Fertility and Pregnancy Outcome. *Geburtshilfe Frauenheilkd.* 2014;74:139-145
51. Rabinovici J, David M, Fukunishi H, Morita Y, Gostout BS, Stewart EA. Pregnancy outcome after magnetic resonance-guided focused ultrasound surgery (MRgFUS) for conservative treatment of uterine fibroids. *Fertil Steril.* 2010;93:199-209
52. Kim YS, Bae DS, Kim BG, Lee JW, Kim TJ. A faster nonsurgical solution very large fibroid tumors yielded to a new ablation strategy. *Am J Obstet Gynecol.* 2011;205:292 e291-295
53. Bouwsma EV, Gorny KR, Hesley GK, Jensen JR, Peterson LG, Stewart EA. Magnetic resonance-guided focused ultrasound surgery for leiomyoma-associated infertility. *Fertil Steril.* 2011;96:e9-e12
54. Yoon SW, Kim KA, Kim SH, Ha DH, Lee C, Lee SY, Jung SG, Kim SJ. Pregnancy and natural delivery following magnetic resonance imaging-guided focused ultrasound surgery of uterine myomas. *Yonsei Med J.* 2010;51:451-453
55. Zaher S, Lyons D, Regan L. Uncomplicated term vaginal delivery following magnetic resonance-guided focused ultrasound surgery for uterine fibroids. *Biomed Imaging Interv J.* 2010;6:e28
56. Morita Y, Ito N, Ohashi H. Pregnancy following MR-guided focused ultrasound surgery for a uterine fibroid. *Int J Gynaecol Obstet.* 2007;99:56-57
57. Gavrilova-Jordan LP, Rose CH, Traynor KD, Brost BC, Gostout BS. Successful term pregnancy following MR-guided focused ultrasound treatment of uterine leiomyoma. *J Perinatol.* 2007;27:59-61
58. Hanstede MM, Tempany CM, Stewart EA. Focused ultrasound surgery of intramural leiomyomas may facilitate fertility: a case report. *Fertil Steril.* 2007;88:497 e495-497
59. Wang T, Wang W, Chen WZ, Wang YX, Ye HY, Tang J. Efficacy and safety of focused ultrasound ablation in treatment of submucosal uterine fibroids. *Zhonghua Fu Chan Ke Za Zhi.* 2011;46:407-411
60. Zaher S, Lyons D, Regan L. Successful in vitro fertilization pregnancy following magnetic resonance-guided focused ultrasound surgery for uterine fibroids. *J Obstet Gynaecol Res.* 2011;37:370-373
61. O'Sullivan AK, Thompson D, Chu P, Lee DW, Stewart EA, Weinstein MC. Cost-effectiveness of magnetic resonance guided focused ultrasound for the treatment of uterine fibroids. *Int J Technol Assess Health Care.* 2009;25:14-25
62. Zowall H, Cairns JA, Brewer C, Lamping DL, Gedroyc WM, Regan L. Cost-effectiveness of magnetic resonance-guided focused ultrasound surgery for treatment of uterine fibroids. *BJOG.* 2008;115:653-662
63. Cain-Nielsen AH, Moriarty JP, Stewart EA, Borah BJ. Cost-effectiveness of uterine-preserving procedures for the treatment of uterine fibroid symptoms in the USA. *J Comp Eff Res.* 2014 May:1-12

# 8 Summary - Samenvatting

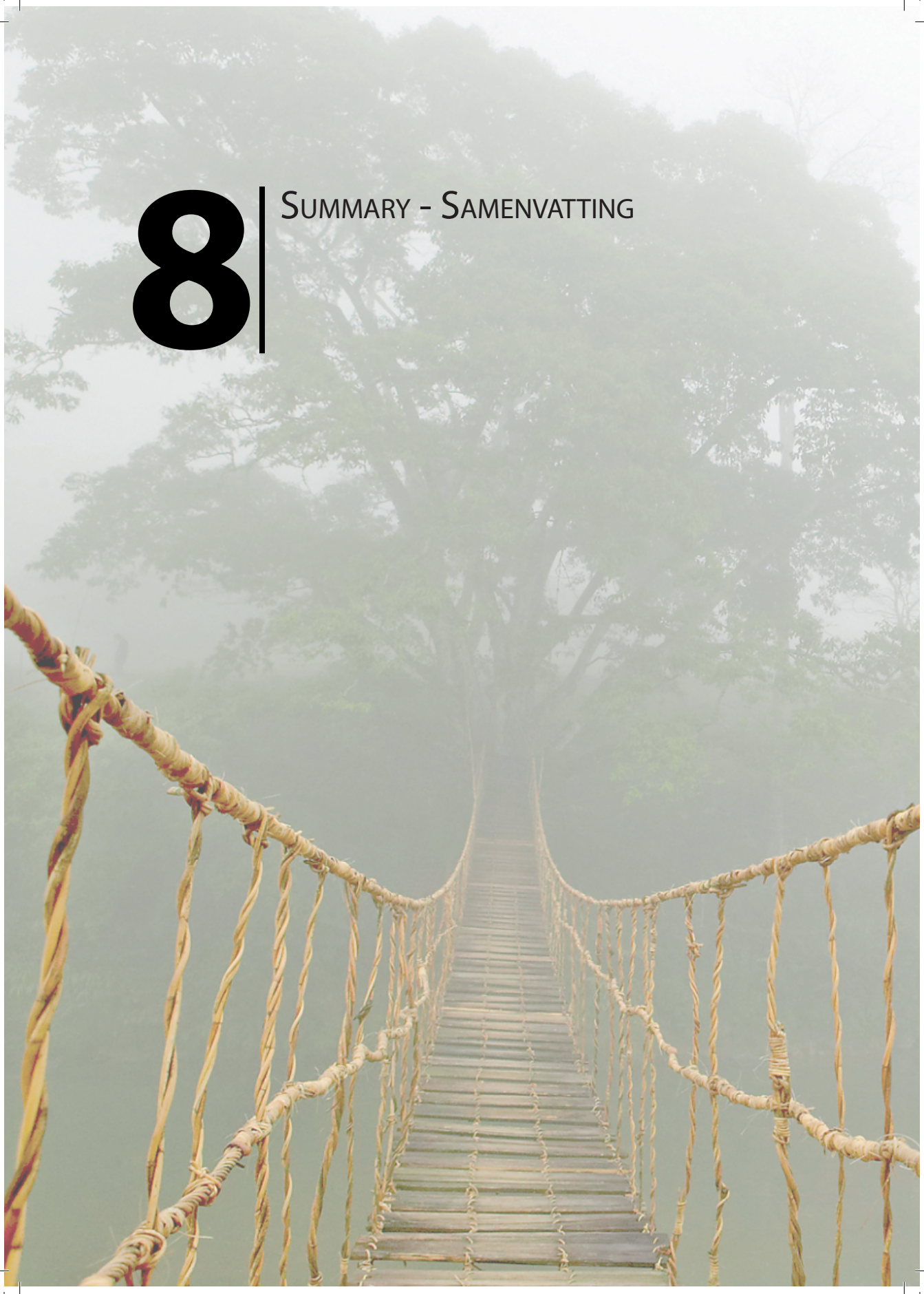

# Summary

Over the past two decades, magnetic resonance-guided high-intensity focused ultrasound (MR-HIFU) has increasingly been used as a non-invasive option for the treatment of symptomatic uterine fibroids. In this thesis, the volumetric MR-HIFU ablation technique of uterine fibroids is investigated. After the general introduction (*Chapter 1*), the first part (*Chapter 2-4*) assesses the implementation of this treatment technique in clinical practice. The second part (*Chapter 5-6*) explores the use of diffusion-weighted magnetic resonance imaging (DWI) for the measurement and prediction of treatment effect of volumetric MR-HIFU ablation.

**Part I. Clinical treatment evaluation**

*Chapter 2* describes the six month clinical efficacy of volumetric MR-HIFU ablation for the treatment of uterine fibroids. The primary endpoint of this study was a clinically relevant improvement in the transformed symptom severity score (tSSS), part of the disease-specific uterine fibroid symptom and health-related quality of life (UFS-QoL) questionnaire, defined as a 10-point reduction. We found that this targeted improvement was achieved in 54% of patients.

In *Chapter 3*, the clinical efficacy of volumetric MR-HIFU is compared to the efficacy of uterine artery embolisation (UAE) in patients treated for symptomatic uterine fibroids. Patients in this study were retrospectively selected and had to meet the eligibility criteria for both radiological treatment options to treat uterine fibroids. We compared the median tSSS, median total health-related quality of life (HRQoL) score, and reintervention rates after unsuccessful initial treatment. The results show that both volumetric MR-HIFU and UAE lead to significant symptom relief and improvement in HRQoL at 3-months follow-up. However, within 12 months, patients treated with MR-HIFU had a significantly higher risk of reintervention compared to the reintervention risk of patients treated with UAE (35% versus 4.5% of patients, respectively).

Since the treatment of larger ablation volumes requires more ultrasound energy, a temperature increase along the ultrasound beam axis in the near field is observed. This could potentially lead to thermal abdominal tissue damage during volumetric MR-HIFU ablation. *Chapter 4* prospectively demonstrates the clinical use of a direct skin cooling (DISC) device added to an MR-HIFU system to maintain a constant temperature (T≈20°C) at the interface between the MR-HIFU table top and the patient's skin during volumetric ablation of uterine fibroids. This proof of concept study shows that it is safe and technically feasible to perform a volumetric MR-HIFU ablation with DISC. In particular, no skin burns, cold injuries or subcutaneous oedema were observed in patients treated with MR-HIFU combined with the DISC device. A future study will investigate whether DISC has a beneficial effect on the clinical efficacy of volumetric MR-HIFU ablation.

**Part II. MRI for prediction and measurement of treatment effect**

In *Chapter 5* we assess the value of DWI and apparent diffusion coefficient (ADC) mapping with different *b*-value combinations for treatment evaluation after MR-HIFU of uterine fibroids. Four combinations of *b*-values were used: (1) all *b*-values (*b*=0, 200, 400, 600, and 800 s/mm$^2$); (2) *b*=0, 200 s/mm$^2$; (3) *b*=400, 600, 800 s/mm$^2$; and (4) *b*=0, 800 s/mm$^2$. The results show that DWI can become a helpful non-contrast-enhanced tool to assess the extent of tissue ablation (defined as non-perfused volume) immediately after MR-HIFU

ablation. A decrease in contrast agent uptake within the ablated region on contrast-enhanced T1-weighted (CE-T1w) MRI resulted in a uniform increased DWI signal intensity, characterised by a decreased ADC when $b$=0 and 200 s/mm$^2$ were used for ADC mapping. Our data suggests that the shutdown of perfusion may partly explain the observed reduction in ADC immediately post-treatment, since the DWI signal attenuation - in the presence of perfusion due to randomly oriented capillary flow - is larger than that caused by diffusion alone. In this line of reasoning, it would be interesting to perform measurements at even lower $b$-values and intravoxel incoherent motion (IVIM) analyses in the future.

In *Chapter 6*, the use of a pre-treatment IVIM model is investigated for tissue characterisation to predict the heating effectiveness of volumetric MR-HIFU ablation on treatment cell level. The mean diffusion coefficient $D$, the mean pseudodiffusion coefficient $D^*$ and the mean perfusion fraction $f$ were measured. The results show a high mean pre-treatment $f$ of over 0.4. Additionally, a significantly higher pre-treatment $D^*$ was found in the treatment cells that acquired suboptimal ablation volumes as determined with CE-T1w MRI data. For absolute quantification of perfusion, future studies with MRI-based perfusion measurement techniques are suggested to measure the volume blood flow within the uterine fibroids and to explore the relationship between perfusion and thermal response after MR-HIFU ablation.

# Samenvatting

Gebaseerd op Ikink ME *et al.* Volumetrische MR-HIFU-behandeling van uterus myomatosus: eerste ervaring in Nederland. *NTOG*. 2012 May;128(4):164-172

**Inleiding**

Vleesbomen (uterusmyomen) zijn goedaardige hormoongevoelige gezwellen uitgaande van de spierlaag van de baarmoeder[1]. Vleesbomen zijn de meest voorkomende goedaardige gezwellen in het vrouwelijke kleine bekken. Circa 70% van de Westerse vrouwen ontwikkelt vleesbomen in de vruchtbare levensperiode[2]. Vleesbomen groeien langzaam en blijven bij de meeste vrouwen onopgemerkt. De meest voorkomende klachten die kunnen optreden bij vleesbomen zijn overmatig bloedverlies tijdens de menstruatie (eventueel samen met bloedarmoede), menstruatiepijn, opgeblazen gevoel in de onderbuik, lage rugpijn, problemen met plassen, problemen met de ontlasting en/of pijn bij het vrijen[3]. Deze klachten kunnen leiden tot een slechtere kwaliteit van leven[4] en een hoger ziekteverzuim[5] waardoor behandeling nodig kan zijn. De vorm van behandeling die zal worden gekozen is afhankelijk van de ernst van de klachten, het aantal vleesbomen, de grootte en de ligging van de vleesbomen in de baarmoeder en een eventuele zwangerschapswens[6]. Er kan gekozen worden voor een operatieve verwijdering van de baarmoeder of voor een behandeling waarbij de baarmoeder behouden blijft. In de afgelopen twee decennia is er een trend waarneembaar naar minimaal-invasieve behandeltechnieken voor vleesbomen. Tot de voordelen behoren minder operatiegerelateerde complicaties (zoals bloedverlies en infectie), minder pijn, minder littekenvorming, kortere herstelperiode en een beter cosmetisch resultaat. De interventieradiologie heeft twee baarmoedersparende behandeltechnieken geïntroduceerd voor de behandeling van symptomatische vleesbomen: uterusmyoomembolisatie[7] en MRI-geleide 'high-intensity focused ultrasound' (MR-HIFU)[8]. Bij een uterusmyoomembolisatie wordt het aanvoerende bloedvat (slagader) naar de vleesboom afgesloten, waardoor de vleesboom zal afsterven en na verloop van tijd zal verschrompelen[9]. Hoewel deze vorm van behandeling veilig wordt geacht, zijn er enkele risico's geassocieerd met een uterusmyoomembolisatie[10]. Het afsluiten van een bloedvat leidt tot zuurstofgebrek waarbij tijdelijk het post-embolisatie syndroom kan optreden (heftige buikkrampen, misselijkheid, braken en koorts). Andere zeldzame complicaties zijn het vervroegd optreden van de overgang, infectie van de baarmoeder of de 'geboorte' van een vleesboom. Om de kans op complicaties tot een minimum te beperken is er een volledig non-invasieve behandeltechniek voor patiënten met vleesbomen ontwikkeld, namelijk MR-HIFU. Bij MR-HIFU worden vleesbomen door de intacte buikhuid heen behandeld door het bundelen van hoogfrequent ultrageluid in een focaal punt (brandpunt) waardoor lokaal een temperatuurverhoging ontstaat (vergelijkbaar met de warmte die ontstaat door het bundelen van zonlicht in een vergrootglas). Dit wordt thermische ablatie genoemd: het weefsel wordt permanent beschadigd door verhitting. Boven een temperatuur van 55-60°C treedt binnen enkele seconden celdood op. Het immuunsysteem zal worden ingeschakeld om de dode cellen op te ruimen, wat na enkele weken zal leiden tot een volumeafname van de vleesboom, vermindering van de klachten en een verbetering in kwaliteit van leven. De behandeling is MRI-gestuurd waardoor het behandelgebied zeer nauwkeurig in beeld gebracht kan worden, de temperatuurverandering in de vleesboom en omliggende weefsels realtime gemeten kan worden[11] en het behandeleffect na behandeling zichtbaar kan worden

gemaakt met contrasttoediening als een non-geperfundeerd, dat wil zeggen niet (goed) doorbloed, weefselvolume[12]. Doordat de temperatuurverhoging zeer lokaal plaatsvindt blijven omliggende weefsels en organen gespaard en is het risico op complicaties klein[13]. Tot op heden zijn er wereldwijd meerdere MR-HIFU-systemen geïntroduceerd. In 2004 werd het eerste commercieel beschikbare MR-HIFU-systeem gelanceerd met een punt-bij-punt-ablatietechniek (ExAblate® 2000, Insightec, Haifa, Israël). In de studies beschreven in dit proefschrift werd gebruik gemaakt van een volumetrische MR-HIFU-ablatietechniek (Sonalleve®, Philips Healthcare, Vantaa, Finland)[14]. Dit MR-HIFU-systeem werd in 2009 wettelijk goedgekeurd voor de behandeling van vleesbomen. Het voordeel van deze nieuwe volumetrische benadering ten opzichte van de punt-bij-punt-ablatietechniek is dat een groter volume in een kortere tijd behandeld kan worden (range 0,1-5,4 ml). Het focale punt wordt langs meerdere concentrische cirkels met toenemende diameter (range 4-16 mm) gestuurd, waarbij de hitteopbouw in het brandpunt maximaal is. Dit proefschrift beschrijft de klinische behandelresultaten van de volumetrische MR-HIFU-ablatietechniek (*deel 1*) en evalueert nieuwe MRI-technieken voor het meten en voorspellen van het behandeleffect van MR-HIFU voor vleesbomen (*deel 2*).



**Deel I. Klinische beoordeling van volumetrische MR-HIFU-behandeling**

Na de algemene introductie (*Hoofdstuk 1*) wordt in *Hoofdstuk 2* de klinische werkzaamheid van de volumetrische MR-HIFU-techniek voor de behandeling van vleesbomen op de middellange termijn (zes maanden) gepresenteerd[15]. De klinische werkzaamheid werd gemeten aan de hand van een ziektespecifieke vragenlijst. Deze vragenlijst kwantificeert zowel de ernst van de klachten als de kwaliteit van leven ten gevolge van vleesbomen. Zes maanden na behandeling blijkt volumetrische MR-HIFU-ablatie in 54% van de behandelde patiënten effectief, met een significante afname van de vleesboomgerelateerde klachten en een significante verbetering in de kwaliteit van leven.

In *Hoofdstuk 3* hebben we de klinische werkzaamheid van volumetrische MR-HIFU-ablatie vergeleken met de werkzaamheid van de langer bestaande uterusmyoom-embolisatie voor de behandeling van vleesbomen in de baarmoeder[16]. De patiënten in deze studie werden retrospectief geselecteerd met het criterium dat alle patiënten voor beide behandelopties in aanmerking zouden moeten kunnen komen. Het effect van beide behandelopties werd vergeleken door middel van de eerdergenoemde ziektespecifieke vragenlijst (ernst van de klachten en kwaliteit van leven) en het risico op aanvullende behandeling bij blijvende of nieuwe vleesboomgerelateerde klachten. Het blijkt dat behandeling met zowel volumetrische MR-HIFU-ablatie als uterusmyoomembolisatie leidt tot een aanzienlijke verlichting van de klachten en verbetering van de kwaliteit van leven. Uterusmyoomembolisatie had echter een sterker effect op dit resultaat dan MR-HIFU. Bovendien hadden patiënten één jaar na embolisatiebehandeling minder kans op een aanvullende behandeling (4,5%) dan de patiënten behandeld met volumetrische MR-HIFU-ablatie (35%). Wij zijn van mening dat dit verschil grotendeels kan worden verklaard door de beperkte non-geperfundeerde weefselvolumes bereikt met MR-HIFU-ablatie (gemiddeld 40% van het totale myoomvolume) tegenover de non-geperfundeerde weefselvolumes die met uterusmyoomembolisatie haalbaar zijn (gemiddeld 95-100% van het totale myoomvolume). De resultaten van de volumetrische MR-HIFU-ablatie zijn gedeeltelijk een weerspiegeling van een aanzienlijke leercurve die gepaard gaat met deze nieuwe behandeltechniek van vleesbomen[17]. Hierdoor valt een verdere toename in het behaalde non-geperfundeerde weefselvolume in de toekomst nog te verwachten.

De behandeling van grotere ablatievolumes vraagt meer ultrageluidenergie, wat kan leiden tot een temperatuurverhoging in de buikhuid[18]. In *Hoofdstuk 4* beschrijven we het concept van het gebruik van een koelelement om de buikhuid tijdens een volumetrische MR-HIFU-behandeling te beschermen tegen verbranding. De veiligheid en technische uitvoerbaarheid van een volumetrische MR-HIFU-behandeling met het huidkoelsysteem werd prospectief onderzocht. Het bleek dat met het gebruik van het huidkoelsysteem alle acht behandelingen op de gebruikelijke wijze konden worden afgerond. Daarbij hebben zich geen ernstige bijwerkingen voorgedaan, met in het bijzonder geen koude- of warmteletsels. In een tweede studie zal worden onderzocht of het huidkoelsysteem een gunstig effect heeft op de klinische werkzaamheid van een volumetrische MR-HIFU-ablatie.

**Deel II. MRI voor het meten en voorspellen van het behandeleffect van volumetrische MR-HIFU-behandeling**

In *Hoofdstuk 5* laten we zien wat de mogelijkheden zijn om met een MRI-techniek, genaamd diffusiegewogen magnetische resonantie (DWI), het behandeleffect in beeld te brengen[19,20]. Met deze techniek kan er zonder het gebruik van contrastmiddel worden geëvalueerd welk gebied van de vleesboom effectief behandeld is. Beeldvorming door middel van DWI is gebaseerd op de verschillen in willekeurige thermische beweging van watermoleculen (diffusie of Brownse beweging). De *b*-waarde bepaalt de mate van diffusieweging in het MRI-signaal. Hoe hoger de *b*-waarde, hoe groter de mate van diffusieweging. Door het verzamelen van MRI-beelden met ten minste twee verschillende *b*-waarden kan de mate van diffusie worden berekend, uitgedrukt in een diffusiecoëfficiënt. Omdat de diffusiecoëfficiënt ook informatie bevat over andere mechanismen die beweging van watermoleculen veroorzaken (zoals watertransport en doorbloeding) wordt er in de praktijk bij voorkeur gesproken over de schijnbare (apparent) diffusiecoëfficiënt (ADC) van water[21]. De berekende ADC-waarden kunnen zichtbaar worden gemaakt in een ADC-map. Gebieden met een verminderde diffusie (bijvoorbeeld bij celdood of verminderde weefseldoorbloeding) vertonen een lage ADC met een laag signaal op de ADC-map. Gebieden met een hoge diffusie (bijvoorbeeld bij celzwelling oftewel vochtophoping) vertonen een hoge ADC met een hoog signaal op de ADC-map. Wij tonen aan dat het gebruik van verschillende *b*-waardencombinaties (laag-laag, hoog-hoog of laag-hoog) invloed heeft op de ADC-waarde vóór en na een MR-HIFU-behandeling van vleesbomen[22]. Het gebruik van een lage-*b*-waardencombinatie leidt in het behandelde gebied tot een aanzienlijke daling in de ADC-waarde, mogelijk ten gevolge van het perfusiedefect na een MR-HIFU-behandeling. Het gebruik van een hoge-*b*-waardencombinatie leidt tot een toename in de ADC-waarde, mogelijk ten gevolge van celzwelling als reactie op de celschade na een MR-HIFU-behandeling. Wanneer de ADC-waarden worden weergegeven in een ADC-map, blijkt dat de ADC-map berekend met de laagste *b*-waarden de beste visuele overeenkomst heeft met het behandeleffect: het non-geperfundeerde weefselvolume zoals weergegeven op de MRI-beelden na contrasttoediening. Deze niet-invasieve MRI-techniek biedt mogelijkheden om het behandeleffect zonder contrastmiddel te visualiseren en tijdens behandeling te controleren zodat het behandelresultaat vergroot en de behandeltijd verkort kan worden.

Niet alle vleesbomen zijn gevoelig voor een MR-HIFU-behandeling[23]. Het succes wordt sterk bepaald door het watergehalte (zichtbaar als veel diffusie met DWI) en de doorbloeding (perfusie) van de vleesboom. In *Hoofdstuk 6* hebben we onderzocht

of vleesbomen kunnen worden gekarakteriseerd met behulp van een diffusie- (*D*) en perfusiecoëfficiënt (*D**) om het behandeleffect van een volumetrische MR-HIFU-ablatie te voorspellen. De *D* en *D** kunnen worden berekend met de MRI-techniek genaamd IVIM (intravoxel incoherent motion imaging)[21,24]. Het blijkt dat in onze studie gemiddeld 40% van het totale MRI-IVIM-signaal van de vleesboom wordt bepaald door perfusie (perfusiefractie *f*). Dit is veel hoger dan bijvoorbeeld wordt beschreven voor het brein, namelijk 4%. Daarnaast bleken de suboptimaal behandelde gebieden in de vleesboom een hogere perfusiecoëfficiënt te hebben. Verdere studies met op MRI-gebaseerde meettechnieken om de bloedstroom in beeld te brengen moeten uitwijzen of weefseldoorbloeding een belangrijke indicator is voor succes van een volumetrische MR-HIFU-ablatie.



**Conclusie**

In *Hoofdstuk 7* beschrijven we het klinische belang van onze studieresultaten en worden overwegingen besproken om volumetrische MR-HIFU-ablatie van vleesbomen in de toekomst verder te verbeteren. Samenvattend is volumetrische MR-HIFU-ablatie nog volop in ontwikkeling. Met nieuwe technische innovaties en aanpassingen kunnen er in de toekomst meer patiënten worden geïncludeerd, grotere myoomvolumes worden behandeld en kan de behandeltijd worden verkort.

## Literatuur

1. Stewart EA. Uterine fibroids. *Lancet*. 2001;357:293-298
2. Baird DD, Dunson DB, Hill MC, Cousins D, Schectman JM. High cumulative incidence of uterine leiomyoma in black and white women: ultrasound evidence. *Am J Obstet Gynecol*. 2003;188:100-107
3. Parker WH. Etiology, symptomatology, and diagnosis of uterine myomas. *Fertil Steril*. 2007;87:725-736
4. Spies JB, Bradley LD, Guido R, Maxwell GL, Levine BA, Coyne K. Outcomes from leiomyoma therapies: comparison with normal controls. *Obstet Gynecol*. 2010;116:641-652
5. Hartmann KE, Birnbaum H, Ben-Hamadi R, Wu EQ, Farrell MH, Spalding J, Stang P. Annual costs associated with diagnosis of uterine leiomyomata. *Obstet Gynecol*. 2006;108:930-937
6. Levy BS. Modern management of uterine fibroids. Acta Obstet Gynecol Scand. 2008;87:812-823
7. Ravina JH, Herbreteau D, Ciraru-Vigneron N, Bouret JM, Houdart E, Aymard A, Merland JJ. Arterial embolisation to treat uterine myomata. *Lancet*. 1995;346:671-672
8. Tempany CM, Stewart EA, McDannold N, Quade BJ, Jolesz FA, Hynynen K. MR imaging-guided focused ultrasound surgery of uterine leiomyomas: a feasibility study. *Radiology*. 2003;226:897-905
9. Lohle PN, Voogt MJ, De Vries J, Smeets AJ, Vervest HA, Lampmann LE, Boekkooi PF. Long-term outcome of uterine artery embolization for symptomatic uterine leiomyomas. *J Vasc Interv Radiol*. 2008;19:319-326
10. Martin J, Bhanot K, Athreya S. Complications and reinterventions in uterine artery embolization for symptomatic uterine fibroids: a literature review and meta-analysis. *Cardiovasc Intervent Radiol*. 2013;36:395-402
11. Mougenot C, Quesson B, de Senneville BD, de Oliveira PL, Sprinkhuizen S, Palussière J, Grenier N, Moonen CT. Three-dimensional spatial and temporal temperature control with MR thermometry-guided focused ultrasound (MRgHIFU). *Magn Reson Med*. 2009;61:603-614
12. Voogt MJ, van den Bosch MA. [MRI-guided 'high-intensity focused ultrasound': non-invasive thermoablation of tumours]. *Ned Tijdschr Geneeskd*. 2010;154:A1824
13. ter Haar GR. High intensity focused ultrasound for the treatment of tumors. *Echocardiography*. 2001;18:317-322
14. Kohler MO, Mougenot C, Quesson B, Enholm J, Le Bail B, Laurent C, Moonen CT, Ehnholm GJ. Volumetric HIFU ablation under 3D guidance of rapid MRI thermometry. *Med Phys*. 2009;36:3521-3535
15. Ikink ME, Voogt MJ, Verkooijen HM, Lohle PN, Schweitzer KJ, Franx A, Mali WP, Bartels LW, van den Bosch MA. Mid-term clinical efficacy of a volumetric magnetic resonance-guided high-intensity focused ultrasound technique for treatment of symptomatic uterine fibroids. *Eur Radiol*. 2013;23:3054-3061
16. Ikink ME, Nijenhuis RJ, Verkooijen HM, Voogt MJ, Reuwer PJ, Smeets AJ, Lohle PN, van den Bosch MA. Volumetric MR-guided high-intensity focused ultrasound versus uterine artery embolisation for treatment of symptomatic uterine fibroids: comparison of symptom improvement and reintervention rates. *Eur Radiol*. 2014;24:2649-2657
17. Okada A, Morita Y, Fukunishi H, Takeichi K, Murakami T. Non-invasive magnetic resonance-guided focused ultrasound treatment of uterine fibroids in a large Japanese population: impact of the learning curve on patient outcome. *Ultrasound Obstet Gynecol*. 2009;34:579-583
18. Fan X, Hynynen K. Ultrasound surgery using multiple sonications--treatment time considerations. *Ultrasound Med Biol*. 1996;22:471-482
19. Bammer R. Basic principles of diffusion-weighted imaging. *Eur J Radiol*. 2003;45:169-184
20. Hagmann P, Jonasson L, Maeder P, Thiran JP, Wedeen VJ, Meuli R. Understanding diffusion MR imaging techniques: from scalar diffusion-weighted imaging to diffusion tensor imaging and beyond. *Radiographics*. 2006;26 Suppl 1:S205-223
21. Le Bihan D, Breton E, Lallemand D, Aubin ML, Vignaud J, Laval-Jeantet M Separation of diffusion and perfusion in intravoxel incoherent motion MR imaging. *Radiology*. 1988;168:497-505
22. Ikink ME, Voogt MJ, van den Bosch MA, Nijenhuis RJ, Keserci B, Kim YS, Vincken KL, Bartels LW. Diffusion-weighted magnetic resonance imaging using different b-value combinations for the evaluation of treatment results after volumetric MR-guided high-intensity focused ultrasound ablation of uterine fibroids. *Eur Radiol*. 2014;24:2118-2127
23. Lenard ZM, McDannold NJ, Fennessy FM, Stewart EA, Jolesz FA, Hynynen K, Tempany CM. Uterine leiomyomas: MR imaging-guided focused ultrasound surgery-imaging predictors of success. *Radiology*. 2008;249:187-194
24. Lemke A, Laun FB, Simon D, Stieltjes B, Schad LR. An in vivo verification of the intravoxel incoherent motion effect in diffusion-weighted imaging of the abdomen. *Magn Reson Med*. 2010;64:1580-1585

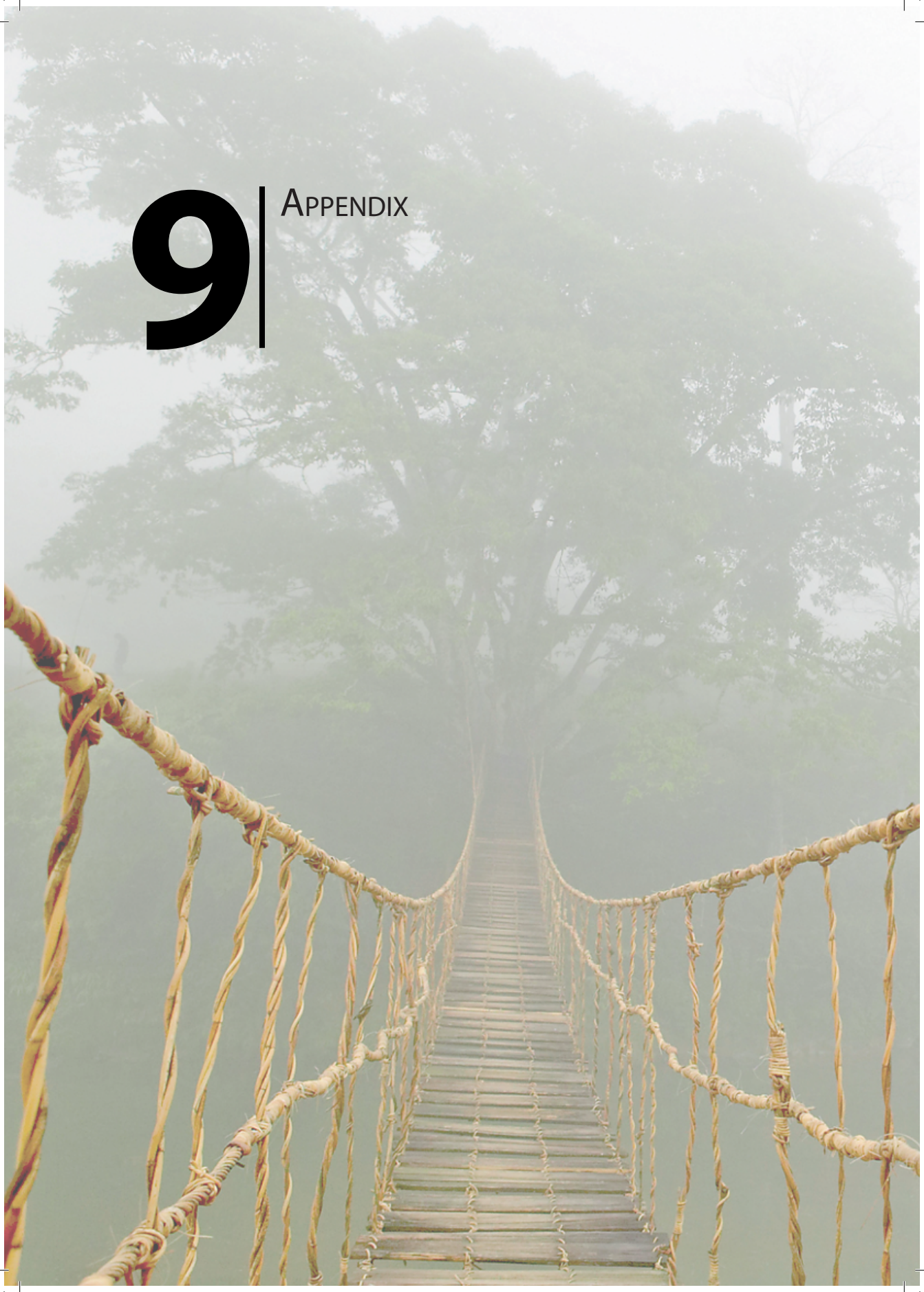

# 9 Appendix

## List of affiliations


| | |
|---|---|
| Bartels, L.W. | Image Sciences Institute, Imaging Division, University Medical Center Utrecht, Utrecht, The Netherlands |
| Bosch, M.A.A.J. van den | Department of Radiology, Imaging Division, University Medical Center Utrecht, Utrecht, The Netherlands |
| Breugel, J.M.M. van | Department of Radiology, Imaging Division, University Medical Center Utrecht, Utrecht, The Netherlands |
| Franx, A. | Department of Obstetrics and Gynaecology, Division Woman and Baby, University Medical Center Utrecht, Utrecht, The Netherlands |
| Frijlingh, M. | Department of Radiology, Imaging Division, University Medical Center Utrecht, Utrecht, The Netherlands |
| Ikink, M.E. | Department of Radiology, Imaging Division, University Medical Center Utrecht, Utrecht, The Netherlands |
| Keserci, B. | Philips Healthcare, Advanced Science and Development, Seoul, South Korea<br>High-intensity Focused Ultrasound (HIFU) Center, Samsung Medical Center, Seoul, South Korea |
| Kim, Y.S. | High-intensity Focused Ultrasound (HIFU) Center, Samsung Medical Center, Seoul, South Korea<br>Department of Radiology and Center for Imaging Science, Samsung Medical Center, Sunkyunkwan University School of Medicine, Seoul, South Korea |
| Lohle, P.N.M. | Department of Radiology, St. Elisabeth Hospital Tilburg, Tilburg, The Netherlands |
| Mali, W.P.Th.M. | Department of Radiology, Imaging Division, University Medical Center Utrecht, Utrecht, The Netherlands |
| Moonen, C.T.W. | Image Sciences Institute, Imaging Division, University Medical Center Utrecht, Utrecht, The Netherlands |
| Nijenhuis, R.J. | Department of Radiology, Imaging Division, University Medical Center Utrecht, Utrecht, The Netherlands |
| Reuwer, P.J.H.M. | Department of Obstetrics and Gynaecology, St. Elisabeth Hospital Tilburg, Tilburg, The Netherlands |

| | |
|---|---|
| Schubert, G. | Philips Healthcare, Philips Medical Systems MR, Vantaa, Finland |
| Schweitzer, K.J. | Department of Obstetrics and Gynaecology, Division Woman and Baby, University Medical Center Utrecht, Utrecht, The Netherlands |
| Smeets, A.J. | Department of Radiology, St. Elisabeth Hospital Tilburg, Tilburg, The Netherlands |
| Stralen, M. van | Image Sciences Institute, Imaging Division, University Medical Center Utrecht, Utrecht, The Netherlands |
| Verkooijen, H.M. | Department of Radiology, Imaging Division, University Medical Center Utrecht, Utrecht, The Netherlands |
| Vincken, K.L. | Image Sciences Institute, Imaging Division, University Medical Center Utrecht, Utrecht, The Netherlands |
| Voogt, M.J. | Department of Radiology, Imaging Division, University Medical Center Utrecht, Utrecht, The Netherlands |

# List of publications

**Journal articles**

**Ikink ME**, van Stralen M, van Breugel JMM, Frijlingh M, Vincken KL, van den Bosch MAAJ, Bartels LW. Intravoxel incoherent motion MRI for tissue characterisation of uterine fibroids before MR-guided high-intensity focused ultrasound ablation. *Manuscript in preparation*.

**Ikink ME**, van Breugel JMM, Schubert G, Nijenhuis RJ, Bartels LW, Moonen CTW, van den Bosch MAAJ. Volumetric MR-guided high-intensity focused ultrasound with direct skin cooling for the treatment of symptomatic uterine fibroids: proof of concept study. *Accepted for publication in Biomed Research International.*

**Ikink ME**, Nijenhuis RJ, Verkooijen HM, Voogt MJ, Reuwer PJHM, Smeets AJ, Lohle PNM, van den Bosch MAAJ. Volumetric MR-guided high-intensity focused ultrasound versus uterine artery embolisation for treatment of symptomatic uterine fibroids: comparison of symptom improvement and reintervention rates. *Eur Radiol*. 2014 Oct;24(10):2649-57.

**Ikink ME**, Voogt MJ, van den Bosch MAAJ, Nijenhuis RJ, Keserci B, Kim YS, Vincken KL, Bartels LW. Diffusion-weighted magnetic resonance imaging using different *b*-value combinations for the evaluation of treatment results after volumetric MR-guided high-intensity focused ultrasound ablation of uterine fibroids. *Eur Radiol.* 2014 Sep;24(9):2118-27.

**Ikink ME**, Voogt MJ, Verkooijen HM, Lohle PNM, Schweitzer KJ, Franx A, Mali WPThM, Bartels LW, van den Bosch MAAJ. Mid-term clinical efficacy of a volumetric magnetic resonance-guided high-intensity focused ultrasound technique for treatment of symptomatic uterine fibroids. *Eur Radiol.* 2013 Nov;23(11):3054-61.

Voogt MJ, van Stralen M, **Ikink ME,** Deckers R, Vincken KL, Bartels LW, Mali WPThM, van den Bosch MAAJ. Targeted vessel ablation for more efficient magnetic resonance-guided high-intensity focused ultrasound ablation of uterine fibroids. *Cardiovasc Intervent Radiol.* 2012 Oct;35(5):1205-10.

**Ikink ME**, Voogt MJ, Bartels LW, Koopman MS, Deckers R, Schweitzer KJ, Verkooijen HM, Moonen CTW, Mali WPThM, van den Bosch MAAJ. Volumetrische MR-HIFU-behandeling van uterus myomatosus: eerste ervaring in Nederland. *NTOG*. 2012 May;128(4):164-172

**Conference proceedings – oral presentations**

**Ikink ME**, van Breugel JMM*, Schubert G, Nijenhuis RJ, Bartels LW, Moonen CTW, van den Bosch MAAJ. Volumetric MR-guided high-intensity focused ultrasound with direct skin cooling for the treatment of symptomatic uterine fibroids: proof of concept study. *International Symposium on Focused Ultrasound*, 12-16 October 2014, Bethesda, United Stated of America.

**Ikink ME***, Nijenhuis RJ, Verkooijen HM, Lohle PNM, van den Bosch MAAJ. Reintervention rate and symptom improvement following volumetric magnetic resonance-guided high-intensity focused ultrasound versus uterine artery embolisation for uterine fibroids: a multicentre study. *European Congress of Radiology (ECR)*, 6-10 March 2014, Vienna, Austria.

**Ikink ME***, Voogt MJ, Verkooijen HM, Lohle PNM, Schweitzer KJ, Franx A, Mali WPTM, Bartels LW, van den Bosch MAAJ. Clinical efficacy of a novel volumetric magnetic resonance-guided high-intensity focused ultrasound technique in the treatment of symptomatic uterine fibroids. *The Graduate Programme Medical Imaging (ImagO) Scientific Conference*, 13 December 2012, Utrecht, The Netherlands.

**Ikink ME***, Voogt MJ, Verkooijen HM, Schweitzer KJ, Franx A, Mali WPTM, Bartels LW, van den Bosch MAAJ. Efficacy of a novel volumetric magnetic resonance-guided high-intensity focused ultrasound technique in the treatment of symptomatic uterine fibroids. *Radiological Society of North America (RSNA) Scientific Assembly and Annual Meeting*, 25-30 November 2012, Chicago, United Stated of America.

**Ikink ME***, Bartels LW, Voogt MJ, Mali WPTM, Vincken KL, van den Bosch MAAJ. Diffusion-weighted magnetic resonance imaging as a predictor for treatment efficacy of volumetric magnetic resonance-guided high-intensity focused ultrasound ablation of symptomatic uterine fibroids. *International Symposium on Focused Ultrasound*, 14-17 October 2012, Bethesda, United Stated of America.

**Ikink ME***, Voogt MJ, Verkooijen HM, Schweitzer KJ, Franx A, Mali WPTM, Bartels LW, van den Bosch MAAJ. Efficacy of a novel volumetric magnetic resonance-guided high-intensity focused ultrasound technique for the treatment of symptomatic uterine fibroids. *Radiologendagen*, 27-28 September 2012, 's-Hertogenbosch, The Netherlands.

**Ikink ME***, Voogt MJ, Mali WPTM, Bartels LW, van den Bosch MAAJ. Volumetric magnetic resonance-guided high-intensity focused ultrasound for the treatment of symptomatic uterine fibroids. *Radiologendagen*, 27-28 September 2012, 's-Hertogenbosch, The Netherlands.

**Ikink ME***, van den Bosch MAAJ. De grenzeloze behandeling van het myoom: MR-HIFU uterus myomatosus. *COBRAdagen*, 18-20 April 2012, Noordwijkerhout, The Netherlands.

**Conference proceedings – poster presentations**

**Ikink ME***, Voogt MJ, van den Bosch MAAJ, Nijenhuis RJ, Keserci B, Kim YS, Vincken KL, Bartels LW. Diffusion-weighted magnetic resonance imaging using different *b*-value combinations for the evaluation of treatment results after volumetric magnetic resonance-guided high-intensity focused ultrasound ablation of uterine fibroids. *Joint Annual Meeting of International Society for Magnetic Resonance in Medicine (ISMRM) and European Society for Magnetic Resonance in Medicine and Biology (ESMRMB)*, 10-16 May 2014, Milan, Italy.

**Ikink ME***, van Breugel JMM, Nijenhuis RJ, Voogt MJ, van den Bosch MAAJ, Vincken KL, Bartels LW. Intravoxel incoherent motion MRI for the characterisation of uterine fibroids before magnetic resonance-guided high-intensity focused ultrasound ablation. *Joint Annual Meeting of International Society for Magnetic Resonance in Medicine (ISMRM) and European Society for Magnetic Resonance in Medicine and Biology (ESMRMB)*, 10-16 May 2014, Milan, Italy.

**Ikink ME***, Voogt MJ, Verkooijen HM, Schweitzer KJ, Franx A, Mali WPThM, Bartels LW, van den Bosch MAAJ. Efficacy of a novel volumetric magnetic resonance-guided high-intensity focused ultrasound technique in the treatment of symptomatic uterine fibroids. *Radiological Society of North America (RSNA) Scientific Assembly and Annual Meeting*, 25-30 November 2012, Chicago, United Stated of America

# Dankwoord

Het zit er bijna op, wie had dat gedacht. Eerlijk gezegd had ik nooit de ambitie om promotieonderzoek te doen, toch ben ik vier jaar geleden de uitdaging van een promotietraject aangegaan. Terugkijkend kan ik concluderen dat ik geen spijt heb van mijn keuze (oké, misschien alleen tijdens de laatste loodjes). Wat heb ik veel geleerd en mijn vaardigheden verder ontwikkeld. Het schrijven van dit proefschrift is hiervan het bewijs, maar vooral de weg ernaar toe maakt promoveren een leerzame en onvergetelijke ervaring. De gesprekken met patiënten, het uitvoeren van de MR-HIFU-behandelingen, de intensieve samenwerking met de MRI-laboranten, de congresbezoeken, het geven van wetenschappelijke en educatieve presentaties, de begeleiding van studenten en co-assistenten geneeskunde, het volgen van cursussen, de nieuwe mensen die ik heb leren kennen, de nodige koffiepauzes, het begin van nieuwe hobby's (spinning en wielrennen), de uitjes met collega's (de Radiology Research Ski Trips (RRSTs), de Joop Zoetemelk Classic, Tour de Haute Veluwe, de Rode Lus, The Color Run, het weekendje Ardennen, kanoën, de vele etentjes): ik had het niet willen missen! Via deze weg wil ik iedereen bedanken die mijn promotietraject tot een succes hebben gemaakt. Een aantal van jullie wil ik graag in het bijzonder noemen.

Allereerst wil ik alle patiënten en verwijzers (huisartsen, radiologen en gynaecologen) bedanken voor het vertrouwen in deze nieuwe non-invasieve behandelmethode voor uterusmyomen. Zonder jullie waren er geen MR-HIFU-behandelingen en was het afronden van dit proefschrift een onmogelijke opgave geweest.

Prof.dr. M.A.A.J. van den Bosch, geachte promotor, beste Maurice, bedankt voor het meedenken over de inhoud van de verschillende studies in dit proefschrift, je enthousiasme en vertrouwen in mijn kunnen. Ik kan mij nog heel goed herinneren dat je in 2012 - op de promotie van mijn voorgangster Marianne Voogt - riep dat ik over twee jaar de doctorstitel zou binnenhalen. Dit heeft mij extra gemotiveerd om door te gaan. Het doel is nu bijna bereikt, ik hoop dat je gelijk krijgt!

Prof.dr. W.P.Th.M. Mali, geachte promotor, bedankt voor het mogelijk maken van mijn promotieonderzoek en de aansturing van 'bovenaf'. Al snel na de start van mijn promotie werd Maurice benoemd tot hoogleraar interventieradiologie en werd u mijn tweede promotor. Desondanks bleef u altijd nauw betrokken bij het MR-HIFU-project en was u goed op de hoogte van de vooruitgang en de mogelijkheden van mijn onderzoek. Ik voel mij vereerd dat ik nog met u heb mogen samenwerken en dat ik dit onderzoek onder uw begeleiding heb mogen afronden.

Dr.ir. L.W. Bartels, geachte co-promotor, beste Wilbert, bedankt voor je grenzeloze inzet, kritische werkwijze en hulp bij de fysische aspecten van dit proefschrift. Je was altijd bereid om mij extra uitleg te geven over de voor mij (voorheen) complexe en ongrijpbare materie van (diffusion-weighted) MRI. Naast het serieuze werk was er ook altijd tijd voor een onverwacht geintje tussendoor, dit heeft het promoveren een stuk dragelijker en luchtiger gemaakt. Hartelijk dank voor de geweldige uitleg en de gezellige samenwerking.

Leden van de beoordelingscommissie - prof.dr. R.H.M. Verheijen, prof.dr. P.J. van Diest, prof.dr. J.J.W. Lagendijk, prof.dr. F.L. Moll en prof.dr. L.J. Schultze Kool -, bedankt dat u zitting hebt willen nemen in deze commissie en dat u mijn proefschrift hebt willen lezen, beoordelen en goedkeuren op de wetenschappelijke inhoud.

Marianne Voogt, ik ben je veel dank verschuldigd voor het opzetten van de MR-HIFU-myoombehandelingen. Ik kwam in een goedlopend onderzoeksproject terecht, waardoor ik jouw wetenschappelijke taken 'gewoon' kon overnemen. Het klinische aspect van het MR-HIFU-project, de combinatie van gynaecologie en radiologie en jouw positieve houding hebben mij destijds over de streep getrokken om de uitdaging van een promotieonderzoek aan te gaan. Je hebt mij zelfs in de ochtenden na mijn nachtdiensten (als ANIOS gynaecologie) weten te inspireren om jouw functie over te nemen. Daarnaast was je altijd bereid om tijd te maken voor overleg, het dicteren van de vele MR-HIFU-verslagen of het nakijken van mijn manuscripten. Bedankt voor alles!

Niels Blanken, Greet Bouwman, Laura Gortzak-Mol en Jørgen Mensinga, wat had ik zonder jullie gemoeten. Het was altijd een feestje om met jullie te werken. Jullie doorzettingsvermogen, flexibiliteit en creativiteit kent geen grenzen. Mede dankzij jullie inspanningen gingen de patiënten altijd met een tevreden gevoel naar huis. Het team was goed op elkaar ingespeeld en dat werd opgemerkt door patiënten en collega's. Ik mis onze gesprekken en de gezelligheid tijdens de MR-HIFU-behandelingen. Ik kijk er met veel plezier naar uit om (als AIOS radiologie) weer met jullie te mogen werken op de klinische werkvloer.

Philips Healthcare, dear Thomas Andreae, Martin Deppe, Max Köhler, Charles Mougenot, Simo Muinonen, Heikki Nieminen, Joy Polefrone, Gerald Schubert, Johan Sjoholm, Paula Syrenius, Teuvo Vaara, Antii Viitala, Lizette Warner, Pirjo Wirtanen, Mika Ylihautala, and all the others who have supported the MR-HIFU treatments in Utrecht. Thank you for all your assistance, it has been a pleasure working with you. In addition, the financial support from Philips Healthcare for printing this thesis is greatly appreciated.

Beste co-auteurs - Marjolein van Breugel, Arie Franx, Marissa Frijlingh, Paul Lohle, Chrit Moonen, Robbert Nijenhuis, Paul Reuwer, Karlijn Schweitzer, Albert Smeets, Marijn van Stralen, Lenny Verkooijen en Koen Vincken -, bedankt voor het inzetten van jullie expertise en voor jullie begeleiding bij het schrijven van dit proefschrift / Dear co-authors - Bilgin Keserci and Young-sun Kim -, thank you for your help and valuable feedback while writing our manuscript.

Anneke Hamersma, Saskia van Amelsfoort-van de Vorst en Marnix van Herwaarden, bedankt voor jullie hulp bij het logistieke proces rondom de MR-HIFU-myoombehandelingen. Jullie hebben mij enorm veel werk uit handen genomen bij het screenen en opwerken van mogelijke kandidaten, het plannen van (follow-up) MRI-scans, het versturen van brieven en vragenlijsten en het reserveren van bedden op de verpleegunit divisie beeld. Door jullie werd het werk een stuk overzichtelijker en kon het onderzoek ook in mijn afwezigheid (tijdens vakantie of congressen) doorgaan.

Karen Schonenberg-van den Hout, jij was mijn vaste aanspreekpunt op de afdeling Radiologie in het St. Elisabeth ziekenhuis Tilburg. Je was altijd bereid om mij te helpen, geen vraag was te gek of bleef onbeantwoord. Hartelijk dank voor de prettige samenwerking, je vriendelijkheid en professionaliteit.

Robbert Nijenhuis, jij hebt mij enorm geholpen met het verzamelen van de data voor hoofdstuk 3 en 4. Ik kan niets anders zeggen dan dat dit het verloop van mijn promotieonderzoek een geweldige 'boost' heeft gegeven. Dank voor al je hulp en inzet.

Stafleden, fellows, arts-assistenten van de afdeling Radiologie, collega's van het Image Sciences Institute (ISI), laboranten, verpleegkundigen van zorgunit beeld, sedatieteam, technisch cluster beeld, digitale beeldbewerking, secretariaat en front-office, bedankt voor jullie tijd en inzet gedurende de afgelopen jaren.

Collega onderzoekers door de jaren heen, bedankt voor de leuke, leerzame en gezellige tijd. Een groot deel van de dag breng je door op het werk. Jullie hebben voor een belangrijk deel mijn opgewekte humeur en mijn positieve energie bepaald. Veel van jullie kom ik gelukkig weer tegen op de werkvloer als arts-assistent in opleiding tot radioloog. Uit ervaring weet ik inmiddels dat het erg prettig is om een bekend gezicht te zien als je aan een nieuwe uitdaging begint. Ik kijk ernaar uit om jullie weer te zien!

Kamergenoten van Q.04.4.306 - Beatrijs Seinstra, Tim Luijkx, Hamza el Aidi, Hanke Schalkx, Alexandra de Rotte, Arthur Adams en Erwin Krikken -, mede dankzij jullie ging ik elke dag met véél plezier naar mijn werk. Lief en leed hebben we met elkaar gedeeld, we hebben gelachen en gehuild. Het was fijn om de ethiek van de dag met jullie te bespreken en vaak kwam voor elk probleem een oplossing. Advies over statistische analyses in SPSS of R-Studio, hulp bij het opmaken van figuren of bij het inkorten van een abstract, het beantwoorden van werkgerelateerde telefoongesprekken: samen kwamen we steeds een stapje verder. Ik kon me door de jaren heen geen betere kamergenoten wensen, ik heb er een aantal vrienden bijgekregen. Arthur, ik wil jou in het bijzonder bedanken voor de opmaak van mijn proefschrift. Jouw oog voor precisie en details hebben dit proefschrift naar een hoger niveau gebracht en een geweldige uitstraling gegeven. Hanke, wat fijn dat jij mijn paranimf wil zijn. Je hebt mij door de moeilijke laatste periode van mijn promotie heen gesleept. Je wist aan elke situatie een positieve draai te geven en mij weer vertrouwen te geven op een goede afloop. Bedankt voor je positieve energie.

Beste familie en vrienden van Roger, bedankt voor jullie enthousiasme en interesse in mijn proefschrift. Karin, veel succes en plezier met je verdere studie en loopbaan. Jij komt er wel!

Lieve grootouders - opa Ikink en oma Rougoor -, ik ben ontzettend dankbaar dat jullie nog zoveel hoogtepunten in mijn leven mogen meemaken. Opa, tussen ons zal altijd iets bijzonders bestaan. Bedankt voor uw knuffels en lieve lach, u beseft niet hoeveel deugt ze mij doen. Ik ben blij dat u nog zo geniet van het leven en ik hoop dat u trots op mij bent. Oma, het is bewonderingswaardig wat u allemaal nog doet op uw leeftijd. Zelfstandig, sportief en leergierig. Ik hoop dat u nog lang actief mag blijven, u bent een groot voorbeeld voor mij!

Lieve Gerjon en Jelmer, we leiden alle drie een druk bestaan en willen zowel op privé- als werkgebied het maximale eruit halen wat erin zit. Jelmer, ondanks je drukke agenda en het tijdsverschil was je altijd bereid om mijn Engelse teksten kritisch te lezen en advies te geven over grammatica of woordgebruik. Ik ben je enorm dankbaar voor je hulp, dit heeft mij veel vertrouwen gegeven in het neerzetten van een goed(lopend) verhaal. Gerjon, wat ben ik blij dat jij tijdens mijn verdediging als paranimf naast mij wil staan. Jij brengt rust en relativiteit rond mijn hedendaagse zorgen. Als ik het even niet meer zie zitten, weet jij mij weer te motiveren. Ons telefoongesprek in de trein naar Den Haag zal ik nooit vergeten. Broertjes, jullie halen het beste in mij naar boven. Bedankt voor alles. Love you.

Lieve papa en mama, het is moeilijk in woorden uit te drukken wat jullie voor mij betekenen. Jullie hebben ons geleerd wat belangrijk is, om gelukkig te zijn en je eigen keuzes te maken in het leven. Dank jullie wel, omdat we mogen zijn zoals we zijn. Bedankt voor jullie onvoorwaardelijke steun en liefde. Jullie zijn de beste, ik hou van jullie!

Allerliefste Roger, een betere en leukere buurman had ik mij niet kunnen wensen. De moeilijke momenten tijdens mijn promotie hebben onze band sterker gemaakt en onze liefde doen groeien. Je was geduldig en hebt urenlang geluisterd. Je bent onmisbaar in mijn leven. Ik ben heel benieuwd wat de toekomst ons gaat brengen. Ik hou van jou!

# Biography

Marlijne Elisabeth Ikink was born on the 6th of June 1984 in Nieuwegein, The Netherlands. In 2002, she graduated from "voorbereidend wetenschappelijk onderwijs" (pre-academic secondary education) with education profile "Natuur en Gezondheid" (Natural and Medical sciences) at the Oosterlicht College in Nieuwegein. She started medical school in 2002 at the Utrecht University, The Netherlands. As part of her medical training she completed, among others, an internship at the department of Radiology, Meander Medical Center in Amersfoort; a research internship at the department of Neonatology, Wilhelmina Children's Hospital in Utrecht; and a final internship at the department of Obstetrics, Wilhelmina Children's Hospital in Utrecht, The Netherlands. After receiving her medical degree in 2008, she started working as a medical intern (ANIOS) in Obstetrics and Gynaecology at the Haga Teaching Hospital in The Hague (2008-2009) and the St. Antonius Hospital in Nieuwegein (2009-2010), The Netherlands. In 2011, she started her PhD project on volumetric magnetic resonance-guided high-intensity focused ultrasound (MR-HIFU) ablation of uterine fibroids under the supervision of Prof.dr. M.A.A.J. van den Bosch, Prof.dr. W.P.Th.M. Mali and Dr.ir. L.W. Bartels. In 2014 this led to the present thesis, in which the results of her PhD research are presented.

She has now started her residency in radiology under supervision of Dr. R.A.J. Nievelstein at the University Medical Center Utrecht, The Netherlands.